Effect of UV Radiation on the Mechanical and Rheological properties of LLDPE and HDPE films

by

Robert Mwangi Fathieh-Ngunjiri

A thesis

presented to the University of Waterloo

in fulfilment of the

thesis requirement for the degree of

Master of Applied Science

in

Chemical Engineering

Waterloo, Ontario, Canada, 2020

AUTHOR'S DECLARATION

I hereby declare that I am the sole author of this thesis. This is a true copy of the thesis, including any required final revisions, as accepted by my examiners.

I understand that my thesis may be made electronically available to the public.

ABSTRACT

The present work reports on the effects of UV-irradiation on the mechanical and rheological properties of films fabricated from high-density polyethylene (HDPE) and linear low-density polyethylene (LLDPE). These resins were selected for study because of their widespread use in the packaging industry. The variables that were investigated include the radiation time, the radiation intensity and the illumination pattern. The illumination pattern was changed by inserting a perforated stainless-steel sheet into the path of the light, thus transforming the pattern of illumination into a series of bright and dark bands.

In general, the study of the response of each film to UV radiation began by examining the interaction between the settings of the compounding and forming operations and the radiation variables. The compounding variables considered were the concentration of photosensitizer (benzophenone) and the concentration of LLDPE in the case of HDPE films while the forming settings included draw-down speed of the films (LLDPE) and the degree of stretching (HDPE).

The reason for studying the interaction between the forming operations and the UV treatment variables was to identify the optimum process settings that would allow the effect of UV treatments to be most clearly manifested. It was found that the optimum settings were low draw-down ratio (LLDPE films), low degree of stretch (HDPE films) and high concentration of benzophenone.

It was found that the screen modifies the effects of radiation intensity to a great extent. In the LLDPE films, increasing the intensity caused the elastic modulus to increase and the elongation at break to decrease. When the screen was introduced, the elastic modulus decreased but the elongation at break and the stress at break increased.

The rheological properties of the LLDPE and HDPE films were studied using a parallel plate rheometer. In the case of the LLDPE films, the viscosity data was fit to the Cross-model, thus allowing the zero-shear viscosity and the shear thinning index to be determined. The HDPE films were not fit to the cross model because none of the samples exhibited a tendency to Newtonian behaviour in the frequency range studied herein.

In the LLDPE films, it was found that irradiation under a screen causes the zero-shear viscosity to decrease by 266,526 Pa.s while radiation intensity and radiation time cause it to increase by 17,632 and 194,159 Pa.s respectively.

Additionally, it was found that irradiation under a screen causes the shear-thinning index to increase by 0.13 while increasing the level of radiation intensity and radiation time causes the shear-thinning index to decrease by 0.12 and 0.11 respectively.

It was also observed that illumination with the screen caused the cross-over modulus to increase relative to illumination without the screen. The cross-over modulus was correlated with the rheological polydispersity index, PI (Z). Without the screen, a film irradiated at an intensity of 47% had a PI (Z) of 4.19. In the presence of a screen, a film treated at the same intensity of UV radiation had a rheological polydispersity of 1.11.

Another measure of polydispersity that was used to characterize the LLDPE films was the ER. It was found that the trends observed for the PI (Z) were reflected in the ER; however, this measure provided addition insight into the effect of illumination pattern on the polydispersity of the high molecular weight chains. In particular, it was found that when the intensity of radiation is increased while the screen is present, the ER decreases. This indicates that the polydispersity of the low molecular weight chains decreases, possibly as a result of chain scission. In contrast, when the screen is absent, increasing the intensity of radiation and the radiation time cause the ER to increase.

In the case of the HDPE films prepared without benzophenone, the study was extended to examine the effect of radiation treatment on the permeability and puncture-propagation tear resistance in addition to the tensile properties. It was found that the effect of the radiation variables on the mechanical properties was highly dependent on the orientation of the films and on the concentration of HDPE. In the machine direction, the screen did not significantly affect either the tensile stress at break or the elongation at break, but in the transverse direction it caused the tensile stress at break to decrease by 6.7 MPa.

The effect of the screen on the puncture resistance was dependent on the concentration of HDPE. When concentration was at the low level, illumination in the presence of the screen caused the

puncture resistance to increase; however, when the concentration of HDPE was at the high level, illuminating the films under a screen caused the puncture resistance to decrease.

Finally, it was observed that none of the radiation variables investigated significantly affected the permeability of the films. The only significant factor in this respect was the concentration of HDPE.

During the second stage of testing the HDPE films, the reflector housing and the emission spectrum of the UV lamp were changed. The lamp was changed to one whose emission spectrum better matched the absorbance of benzophenone and polyethylene while the reflector housing was changed to one with a more uniform illumination. Under these new conditions, it was found that illumination in the presence of the screen caused the tensile stress at break in the machine direction to increase by 9.6 MPa but it did not affect the tensile stress at break in the transverse direction. A similar effect was observed on the tensile strain at break.

The scope of the rheological investigation was extended to include a second screen with smaller holes and a hexagonal pitch (called screen 1). The screen used thus far had wider holes and a square pitch (this screen was called screen 2). It was found that samples irradiated using screen 1 had a higher viscosity at low shear rates and were more shear thinning than films irradiated under screen 2. Investigating the crossover moduli of films irradiated under this experimental set-up (new housing, lamp and 10 wt. % benzophenone) showed that all of them were highly crosslinked.

ACKNOWLEDGEMENTS

DEDICATION

I wish to dedicate this work to God, in thanks for enabling me to catch a glimpse of the beauty of His creation.

Table of Contents

LIST OF FIGURES

LIST OF TABLES

1 INTRODUCTION

Polyethylene is one of the simplest synthetic polymers known to man. It is composed of repeating ethylene units connected to each other by covalent bonds. Despite its structural simplicity, it has excellent mechanical, electrical, optical and chemical properties and thus is used in a wide range of applications.

This study will focus on two commercially important types of polyethylene: linear low-density polyethylene (LLDPE) and high-density polyethylene (HDPE). High density polyethylene is made from the polymerization of ethylene gas at low pressure and temperature in the presence of a catalyst [1] . Linear low-density polyethylene results from the copolymerization of ethylene with α-olefins. Copolymerization results in the formation of branches of uniform length randomly distributed along a given chain [2] [1].

Both LLDPE and HDPE are used widely in the packaging industry. Often they are combined with other materials in the form of multilayer films. This is done in order to modify their physical properties such as permeability and puncture resistance. This presents challenges during disposal as multilayer films are difficult to recycle. Accordingly, there is significant academic and industrial interest in developing single-layer films with properties comparable to those of multilayer films.

Objective

The purpose of the present study is to explore the potential of UV radiation to modify the properties of films made from LLDPE and HDPE. The properties examined include ductility, stiffness, strength, viscosity, linear viscoelasticity, puncture resistance and air permeability. A unique approach taken in this study is that the effect of changing the illumination pattern using a photo-masking screen is examined.

Based on previous research studies, it is expected that radiation treatment will induce crosslinking [3], chain scission [4] and long chain branching [5] in the films. The main research question is, therefore, whether changing the illumination pattern will modify the effect of radiation, perhaps giving rise to new properties resulting from locally induced structures.

Thesis Outline

Chapter 1: This chapter introduces the research work and describes its principal objective

Chapter 2: This chapter describes the present condition of the plastics industry. It aims to contextualize this study in the needs of the plastics industry.

Chapter 3: This chapter presents an introduction to photochemistry then moves to a review of previous work on the photochemistry of polyethylene.

Chapter 4: This section introduces the experimental and statistical methods applied in this study.

Chapter 5: This chapter presents and discusses the results of the work.

Chapter 6: Comments on the significance of the present work are presented here and suggestions for avenues of further exploration offered.

2 THE PRESENT STATE OF THE PLASTICS INDUSTRY

Human society has benefited from the use of polymers since about 1600 BC when ancient Mesoamericans processed natural rubber into balls, figurines and bands [3].

While natural polymers have been in use for several centuries, synthetic polymers are a relatively new category of materials. They are often made from fossil fuels and are generally divided into two categories: thermosetting and thermoplastic polymers. Thermoplastic polymers, also known simply as "plastics" are a class of synthetic polymers that are commonly distinguished by their ability to be melted from the solid phase. In contrast, thermosetting polymers cannot be melted once they are synthesized.

Polyethylene is one of the most common plastics in production today. It was discovered by Reginald Gibson and Eric Fawcett of Imperial Chemical Industries in the 1930's [3]. Since then, a large variety of production processes have been discovered and refined, leading to a vast range of types of polyethylene. Usually, these are characterized according to the average density of the resin:

1. Linear low-density polyethylene (LLDPE): 0.925 $g.cm_{-3}$
2. Low-Density Polyethylene (LDPE): 0.930 – 0.935 $g.cm_{-3}$
3. Medium-Density Polyethylene (MDPE): 0.935 – 0.945 $g.cm_{-3}$
4. High-Density Polyethylene (HDPE): 0.945 – 0.965 $g.cm_{-3}$

Since their discovery in the early 20th century, global production of plastics has increased from 2 million tons in 1950 to more than 400 million tonnes in 2015 [4]. This growth reflects the increasingly important role plastics have played in shaping our modern world.

The success of plastics is closely connected to the rapid expansion in knowledge of the chemistry and physics of polymers. This has enabled polymer scientists to develop plastics which exhibit a wide range of physical and chemical properties. This in turn means that a specific plastic can be developed to exactly meet a specific need in society. An example of the range of applications of plastics is listed in Table 2-1.

Table 2-1: Global primary plastics production and primary waste generation in 2015 [4]

Market Sector	2015 Primary Production ($\times 10^6\ tones$)	2015 Primary Waste Generation ($\times 10^6\ tones$)	Average lifetime (years)
Packaging	146	141	0.5
Transportation	27	17	13
Building and Construction	65	13	35
Electrical/ Electronic	18	13	8
Consumer & Institutional Products	42	37	3
Industrial Machinery	3	1	20
Textiles	59	42	5
Other	47	38	5
Total	**407**	**302**	**-**

Table 2-1 illustrates that the largest application of plastics is in packaging, which accounted for close to 36% of the global production of plastics as of 2015. It also illustrates that concomitant with the growth in the production of plastics is the challenge of the generation of plastic waste. In 2015 alone, 302 million tons of plastic waste was produced globally. This challenge is particularly acute in the packaging sector because the average lifetime of packaging film is about six months from when it is produced [4]. This means that packaging waste is produced more rapidly and in greater quantity than other kinds of plastic waste [8].

A significant component of plastic packaging is plastic flexible films. For example, in the United Kingdom, plastic films represent 34% of total plastic packaging [5]. The global volume of consumer flexible packaging is expected to increase from 27.4 million tonnes in 2017 to 33.5 million tonnes in 2022. [5] The applications of plastic films in the packaging industry are summarized in Figure 2-1 [5].
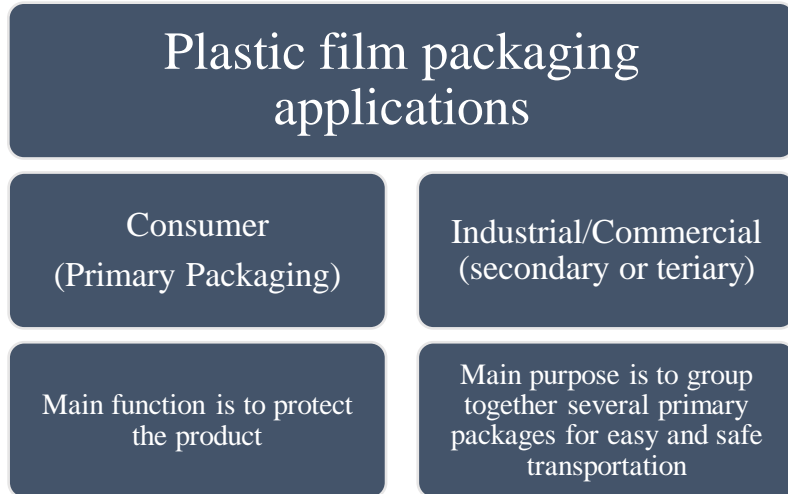
Figure 2-1: Main applications of plastic film in the packaging industry.

Most primary packaging is made of either HDPE or LLDPE while most secondary packaging is made of LDPE [5]. There are two main groups of plastic films: monolayer films and multilayer films. Monolayer films are usually 20 – 200 µm thick and are mostly used for secondary packaging or in the agricultural and building applications.

Multilayer film is used in primary packaging. As the name suggests, such film is usually made up of several layers of plastic. The number of layers can range from 2 – 17. Multilayer films account for up to 17% of global plastic production [5]. The production methods for both monolayer and multilayer films are summarized in Table 2-2.

Table 2-2: Plastic film production processes and applications

Type of film	Processing method		Applications
Monolayer	Extrusion	Blown film	Bags, agricultural and construction films, stretch films, can liner
		Cast film	Textile packaging, flower wrapping, coating substrates
Multilayer	Co-extrusion	Blown film	Food and chemical packaging
		Cast film	Packaging
		Coating	Candy wrappers, snack food bags

	Lamination	Medical packaging, condiment packages, soup sachets, cable wrap
Lamination	Adhesive	Food packaging, lidding foil, chemical storage, outdoor exposure film

The share of plastics in municipal solid waste in middle- and high-income countries has seen a steady increase from 1% in 1960 to 10% in 2005. 50% of this waste is films [5]. Given that about 50% of manufactured polyethylene is used to make plastic films [3], this implies that a large percentage of plastic packaging waste is made of polyethylene [8].

Presently, management strategies for plastic waste include recycling, incineration, pyrolysis and discarding into the environment. As of 2015, 12% of all plastics were incinerated, 9% were recycled (of which 10% have been recycled more than once) and 60% were discarded and are accumulating in landfills [4].

The effect of plastic waste on the environment is two-fold. First, because of their chemical inertness, they are mostly impervious to biological breakdown. This means that when discarded into the environment, they accumulate, rather than decompose. When combined with the increase in the production of plastic, especially for packaging, more and more space will be needed to dispose of plastic waste. Second, most plastics are sensitive to ultraviolet radiation from the sun. This radiation causes them to fragment into particles that reach up to micrometres in size. The effect of these 'micro-plastics' on marine and freshwater environments is a growing concern [4].

Consideration of the aforementioned points inevitably leads to the conclusion that the disposal of plastic waste is not only unsustainable but also harmful at least to marine ecosystems. Indeed, while the full impact of the accumulation of plastic waste cannot yet be fully estimated, society cannot ignore the harm that it has had so far. It is therefore imperative that the proportion of plastics that are discarded into the environment be significantly minimized and if possible, entirely eliminated.

We propose that this objective can be achieved if effort is directed towards developing strategies which allow society to derive some secondary benefit from sustainable disposal of plastic waste. This benefit can be energy (pyrolysis or incineration) or the production of new materials from plastic waste (recycling). Both of these solutions are in development and much work will need to be done to refine them before they can be applied to process significant proportions of the global plastic waste.

We feel that a special focus on waste from plastic films is required since they comprise the largest share of the largest sector of the plastics industry. Accordingly, our study will focus on the development of a self-reinforced plastic film using ultraviolet radiation. The main motivation for producing such a film is that it would be easier to recycle because it would be composed of just one type of resin.

Flexible films are usually considered a non-recyclable fraction of the waste stream and thus sent to landfill or energy recovery. This is because their small thickness and low bulk density pose challenges during reprocessing and thus makes recycling uneconomical.

Recycling multilayer films is especially challenging because of the large variety of materials used to make a single film. This means that conventional recycling processes cannot be effectively applied to them. New technologies are therefore being developed to recycle these materials. Examples of these include delamination [6], [7] and selective dissolution [8]. While these methods are promising, they are not yet economically viable nor are they efficient enough to process waste in bulk [5].

The development of monolayer self-reinforced films seeks to tackle the problem at its source by developing materials that play the same role, but which are easier to recycle.

3   LITERATURE REVIEW

Introduction to photo-polymerization

Photo-polymerization is a process which utilizes energy from the electromagnetic spectrum to initiate and control the synthesis or modification of macromolecules. As a method in chemistry, photo-polymerization is used by both living and non-living systems.

In living systems, photo-polymerization is applied by green plants to synthesize starch from carbon dioxide and water using radiation from the sun.

In the laboratory, photochemistry emerged as a method for the synthesis and modification of organic molecules early in the 20th century [9]. One of the early contributors to this field, Giacomo Ciamacian, even saw in photochemistry a solution to society's dependence on fossil fuels [9]. Since that time the use of the electromagnetic spectrum to control the formation, structure and properties of polymeric materials has emerged as one of the most powerful paradigms in polymer science [10].

It is interesting to note that in his paper [9], Giacomo notes that there exists a close connection between photochemistry and the "deepest speculations of quantum mechanics". Since his time, a great deal of effort has been expended into understanding the mechanisms involved in light driven reactions and today the field is quite mature. The purpose of this section is to summarize the aspects of photochemistry which have a bearing on the study of the photo-polymerization of polyethylene and then to survey the photo-polymerization reactions of polyethylene itself.

Advantages of light-driven reactions

Light driven polymerizations offer several advantages over thermally driven methods.

First, they allow highly selective reactions to occur at ambient conditions [9] [10] [11]. The reason for this is the large difference in energy available for chemical reactions in thermally and photo-induced systems. For example, a thermal bath at 25_oC supplies one-hundredth of the energy available in one mole of photons at 350-450 nm. In addition to this, this energy can be accepted by specific chromophores that have been introduced into a system.

Furthermore, light driven reactions enable the organic chemist to achieve an unparalleled degree of spatiotemporal control over chemical reactions. This is facilitated by the intersection of three factors. One of these is recent developments in the design and manufacture of light sources [11]. These developments have made light sources cheaper and more precise. At present there are three sources that are used to drive chemical reactions: fluorescent lights, lasers and light emitting diodes (LEDs). Each of these sources facilitates the control of the position, intensity, wavelength and duration of radiation.

The second phenomenon, which is intimately tied to the first, is the manner in which electromagnetic radiation propagates through space-time. Often, electromagnetic radiation travels through a void in the form of waves and rays. These rays can be easily diffracted, focused or diffused through the use of optical instruments such as mirrors, lenses, diaphragms or screens. It is thus possible to develop optical ensembles which are tailor made to facilitate interactions with reacting systems at precisely controlled positions.

The third factor is the way that matter itself interacts with light. Some reactions such as photo-isomerization only proceed in the presence of light. This means that it is possible to switch these reactions on and off by simply switching the light source on or off. Temporal control has been successfully applied to exert greater control over several living polymerization mechanisms.

Practically, spatial and temporal control of photo-polymerization reactions is achieved by utilizing the properties described above to initiate and control a particular polymerization mechanism. Spatiotemporal control has been successfully applied to atom transfer radical polymerization (ATRP) [12] [13] and reversible addition-fragmentation chain transfer (RAFT) [14] [15].

An interesting illustration of spatiotemporal control was illustrated by the works of Polema et al [12], [16]. They began by illustrating how visible light can be used to initiate the polymerization of methacrylates by using an iridium-based catalyst, Ir (ppy)$_3$. The catalyst acts as a photo-initiator for atom transfer radical polymerization (Photo-ATRP) [16]. They then showed that the propagating polymer chains could be returned to their dormant state by simply switching the light source off and can be re-initiated by switching it back on.

Subsequently they showed that spatial control could be achieved by combining photo-ATRP with a photomask to control the location and intensity of incident light on the polymer surface [12]. An illustration of this process is shown in Figure 3-1.
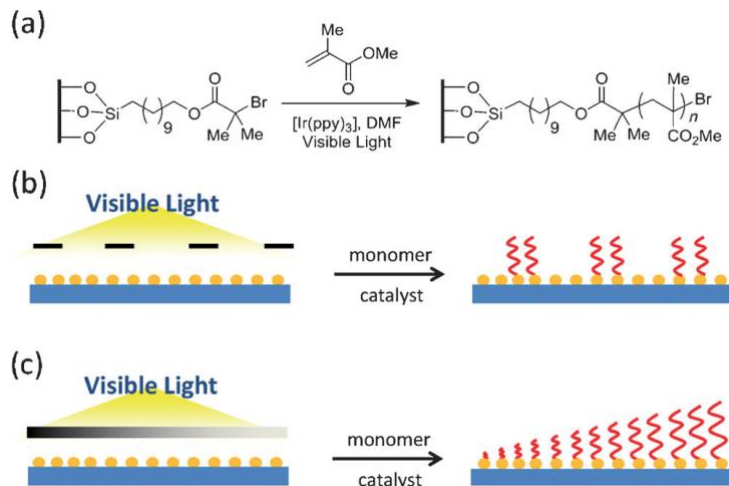
Figure 3-1: Illustration of fabrication of polymer brushes uniformly functionalized with trichlorosilane-substituted α-bromoisobutyrate-based initiators. (a) Polymerization reaction. (b)Use of a photomask for patterns (c) Use of neutral density filter for gradient structures.

By doing this, a variety of sub-micron 3-D structures could be synthesised on the surface by altering the properties of the photomask. Examples of these features are shown in Figure 3-2.
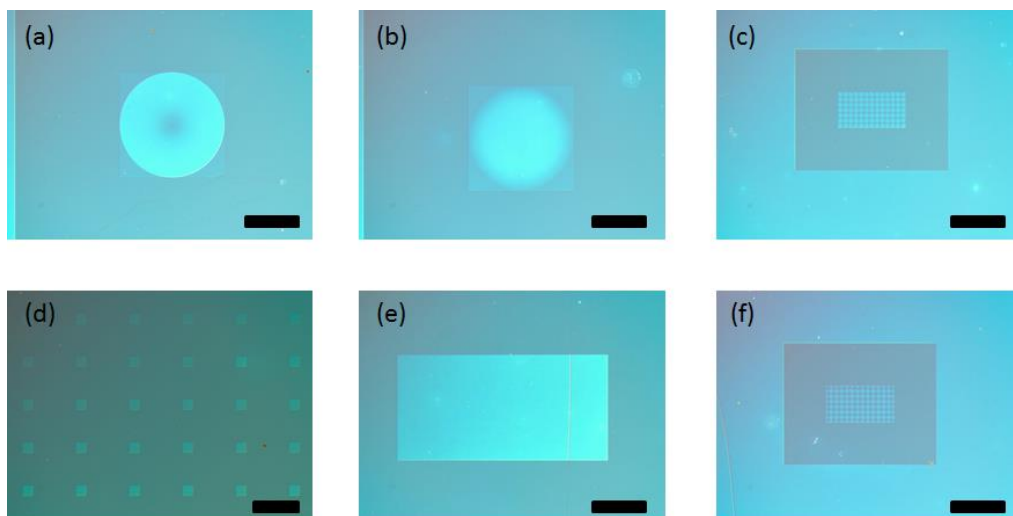
All scale bars are 500 microns

Figure 3-2: Optical micrographs of 3-D polymer brush structures obtained by irradiating through a grayscale mask with the following features: (a) A negative lens (b) Positive lens (c) Positive micro-lens array (d) Squares of varying height (e) Macroscopic gradient (f) negative micro-lens array [12]. Reprinted from J. E. Poelma, B. P. Fors, G. F. Meyers, J. W. Kramer and C. J. Hawker, "Fabrication of complex three-dimensional polymer brush nanostructures through light-mediated living radical polymerization," *Angewandte Chemie - International Edition,* vol. 52, no. 27, pp. 6844-6848, 1 7 2013 with the permission of John Wiley and Sons.

Materials with precisely controlled architectures are being used in a wide range of applications. So far, the applications of such materials include: antifouling coatings, chemical sensing, bio-functional interfaces and stimuli-responsive materials. [12] [15].

Quantum Mechanical Principles of Photochemical Reactions

In contrast to thermal systems where activation energy is overcome by an increase in temperature (and thus the average kinetic energy of the reacting molecules), photochemical systems proceed through the production of energetic molecular species through photoexcitation [11]. The photoexcitation process can be illustrated using a Jablonski diagram, shown in Figure 3-3.
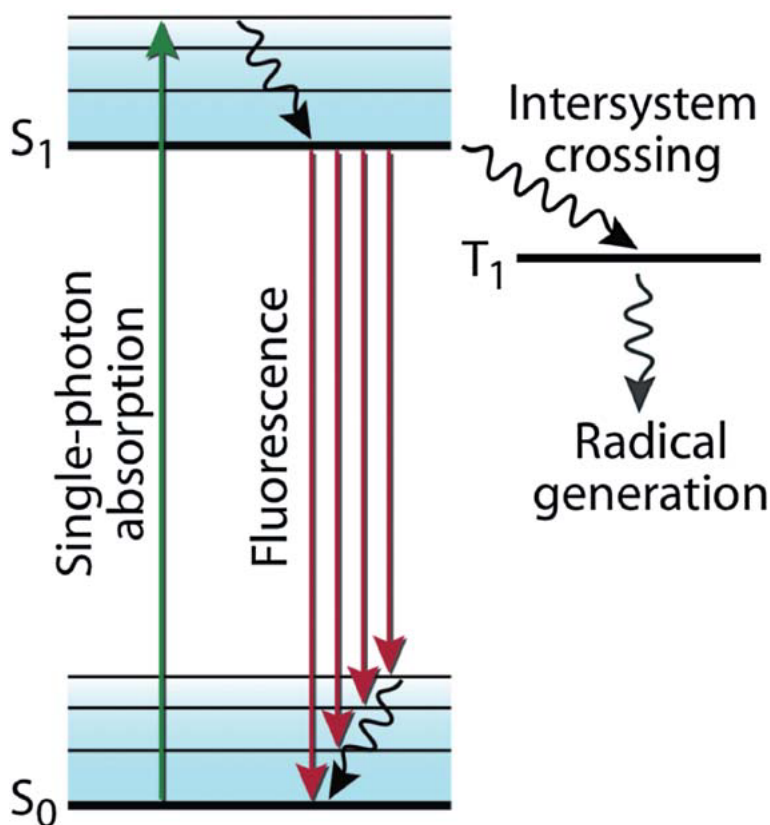
Figure 3-3: Jablonski diagram showing excitation of a chromophore from a stable ground state S_0 to an excited state S_1. From S_1 the system undergoes intersystem crossing (ISC) to a triplet state, T_1. The system can either decay back to S_0 or can undergo a variety of chemical reactions which occur from T_1 [10]. Republished with permission of the Royal Society of Chemistry, from "*The power of light in polymer science: Photochemical processes to manipulate polymer formation, structure, and properties*", S. Chatani, C. J. Kloxin and C. N. Bowman, vol. 5, Royal Society of Chemistry, 2014, pp. 2187-2201 permission conveyed through Copyright Clearance Center, Inc.

Figure 3-3 illustrates that a chromophore (a species which absorbs electromagnetic radiation at a particular wavelength) interacts with the electromagnetic spectrum by absorbing the energy of a photon and using it to promote an electron from its ground state, S_0 to an excited singlet state, S_1. In a singlet excited state, the excited electrons retain opposite spin. For this to occur, the

chromophore must have an energy level that corresponds to the energy of the radiation [17]. Furthermore, depending on the functionality, organic compounds can have absorption bands in the ultraviolet, visible or even the infrared regions of the electromagnetic spectrum [11] [17]. The wavelength absorbance ranges of various functionalities are shown in Table 3-1.

Table 3-1: Approximate wavelength ranges for the lowest energy absorption band of representative organic compounds [17]

Functionality	Absorption maxima (nm)
Monoalkenes	190 – 200
Acyclic dienes	220 - 250
Cyclic dienes	250 – 270
Aryl-substituted alkenes	270 – 300
Saturated ketones	270 – 280
α, β −unsaturated ketones	310 – 330
Benzene derivatives	250 – 280
Aromatic ketones and aldehydes	280 - 300

Most photochemical reactions involve unsaturated groups, mainly alkenes, carbonyl groups and arenes. In compounds with these functionalities, the transition from S_0 to S_1 involves the promotion of a valence shell electron to an antibonding π^* orbital.

The manner in which the valence electron is excited from its ground state is governed by three general principles [17]:

1. In general, the excitation of an electron is from a filled orbital to an empty one. In many cases, the excitation is from the highest occupied molecular orbital (HOMO) to the lowest unoccupied molecular orbital (LUMO). Hence, in general, photo excitation involves the unpairing of electrons.

2. At the instant of excitation, only electrons are reorganized. Nuclei retain their ground state geometry. This excitation is called a vertical transition. This is called the Frank-Condon Principle. A consequence of this principle is that the excited state is initially in

non-minimal energy geometry. From here, the excited state decays rapidly to its minimum energy geometry through a series of vibrational processes that transfer thermal energy to the environment. This process is called internal conversion

3. Electrons do not undergo spin inversion at the moment of excitation. This is a consequence of the principle of the conservation of spin. Although inversion of spin may occur, it is a separate excitation event.

In the absence of any chemical reactions, the energy of the chromophore decays back to S_0 by fluorescence emission or through heat dissipation [10], [11], [17]. Sometimes chemical reactions can occur from the excited singlet state though this is rare when the chromophore is in solution [17]. This occurs because the rate of chemical reaction is fast relative to vibrational relaxation. When this occurs, a reaction is said to involve a "hot excited state".

Alternatively, the chromophore can undergo intersystem crossing (ISC) to T_1. This involves the inversion of the spin of an electron in a half-filled orbital to give a triplet state. A triplet state is characterized by both unpaired electrons having the same spin. The triplet state also adopts a minimum energy molecular geometry. From here, it can either undergo intersystem crossing back to S_0 or it can undergo chemical reactions such as isomerization, bond formation or bond cleavage from T_1.

One of the main challenges in characterizing photochemical reactions is to determine whether a reaction proceeds from a singlet or triplet excited state. This depends on the relative rates of intersystem crossing and reaction. If intersystem crossing is slow compared to a chemical reaction, then the reaction will proceed from the singlet state. If intersystem crossing is faster, then the reaction will proceed from the triplet excited state.

An alternative to the direct photoexcitation of molecules in a reacting system is photosensitization. Here, the main chromophore is a molecule called a sensitizer. The sensitizer transfers a characteristic energy, E_T from its excited triplet state to the ground state of the reactant molecule. This energy transfer occurs with the net conservation of spin. Therefore, it produces a reactant in an excited triplet state.

The mechanism for triplet photosensitization is summarized in Table 3-2.

Table 3-2: Summary of mechanism for photosensitized triplet excitation

Sensitizer → Sensitizer^{1,*}	Sensitizer singlet formation
Sensitizer^{1,*} → Sensitizer^{3,*}	ISC of sensitizer singlet to triplet state
Sensitizer^{3,*} + Reactant → Sensitizer + Reactant^{3*}	Energy transfer to reactant

To be effective, the choice of photosensitizer must conform to the following criteria [17]:

1. It must be excited by the wavelength of radiation used for a specific reaction.
2. It must be present in sufficient concentration so as to absorb more strongly than other molecules in the reacting system.
3. Its intersystem crossing rate must be faster than the rate of energy transfer to the reactant molecule from the singlet state.
4. The energy of its triplet state must be higher than that of the reactant. Otherwise the energy transfer will be endothermic and cannot compete with other transformations.
5. The triplet excited sensitizer must be able to transfer energy to the desired reactant.

From the foregoing, it is possible to characterize the response of a chromophore to electromagnetic radiation as either photo-physical or photochemical. Photo-physical events include fluorescence, phosphorescence or heat dissipation and are caused by the decay of the molecule from an excited state (S_1 or T_1) back to the ground state (S_0). The rate of decay from states by fluorescence is higher than the rate by phosphorescence [17]. Examples of photochemical events include isomerization, bond formation or bond cleavage. These mostly occur from T_1 and lead to the formation of new molecules. The probability of a specific photo-physical or photochemical event occurring is measured using the quantum yield, φ.

Since photochemical processes are very fast, special techniques are used to determine the rate measurements used to determine the quantum yield. One example is flash photolysis in which the excitation is affected by a short pulse of light in an apparatus used to monitor very fast spectroscopic changes. The rate of various events can be determined from these changes. Often, a molecule called a quencher is introduced to the reacting system. A quencher is a molecule which accepts energy from an excited reactant, thus deactivating it and preventing further reaction. The quantum yield is then measured as a function of quencher concentration and can be evaluated using the following equation:

$$\varphi = \frac{k_r}{k_r + k_q[Q] + k_n}$$

Equation 1: Dependence of quantum yield on the relative rates of reaction (k_r), quenching (k_q) and nonreactive decay to ground state (k_n)

A plot of the inverse of quantum yield versus quencher concentration is called a Stern-Volmer plot. From this plot it is possible to determine the rate of a particular reaction. Though this method is well-established in the field, it would be more appropriate from a statistical perspective to plot the quantum yield against the quencher concentration and then to apply non-linear regression to determine the unknown reaction rates. This is because taking the inverse of the data also has the effect of transforming the experimental error associated with the measurements. The consequence of this is that it might not possible to obtain reliable estimates of the reaction rates from the transformed data [22].

The quantum yield is determined by several factors. The most important factor is the molecular structure of the chromophore itself [11]. The molecular structure determines the possible energy transfer pathways, the lifetimes of the excited states and its molar extinction coefficient, ε, a measure of how strongly a chromophore absorbs light at a particular wavelength.

Considering the possible energy transfer pathways and lifetimes of specific excited states, photochemical reactions are of particular interest for three major reasons. First, excited states have excess energy and thus can undergo reactions that would be highly endothermic if initiated from the ground state. Furthermore, the population of one or more antibonding molecular orbitals in the excited state allows the occurrence of chemical transformations that are electronically forbidden to ground state species. Finally, both singlet and triplet states have unpaired electrons. This permits the formation of intermediates that are unavailable under thermal conditions.

Another factor that determines the quantum yield is the chemical environment of the chromophore. In particular, the solvent type and the temperature of the mixture play a significant role. In general, the characteristics of a solvent, for example polarity, affect the interaction between a chromophore's electron manifold and incident photons. Furthermore, the solvent itself as well as other molecules in a reaction mixture provide alternative pathways for energy transfer

through interaction with the excited chromophore. Temperature affects how frequently these interactions occur. [11]

Finally, the intensity and wavelength of the incident light itself affect the quantum yield. The energy of the photons emitted from a light source is inversely related to the wavelength of the light as illustrated in Equation 2.

$$E = h.c\frac{1}{\lambda} = h.c\, v$$

Equation 2: Quantized energy of a photon of light

where: h = Plank's Constant, 6.26×10^{-34} $m_2.kg.s_{-1}$

c = speed of light in vacuum, $3.0 \times 10_8$ $m.s_{-1}$

λ = wavelength of incident radiation in m

v = frequency of incident radiation

Thus, changing the irradiation wavelength changes the photon energy and this affects the likelihood of electron transitions to higher energy orbitals. The wavelength dependence of photoexcitation pathways is reflected in the dependence of the molar extinction coefficient on the wavelength of the incident radiation. Radiation intensity is related to the quantity of photons entering a system. Hence, increasing radiation intensity increases the number of electron available for interaction with chromophores.

Photochemical reactions fundamentally involve the unpairing and repairing of electrons; however, the structure of excited states and intermediates play a crucial role in determining the final products of a photochemical reaction. Mechanisms for photochemical reactions can therefore be presented at different levels of detail.

The most basic level, which is the one which shall be primarily used in this thesis, is, to recognize the unpairing/repairing sequence that is involved in bond breaking and bond forming. At a second level of detail, the orbitals that are involved in a reaction can be described. This level of detail permits the recognition of orbital symmetry effects and/or stereo-electronic effects.

A potential energy diagram represents transitions between the reactant, its excited structures and the products. It aims to trace the minimum energy path across a potential energy surface from

excitation to product. Since photo-chemical reactions can involve several excited states, each with its own potential energy surface, there are several energy plots representing these states. Some plots can map progress in one structural change, such as bond breaking or bond twisting about a bond. Potential energy diagrams can also map the composite changes that occur in the reactant, excited state and the product. An example of such a diagram is shown in Figure 3-4.
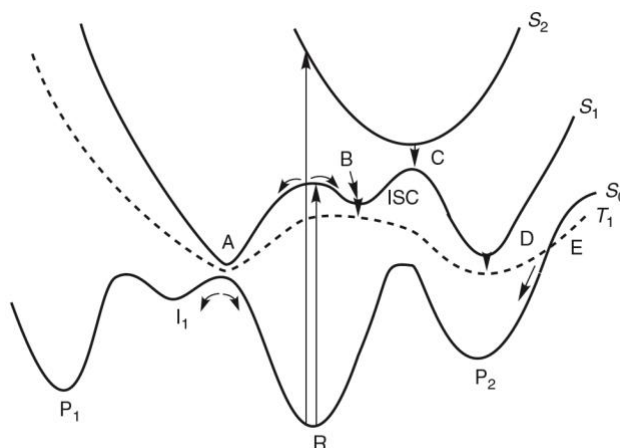
Figure 3-4: A potential energy diagram showing energy transitions between excited states leading to the formation of products [17]. Reprinted by permission from Springer Nature Customer Service Centre GmbH: Springer Nature, Advanced Organic Chemistry by Carey F.A., Sundberg R.J. Copyright © (2007)

Figure 3-4 depicts excitation to both S_1 and S_2, the first and second singlet states. Singlet species return to the ground state at point A and may return either to reactant, R or product at P_1. Intersystem crossing occurs at point B or D and provides the triplets state, T_1 which gives product P_2.

For many reactions, it has been found that the transition between an excited state and the ground state involves a conical intersection (CI) which can be envisioned as a funnel that permits transition from one state (energy surface) to another. Two points about the conical interface are noteworthy. First, the rate of conversion between the excited state and the ground state is dependent on the similarity between it and the corresponding ground state molecular ensemble. Second, several conical interfaces can exist for the excited states of a typical polyatomic molecule. Conical intersections can proceed along any direction on a plane and can reach more than one minimum (product). Thus, the ultimate outcome of a reaction is determined by dynamic

18

factors at the CI such as the direction of rotation of a molecule at a preceding stage in the reaction. This is illustrated in Figure 3-5.
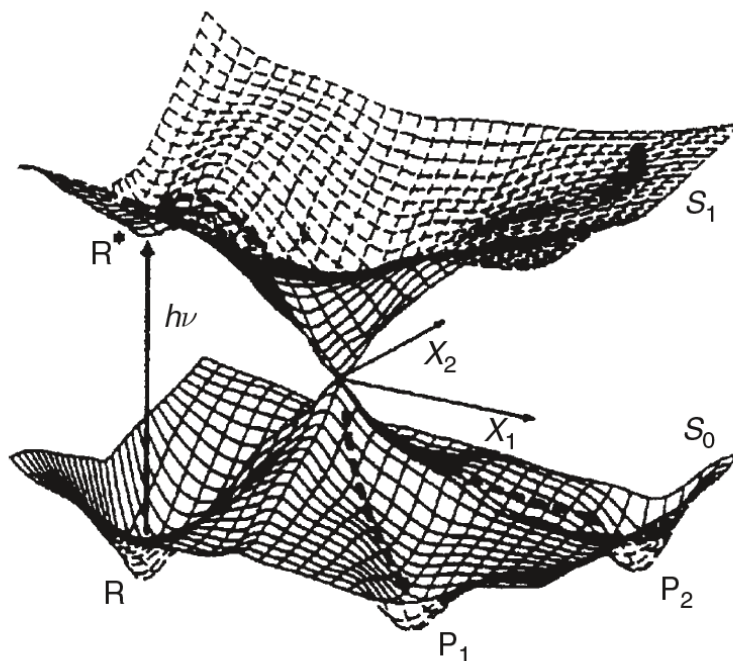
Figure 3-5: Illustration of the potential energy surfaces of the ground S0 and excited singlet S1 state in a photochemical reaction. Two paths lead from the conical intersection to products P1 and P2 [17]. Reprinted by permission from Springer Nature Customer Service Centre GmbH: Springer Nature, Advanced Organic Chemistry by Carey F.A., Sundberg R.J. Copyright © (2007)

In the case shown in Figure 3-5, the different products are formed as a result of differences in the components of motion in the x_1 and x_2 directions.

Each of the levels of description outlined in the preceding paragraphs permits different levels of insight into the causes of different phenomena associated with photochemical reactions.

Photochemical Reactions in Polyethylene

One of the earliest quantitative studies of the radiation chemistry of polyethylene was published by Charlesby in 1952 [18]. He discovered that when polyethylene is exposed to ionizing radiation, a new material is formed with the following properties:

1. It does not melt at 115_oC, the usual melting point for low density polyethylene.
2. It is resistant to hot organic solvents.
3. It exhibits rubber-like elasticity at temperatures above 115_oC.

He attributed these properties to crosslinking of the polymer chains. Furthermore, he studied weight changes in samples as a way to elucidate a simple mechanism for crosslinking. The result is shown in Figure 3-6.
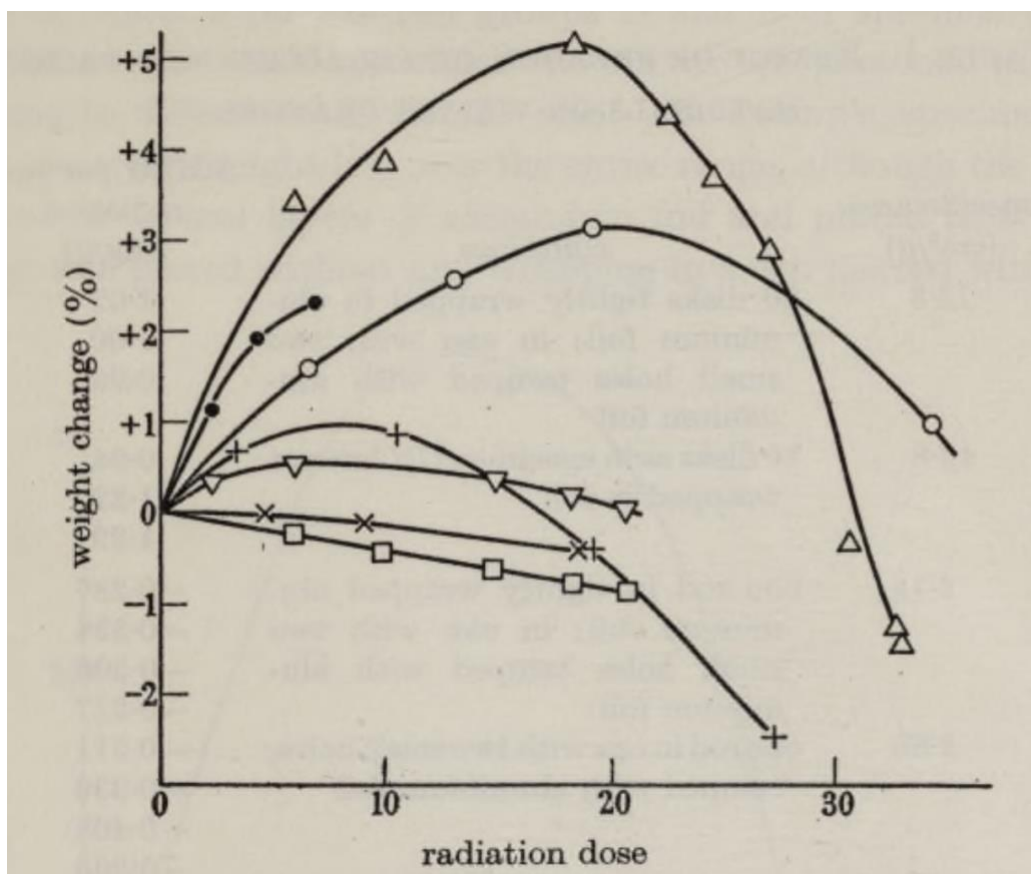
Figure 3-6: Weight changes in samples of polyethylene with radiation dose:
$o, granules\ in\ clear\ glass$; $\Delta, granules\ in\ copper\ gauze$;$\times, cylinders$; $\bullet$
$, granules\ in\ copper\ gauze$; $\nabla, disks\ in\ copper\ gauze$; $+, paraffin\ granules$. Republished with permission of The Royal Society (U.K.), from Proceedings of the Royal Society A, Mathematical, Physical and

Figure 3-6 shows that initially, as radiation dose is increased, the mass of the samples increases to maximum value but then decreases sharply after. Charlesby attributes this increase to an oxidation process that occurs mostly on the surface of the polymer while the decrease is attributed to hydrogen and small hydrocarbon release occurring in the bulk of the polymer. The release of hydrogen gas is associated with crosslinking while the release of small hydrocarbons is associated with scission of the polymer chains.

One key result from Charlesby's study is that the yield of crosslinks is sensitive to the thickness of the samples. The oxidation reaction occurs mostly on the surface of the sample and leads to the formation of a waxy layer on the surface of the film. If the surface area to volume ratio of the sample is very high, the sample will mostly undergo oxidation because much of its surface is available for reaction with atmospheric oxygen.

Following this pioneering work, Oster, Oster and Morrson explored the possibility of crosslinking polyethylene using ultraviolet radiation [19]. They adduced the following reasons for considering ultraviolet radiation:

1. UV radiation is less lethal to human beings than ionizing radiation.
2. UV lamps can cover a larger surface area than the piles that were used in Charlesby's study.
3. Low selectivity of the crosslinking reaction over bond scission when polyethylene is exposed to gamma radiation.

Building on Charlesby's proposed mechanism, they proposed that UV radiation in the range of 200 – 300 nm would be sufficient to abstract hydrogen from the polymer backbone. Their results validated this proposition. Furthermore, they found that the addition of a photosensitizer leads to a 1000-fold increase in the crosslinking efficiency. The photosensitizer they proposed was benzophenone. Furthermore, Oster et at al demonstrated that in addition to crosslinking, it is possible to perform graft copolymerization by incorporating monomer onto the surface of the polyethylene films.

Oster et al also reported one of the earliest measurements of the quantum yield of the crosslinking reaction in the presence of benzophenone. The value they reported was 0.09. This

value was later disputed by a subsequent study published by Charlesby et al in 1959 [20]. Their study asserted that the quantum yield in oxygen at 253 nm is 0.175 while at 365nm it is 0.0222.

The observations described above can be correlated with changes in the absorbance spectrum of polyethylene both in the absence and presence of benzophenone. One of the most comprehensive studies on the absorbance of polyethylene in the range studied by Charlesby and Oster et al was published by Roger Partridge in 1966 [21]. The spectrum is shown in Figure 3-7.
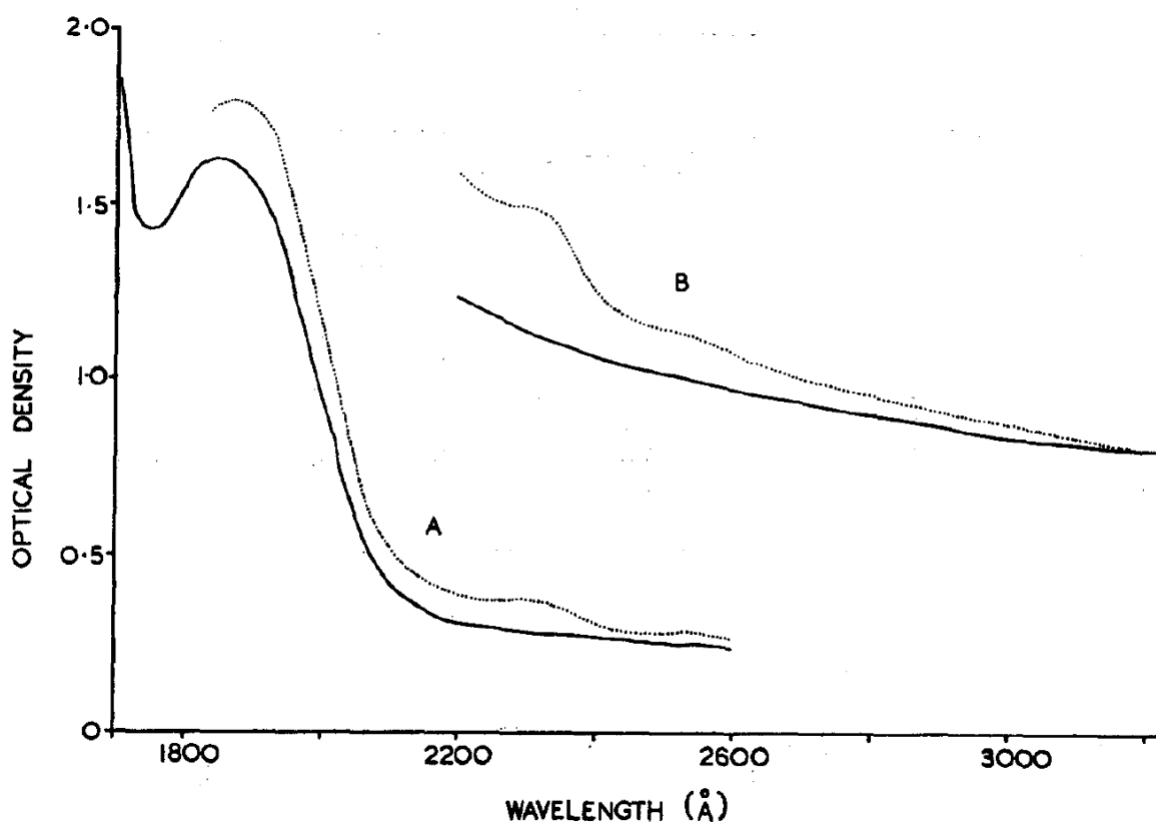
Figure 3-7: Absorption spectrum of 1mm (A) and 4 mm (B) polyethylene films. ---, Normal absorption; ___, absorption after hexane treatment. Reprinted from R. H. Partridge, "Near-ultraviolet absorption spectrum of polyethylene," *The Journal of Chemical Physics,* vol. 45, no. 5, pp. 1679-1684, 1966, with the permission of John Wiley and Sons.

Figure 3-7 shows that there are two distinct regions in the absorbance spectrum of polyethylene (before hexane treatment):

I.   A single peak centred around 185 nm

II.   A series of small peaks from 193 – 334 nm

Another interesting observation is that the small peaks in region II can be removed if the sample is soaked in hexane for a period of time roughly proportional to the thickness of the sample. One of the materials responsible for the absorption peaks in region II was found to have a carbonyl group. When the sample was exposed to air at room temperature the peaks in region II returned, indicating that they could be formed from the room temperature oxidation of polyethylene.

Partridge suggests that the compounds in region II constitute the sole means through which polyethylene by itself can absorb UV at 254 nm to form crosslinks. This could explain why Oster, Oster and Morrson [19] report a low efficiency of crosslink formation in unsensitized polyethylene. Region I is essentially a single peak centred at about 185 nm. Partridge ascribed this peak to unsaturation in the polymer backbone. The main form of unsaturation in low density polyethylene is of vinylidene type.

When benzophenone is added onto polyethylene, a new peak centred at about 254nm appears in the absorbance spectrum of polyethylene. This is shown in Figure 3-8.
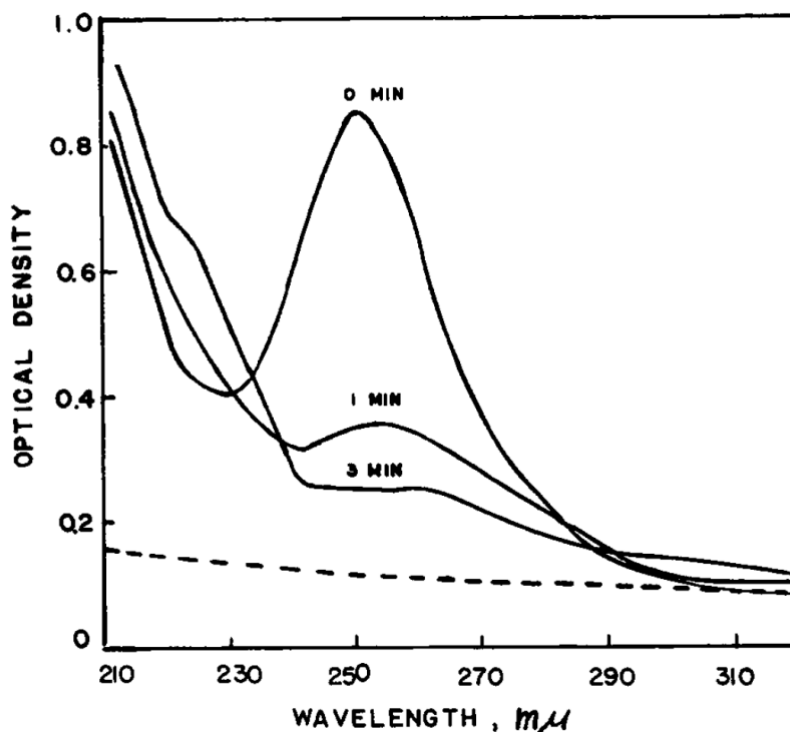
Figure 3-8: Spectral changes in polyethylene photo-sensitized with benzophenone. The initial benzophenone concentration was 0.25%. Dotted line represents unsensitized polyethylene [19].

Reprinted from G. Oster, G. K. Oster and H. Moroson, "Ultraviolet induced crosslinking and grafting of solid high

polymers," *Journal of Polymer Science,* vol. 34, no. 127, pp. 671-684, 1 1959., with the permission of John Wiley and Sons.

Figure 3-8 shows that a sharp peak is present before irradiation. This peak broadens and disappears after about 3 minutes of radiation. This corresponds with the consumption of benzophenone.

Charlesby et al [20] compared the UV absorption spectrum of polyethylene after radiation with the spectrum before radiation. This is shown in Figure 3-9
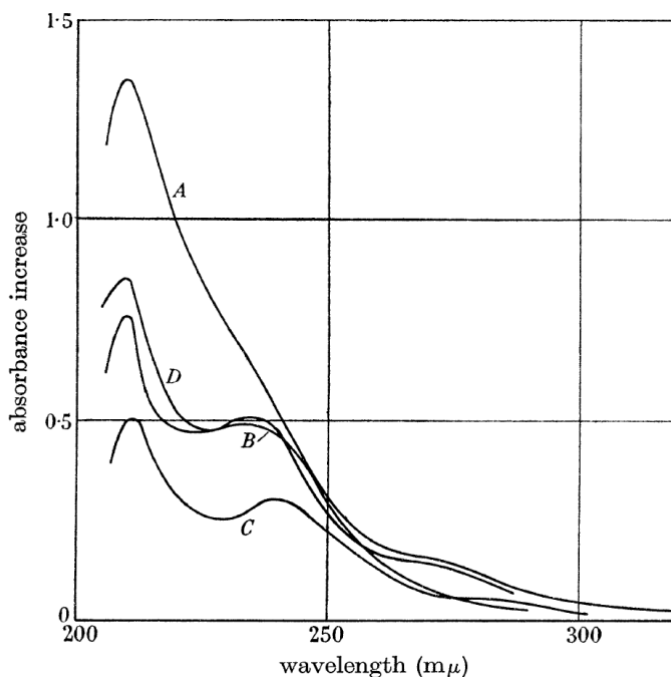
Figure 3-9: Absorbance changes relative to pure materials after irradiation. (A) Polyethylene, 0.002 inches, initial benzophenone content, 0.2; (B), as A, but corrected for absorbance due to benzpinacol;. (C), n-Octane, initial benzophenone content 0.001% irradiated in nitrogen, path length 1.0 cm, corrected for absorbance due to benzpinacol.; (D), Polyethylene, 0.005 in, after 15 Mrads electron radiation in air [20]. Republished with permission of The Royal Society (U.K.), from Proceedings of the Royal Society A, Mathematical, Physical and Engineering Sciences, "Crosslinking of Polyethylene and Paraffins by Ultra-Violet Radiation in the Presence of Sensitizers," A. Charlesby, C. S. Grace and F. B. Pilkington., Volume 268, Issue 1333 Copyright ©; permission conveyed through Copyright Clearance Center, Inc.

The first notable feature in Figure 3-9 is an absorbance peak centred around 215 nm. This is attributed to benzpinacol, a known product of photochemical reactions of benzophenone in alcohols. Benzpinacol is formed when benzophenone abstracts hydrogen from a molecule. The second notable feature is that in each case, the absorbance of the radiated sample is higher than

the unirradiated sample at each wavelength. This suggests that in addition to benzpinacol, there are products of benzophenone reaction with polyethylene which absorb ultraviolet light. This means that polyethylene is "photo-darkening" to ultraviolet light. This phenomenon effectively limits the depth to which cross-linking can occur in an irradiated sample.

The nature of the other photo-reduction products of benzophenone in polyethylene was investigated by Qu et al [22] using a combination of fluorescence spectroscopy, electron spin resonance spectroscopy, 13C and 1H nuclear magnetic resonance spectroscopy. Their results confirmed Charlesby's conclusion that benzpinacol was the main photo-reduction product. Additionally, they identified two new products: an isomer of benzpinacol, 1-phenyl-hydroxymethylene-4-diphenyl-hydroxymethyl-2, 5-cyclohexa-diene and two kinds of α-alkylbenzhydrols. This allowed them to place the mechanism proposed by Charlesby et al on firmer experimental footing. This reaction mechanism is shown in Figure 3-10.
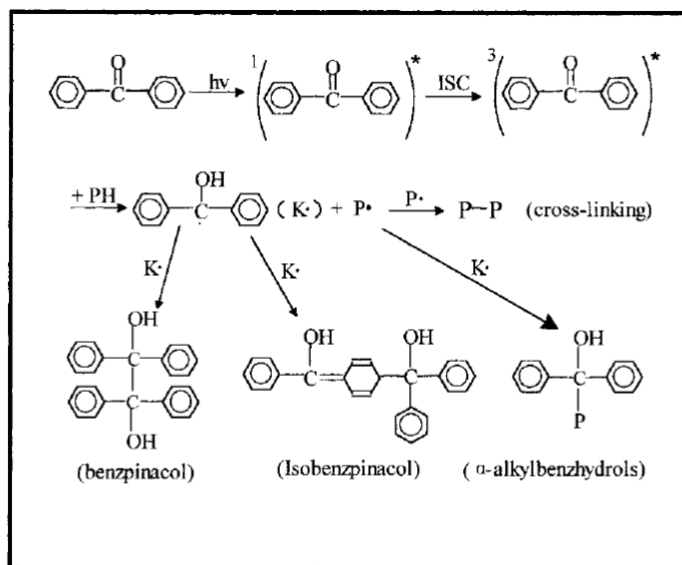
Figure 3-10: Mechanism for benzophenone photo-reduction and crosslink formation in polyethylene. Reprinted from B. Qu, Y. Xu, L. Ding and B. Rånby, "New mechanism of benzophenone photoreduction in photoinitiated crosslinking of polyethylene and its model compounds," *Journal of Polymer Science, Part A: Polymer Chemistry,* vol. 38, no. 6, pp. 999-1005, 15 3 2000, with the permission of John Wiley and Sons.

Figure 3-10 show that when benzophenone absorbs a quantum of radiation, it promotes a valence electron to a higher orbital, thereby attaining an excited singlet state. The singlet state quickly undergoes intersystem crossing to a triplet state. This triplet state is capable of abstracting

hydrogen from a tertiary carbon atom thereby forming a diphenylhydroxymethyl radical (also called a semi-pinacol or ketyl radical). The ketyl radical, K* is able to combine with another ketyl radical to form either benzpinacol or its isomer, isobenzpinacol. Alternatively, it can combine with a polymer radical to form α-alkylbenzhydrol. Finally, adjacent polymer radical can combine, forming a crosslink.

As established by Charlesby [18], the crosslinking reaction occurs in parallel with oxidation reaction. The oxidation reactions in UV irradiated polyethylene have been a subject of intense study because oxidation often leads to the deterioration of important properties of the resin.

Hsu et al [23] suggest that oxygen diffuses into the amorphous layer and reacts with tertiary carbon atoms in the presence of UV light to form polymer alkoxy radicals. These radicals initiate a set of chemical reactions which lead to the formation of several smaller organic molecules. These, according to a study published by Lacoste and Carlsson [24] include:

1. Ketones
2. Alcohols
3. Carboxylic acids
4. Esters

The consequence of these oxidation reactions is the scission of polymer chains and thus a reduction in molecular weight, recrystallization and ultimately a decrease in mechanical properties.

4 EXPERIMENTAL

Materials

The resins used in this work were a linear low-density polyethylene (LLDPE, ExxonMobil LL1001) resin supplied by Ingenia Polymers Corp. and a high-density polyethylene (HDPE, Nova Sclair 19H) resin supplied by Nova Chemicals. The LLDPE had a density of 0.918 g/cm$_3$ and melt index of 0.5 g/10 min at 190°C and load of 2.16 kg while the HDPE had a density of 0.96 g/cm$_3$ and a melt index of 0.38 g/10 min at 190°C and a load of 2.16 kg. Benzophenone (BP), also known as diphenyl ketone, was used as the photosensitizer. It was supplied by Sigma-Aldrich Canada.

Methods

4.1.1 Compounding and Film Production

LLDPE Films

The LLDPE resin was compounded with benzophenone in a 27 mm Leistritz corotating extruder and films were produced using a flat die (10" width, gap 0.015") and a three-roll stack. Various samples were produced using different conditions as shown in Table 4-1.

Table 4-1: Batches of LLDPE prepared

Batch ID	Line Speed (ft/min)	Draw-Down Ratio (DDR)	Benzophenone Concentration (g/min)	Thickness (mm)
PE 1	12	2.8	0	0.24
PE 1A	12	2.8	1.1	0.24
PE 1B	12	2.8	2.2	0.24
PE 2	24	5.6	0	0.22
PE 2A	24	5.6	1.1	0.22
PE 2B	24	5.6	2.2	0.22
PE 3	36	8.4	0	0.19

PE 3A	36	8.4	1.1	0.19
PE 3B	36	8.4	2.2	0.19

HDPE Films

The HDPE samples tested in this work were commercial films produced according to a proprietary method using the Nova 19H HDPE resin and very small amounts of LLDPE. Due to the production method, these films exhibited unusually high elongation, high modulus and high elastic recovery in the machine direction but not in the transverse direction. The films that were tested in this study had a benzophenone concentration of 5 wt. %.

4.1.2 UV Radiation

Films were irradiated using a 1.8 kW CON-TROL-CURE® VersaCure Modular UV System supplied by UV Process Supply, Inc. This system enables the relative intensity of the UV light to be varied from 47% to 99.8% of the maximum intensity. The available lamp set points and the associated light intensity are shown in Table 4-2.

Table 4-2: Set points of modular system and associated relative intensity of UV light

Set Points	Light Intensity (%)
1	47.0
2	51.8
3	56.6
4	61.4
5	66.2
6	71.0
7	75.8
8	80.6
9	85.4
10	90.2
11	95.0
12	99.8

Two 10-inch, medium pressure lamps were used in combination with the modular system to irradiate the films. One lamp was filled with mercury vapour while the other was filled with a

mixture of mercury and lead vapour. The emission spectra of the two lamps are compared in Table 4-3

Table 4-3: Main emission bands of UV lamps used to study the effect of radiation on HDPE and LLDPE films

Lamp type	UVC: 180 – 280 nm	UVB: 280 – 315 nm	UVA: 315 – 380 nm
Mercury vapour	N/A	305	365
Mercury + Lead vapour	217	283	364,368

As it can be seen in Table 4-3, adding lead vapour introduces several changes to the emission spectrum of the mercury lamp. In the UVA region, it introduces a new peak at 368 nm while in the UVB region, it blue shifts the emission peak to 283 nm. Finally, it introduces a peak in the UVC region at 217 nm.

Two different reflector housings were used in this study. One had a ¾ inch ellipse reflector while the other had a parabolic reflector. The ray traces from these reflectors are shown in Figure 4-1.
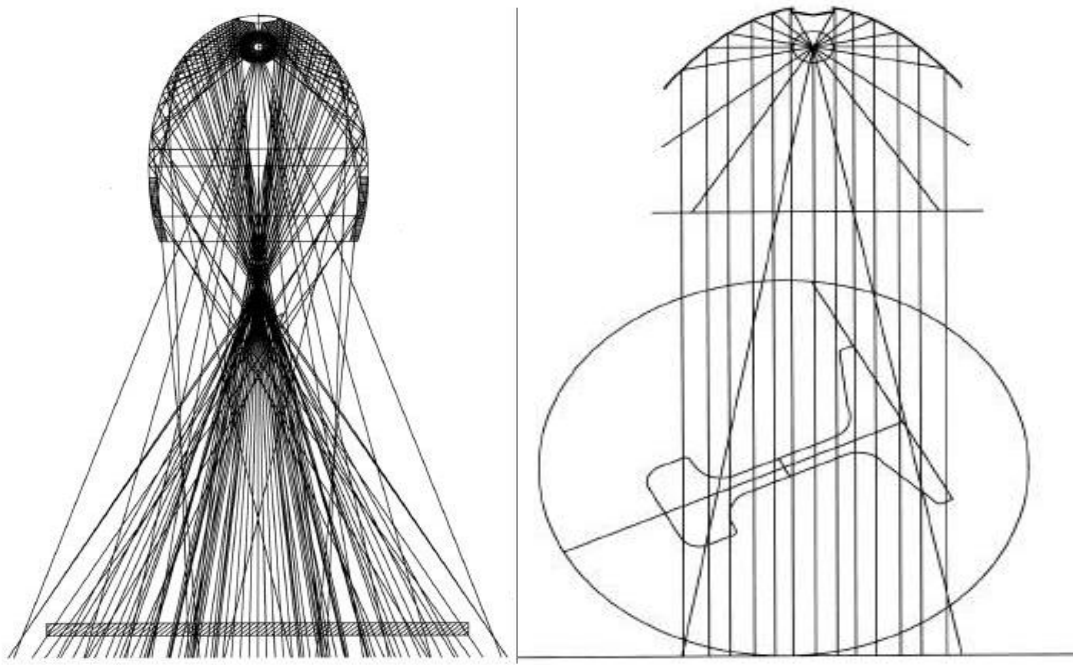
Figure 4-1: Ray traces of Ultraviolet light emerging from 3/4 ellipse (left) and parabolic (right) reflector housing [25]. Reprinted from "*Three-Dimensional Ultra-Violet Curing of Liquid and Powder Coatings*" courtesy of UV Process Supply, Inc, copyright © 2000

The elliptical reflector results in the development of a three-dimensional focal region at a distance of about 10 inches from the top of the housing [25]. This enables solid samples with complex shapes or liquids to be irradiated evenly. However, the drawback of this reflector geometry is that the beam diverges away from the focal region, resulting in some rays hitting the sample at angles less than 90°. This in turn causes the radiation intensity to vary over the surface that is being illuminated. It is highest at the focal region and then decreases further away.

The parabolic reflector eliminates this problem by collimating the rays immediately after they leave the lamp. This results in even illumination intensity over the illuminated surface.

The addition of lead to the mercury increased the intensity of 260 nm peak. The lamps were used to detect the effect of wavelength on the properties of the film. Both of the UV lamps and the reflector housing were supplied by UV Process Supply Inc.

Two perforated steel sheets were used as photomasks to study the effect of changing the illumination pattern on the films. The properties of the screens are listed in Table 4-4.

Table 4-4: Properties of the screens used to change illumination pattern on the film

Property	Screen 1	Screen 2
Hole diameter (inches)	0.0156	0.0330
Centre to centre distance	0.055	0.055
Thickness (inches)	0.0225	0.0225
Orientation of centres	60° staggered centre	Straight line centres

UV irradiation of the films was carried out in a radiation chamber specifically designed to allow the distance between the radiation source and the films to be optimized. An illustration of the chamber is shown in Figure 4-2.

The illumination distance was optimized by studying the development of an illumination pattern when the screens were used. The optimal location was defined as the one at which sharply defined dark and light bands could be seen on a substrate. The distance between the lamp and the screen at which these bands were visible was 47.5 cm.

Figure 4-2: UV radiation chamber.

4.1.3   Mechanical Testing

The modulus of elasticity, ultimate tensile strength and the elongation at break of the films were determined as per ASTM D882 using a tensile testing machine (Instron Co. model 3319, USA). Each of the films was tested in the machine and in the transverse direction. The films were cut using a single blade shear cutter. In accordance with the ASTM standard, the gauge length and

the rate of grip of separation were matched with the ductility of the films. The dimensions used are summarized in Table 4-5.

Table 4-5: Dimensions and rate of grip separation used for tensile testing of films

Sample	Elongation at break	Machine Direction			Transverse Direction		
		Length (mm)	Width (mm)	Rate of Grip separation (mm/min)	Length (mm)	Width (mm)	Rate of Grip Separation (mm/min)
LLDPE films	Greater than 100%	50	20	500	50	20	500
HDPE films	between 20% and 100 %	100	20	50	125	20	12.5

Since the films exhibited a tendency to fail at the grips, two layers of pressure sensitive tape were applied onto the grips so as to increase the radius of curvature of the edges where the grips come into contact with the test area of the specimens.

4.1.4   Puncture-Propagation Tear Resistance testing

The puncture -propagation tear resistance of HDPE films was determined according ASTM D2582. Rectangular specimens, each measuring 200 mm were cut from the films for testing. These samples were then clamped onto a tear testing machine supplied by Testing Machines Inc. The tear resistance was determined by dropping a weighted carriage fitted with an alignment marker from a height of 508 mm and measuring the tear length to the nearest 0.5 mm. Five tear tests were performed for each film specimen and the results averaged.

4.1.5   Rheological Testing

A parallel plate viscometer (AR2000, TA Instruments, USA) was used to study the linear viscoelastic properties of the irradiated polyethylene films. During strain sweep, a range of 0.1 – 100% strain at a frequency of 6.28 rad/s was used. During frequency sweep a strain of 0.5% with a frequency range of 0.01 – 100 Hz was used. Both tests were run at a temperature of 180°C.

For the LLDPE films, samples for rheological testing were cut directly from the irradiated films using a hydraulic press and a 25 mm die. For the HDPE films, three samples, each measuring 5cm x 5cm were first cut from the irradiated films and pressed together in a Carver laboratory compress machine set at 180°C and 10,000 pounds ram force for 5 minutes. This was done in order to relieve the residual stresses in these films. It was observed that the moulding method used to prepare these films induced a high degree of residual stress. This residual stress caused the films to shrivel when they came into contact with the surface of the rheometer. After pressing these films, samples for rheological testing were cut using a hydraulic press and a 25 mm die.

4.1.6 Design of Irradiation Experiments

For the LLDPE samples a fully replicated 2-level factorial design was implemented to test the effect of line speed, benzophenone concentration, illumination pattern and intensity on the modulus of elasticity of the films. The levels of the design are shown in Table 4-6.

Table 4-6: Factors and levels used in design of experiments

Factor	Low Level	High Level
Radiation Intensity (A)	47%	99.8%
Radiation time (B)	30 sec	180 sec
Screen (C)	Screen OFF	Screen 2
Benzophenone Concentration (D)	0 g/min	2.2 g/min
Line Speed (E)	12	24

For the HDPE samples, the levels of the factorial design are shown in Table 4-7.

Table 4-7: Design levels for the factorial design on the HDPE samples

Factor	Code	Low level	High Level
Concentration of HDPE (%)	A	95	100
Degree of Stretch	B	Low (Precursor)	High (Stretched)
Screen	C	OFF/Screen 1	Screen 2
Radiation time (sec)	D	30	120
Radiation Intensity (%)	E	47	99.8

5 RESULTS AND DISCUSSION

A study on the effect of compounding and radiation conditions on the tensile properties of LLDPE films

5.1.1 Introduction

A factor screening test was performed to examine how the compounding variables (line speed and benzophenone concentration) interact with the radiation treatment variables (radiation intensity, radiation time and illumination pattern). The objective of this study is to determine an optimum setting for the compounding variables at which an exhaustive investigation of the effect of the radiation variables on the mechanical and rheological properties of the films can be undertaken.

The tensile properties that were examined in this study are the elastic modulus, and the tensile stress at break. The elastic modulus is a measure of the stiffness of the film while the stress at break is a measure of the overall loading that the material can withstand before rupture. Taken together, these tensile parameters indicate the mechanical conditions under which the film can be used effectively.

For the factor screening tests, the elastic modulus and the tensile stress at break in the machine direction were studied; however, during subsequent tests, all tensile properties were studied in both the machine and transverse direction.

The effects and significance levels of the radiation and compounding variables on the elastic modulus are listed in Table 5-1 .

Table 5-1: Effects and P-values of radiation and compounding variables on the elastic modulus of LLDPE films

Factor	Effect (MPa)	F_0	P-value	90% confidence interval
A	8.76	2.76	0.11	8.82
B	-5.49	1.08	0.31	8.82
C	-6.63	1.58	0.22	8.82
D	-0.34	0.00	0.95	8.82
E	-95.49	327.54	0.00	8.82
AB	-5.75	1.19	0.28	8.82
AC	-11.26	4.56	0.04	8.82
BC	3.81	0.52	0.48	8.82
AD	6.91	1.72	0.20	8.82
BD	2.86	0.29	0.59	8.82
CD	-3.51	0.44	0.51	8.82
AE	-9.66	3.35	0.08	8.82
BE	1.49	0.08	0.78	8.82
CE	5.11	0.94	0.34	8.82
DE	-6.35	1.45	0.24	8.82
ABC	6.95	1.73	0.20	8.82
ABD	-3.14	0.35	0.56	8.82
ACD	-4.73	0.80	0.38	8.82
BCD	7.76	2.16	0.15	8.82
ABE	7.80	2.19	0.15	8.82
BCE	-5.66	1.15	0.29	8.82
ADE	-7.09	1.81	0.19	8.82
BDE	-1.05	0.04	0.84	8.82
CDE	2.35	0.20	0.66	8.82
ABCD	4.01	0.58	0.45	8.82
ABCE	-4.54	0.74	0.40	8.82
ABDE	1.73	0.11	0.74	8.82
ACDE	1.95	0.14	0.71	8.82
BCDE	-6.76	1.64	0.21	8.82
ABCDE	1.40	0.07	0.79	8.82

Table 5-1 indicates that the most significant process condition is the line speed, E with an effect of -95.49 MPa and a p-value of 1.06×10^{-18}. This p-value indicates that this effect is significant at a confidence level higher than 99%. The negative value of the effect indicates that increasing the line speed decreases the modulus of the film as shown in Figure 5-1. This makes sense since higher line speeds (and DDR) impart higher molecular orientation during film manufacturing and therefore there is less room for stretching during subsequent processing (as in the tensile testing experiment).
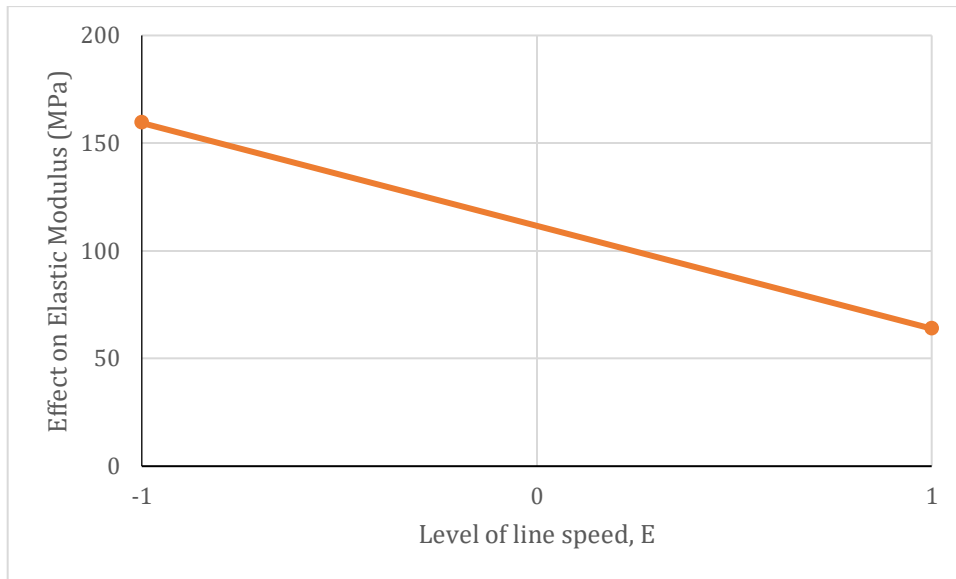
Figure 5-1: Effect of the line speed on the average modulus of the films

Figure 5-1 shows that increasing the line speed from the low level to the high level cause the average modulus to drop by 95.49 MPa. This indicates that the film undergoes a significant reduction in stiffness as a result of increasing the line speed.

Table 5-1 also indicates that the interaction of the screen and the radiation intensity is significant. The effect of this interaction is -11.26 MPa. It is the second most significant factor after the line speed with a p-value of 0.04. The marginal means plot for this interaction is shown in Figure 5-2.
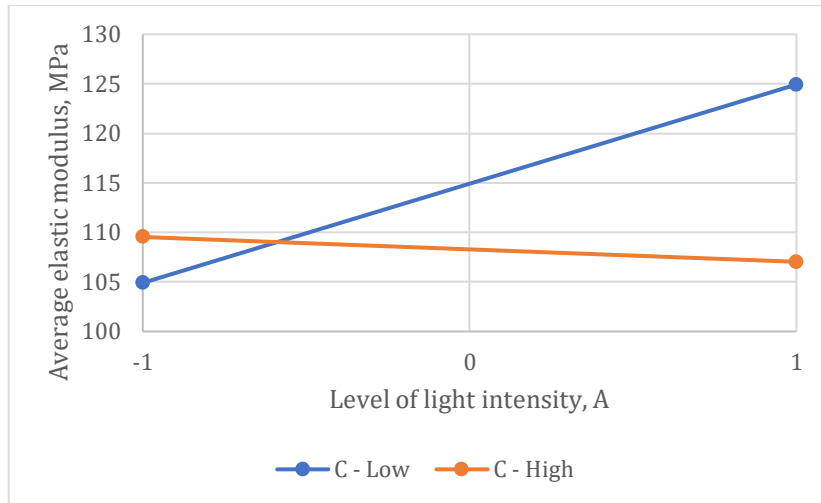
Figure 5-2: Marginal means plot showing the effect of the interaction between light intensity (A) and the screen (C) on the average elastic modulus

Figure 5-2 shows that the effect of the screen is dependent on the level of light intensity. When the screen is present, increasing the light intensity causes the elastic modulus to decrease from 109.54 MPa to 107.03 MPa. When the screen is not present, increasing the intensity causes the average elastic modulus to increase from 104.91 MPa to 124.93 MPa.

The final significant parameter is the interaction between light intensity and line speed. The effect of this interaction is -9.66 MPa and it has a P-value of 0.08, indicating that it is significant at the 10% significance level but not at the 5% significance level. The marginal means plot for this interaction is shown in Figure 5-3.
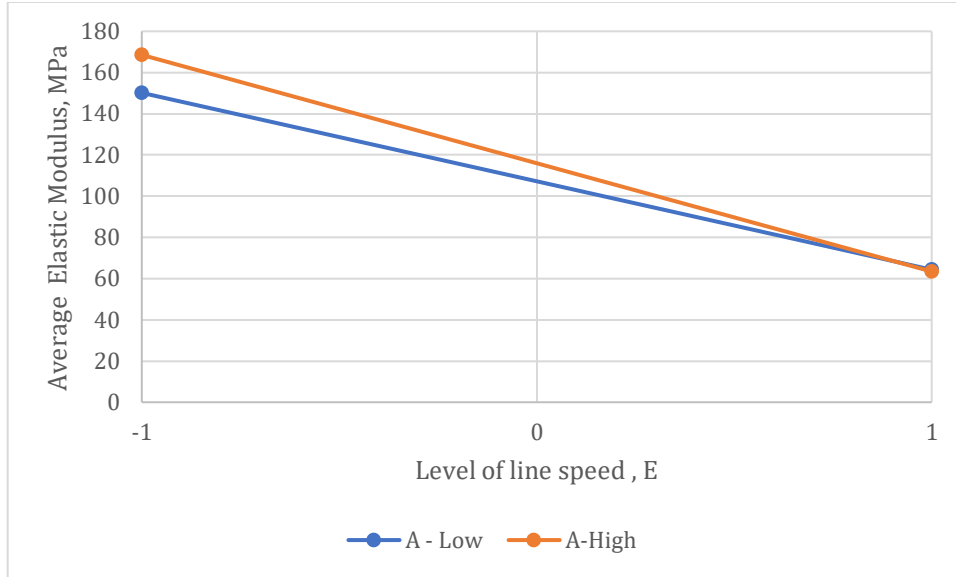
Figure 5-3: Marginal means plot showing the interaction between light intensity (A) and line speed (E) on the average modulus of elasticity

Figure 5-3 indicates that regardless of the level of the light intensity, increasing the line speed from the low level to the high level causes the average elastic modulus to decrease. Moreover, at the high level of line speed, the average modulus is the same for both levels of light intensity. The effect of radiation intensity is more significant at the low level of line speed, with the highest modulus occurring when radiation intensity is high.

The effects listed in Table 5-1 were used to construct an empirical model describing the effect of processing and radiation on the elastic modulus of the LLDPE samples. The model is shown in Equation 3.

$$\hat{y}_i = \hat{\beta}_0 + \widehat{\beta_E} x_E + \widehat{\beta_{AC}} x_{AC} + \widehat{\beta_{AE}} x_{AE}$$

Equation 3: Model describing effects of processing and radiation on modulus of LLDPE films

Table 5-2: Values of parameters in equation describing effects of compounding and radiation variables on elastic modulus

Model terms	Value (MPa)
β_0	111.60
β_E	-47.75
β_{AC}	-5.63
β_{AE}	-4.83

The ANOVA table for this model is shown in Table 5-3 and Table 5-4.

Table 5-3: ANOVA for regression model for effect of compounding and radiation parameters on elastic modulus of LLDPE films

Source	Sum of Squares	Degrees of Freedom	Mean Square	F_0	P-value
Model	149,428.21	3	49,809.40	111.82	2.30E-17
E	145,907.09	1	145,907.09	327.54	1.06E-18
AC	2,029.34	1	2,029.34	4.56	0.04
AE	1,491.78	1	1,491.78	3.35	0.08
Residual	26,175.27	60	436.25	0.98	
Lack of Fit	11,475.12	27	425.00	0.95	0.545626841
Pure Error	14,700.14	33	445.46		
Total	175,603.48	63	2,787.36		

Table 5-4: Adequacy diagnostic checks for regression model describing effect of processing and radiation conditions on modulus of LLDPE films

Diagnostic	Value
R^2	0.8509
R^2_{adj}	0.8435
PRESS	34,188.11
R^2_{pred}	0.8053

Table 5-3 illustrates that the model as a whole has a p-value of 2.30×10^{-17} indicating that it would pass a confidence test conducted at the 99% significance level. Furthermore, Table 5-4

indicates that the model accounts for about 85% of the variability in the data. This value decreases to 84% when the coefficient of determination is adjusted for the number of parameters in the model. Finally, Table 5-4 indicates that the model could account for 80% of the variability in new data in the range within which the experiment was conducted. Taken as a whole, these diagnostics show that the model provides a good description of the effect of the compounding and radiation variables on the elastic modulus of the films.

For the tensile stress, radiation treatments were carried out at 100% relative light intensity. The effects of the remaining radiation and compounding variables on the stress at break are listed in Table 5-5.

Table 5-5: Effects and p-values of radiation and compounding variables on the stress at break of LLDPE films.

Factor	Effect (MPa)	F_0	P-value	95% Confidence Interval
B	0.097		-	1.79
C	-0.114		-	1.79
D	0.253		-	1.79
E	-2.948	437.78	8.23×10^{-11}	1.79
BC	0.005		-	1.79
BD	0.235		-	1.79
CD	0.127		-	1.79
BE	0.190		-	1.79
CE	-0.028		-	1.79
DE	-0.573	16.53	1.57×10^{-3}	1.79
BCD	-0.095		-	1.79
BCE	-0.114		-	1.79
BDE	-0.148		-	1.79
CDE	-0.347	6.07	0.03	1.79
BCDE	0.004		-	1.79

Since this experiment was not fully replicated, a normal probability plot (Figure 5-4) was used to determine which effects are least likely to be statistically significant.

41
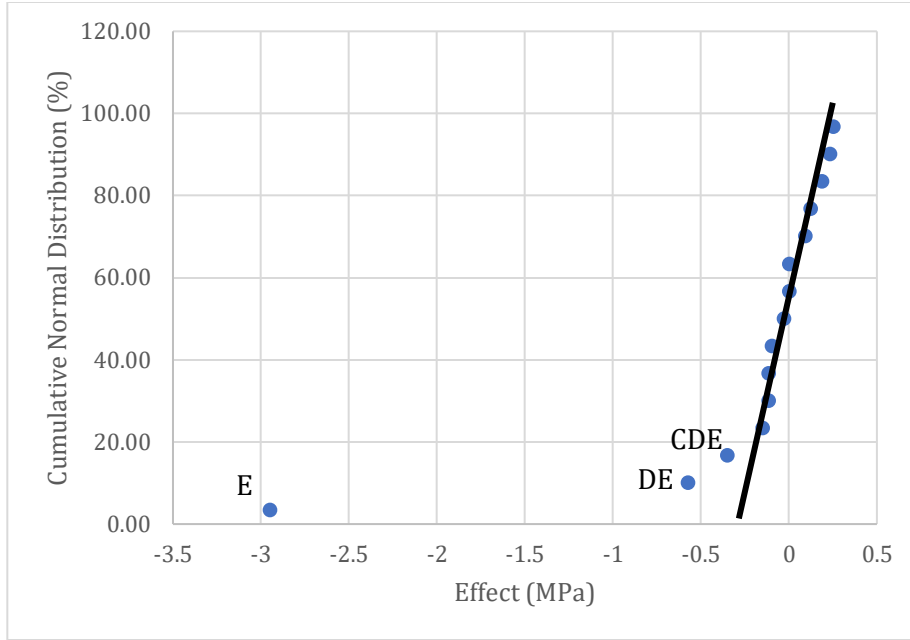
Figure 5-4: Normal probability plot of effects of radiation and compounding variables on the tensile stress at break.

Figure 5-4 shows that the majority of the effects lie along a straight line, showing that they follow a normal distribution. The only factors which deviate significantly from the distribution are the line speed (E), the interaction between the line speed and the concentration of benzophenone (DE) and the interaction between the illumination pattern, benzophenone concentration and line speed (CDE). The sum of squares of the other factors were pooled and used as an estimate of the error sum of squares. This value was then used to compute p-values for the three significant variables.

The effect of line speed on the stress at break is similar to its effect on the elastic modulus. The effect of line speed is -2.95 MPa with a p-level of 8.23×10^{-11} MPa. The marginal means plot for this factor shown in Figure 5-5 indicates that increasing this factor from the low level to the high level causes the average tensile stress at break to drop by 2.95 MPa.

42
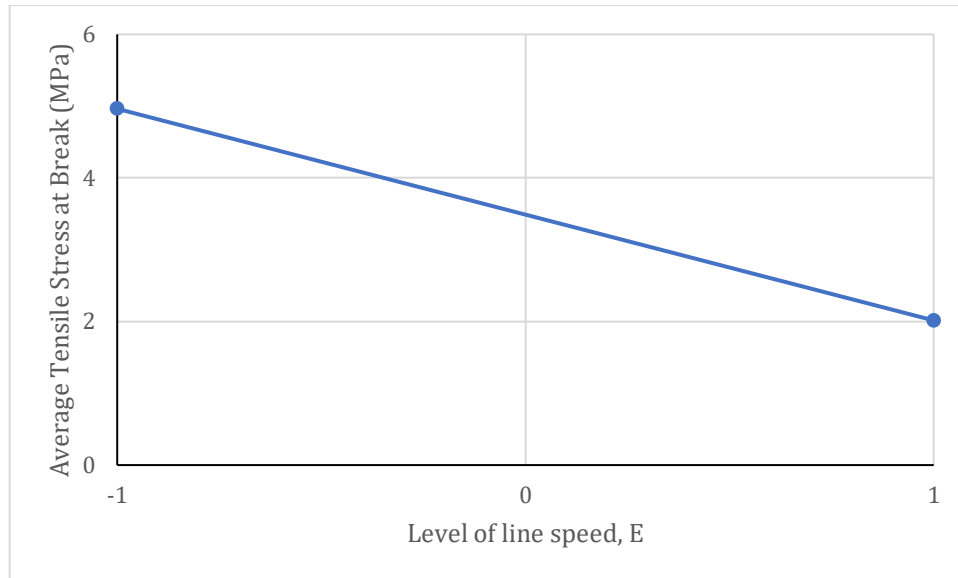
Figure 5-5: Marginal means plot showing the effect of line speed, E on the average tensile strength of LLDPE films

After line speed, the next most significant factor is the interaction between benzophenone concentration and the line speed. The effect of this interaction is -0.57 MPa and it has a p-value of 1.57×10^{-3}; indicating that it is significant at both the 95% and 99% confidence levels. This interaction can be better understood by looking at Figure 5-6.
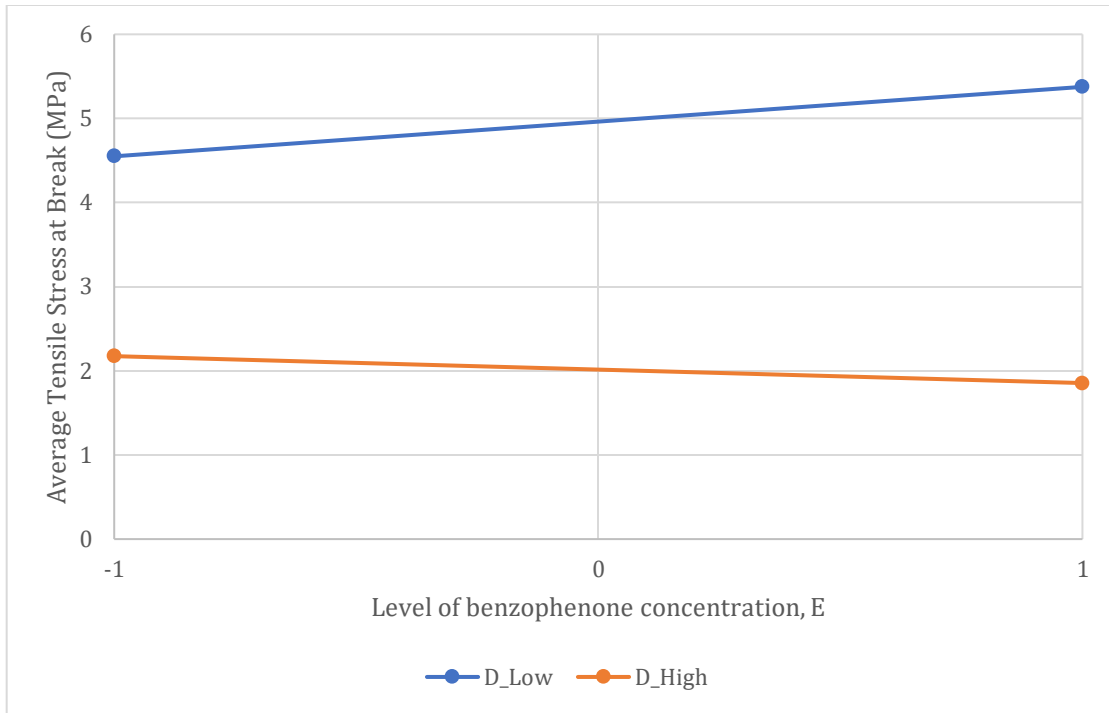
Figure 5-6: Marginal means plot illustrating the effect of the interaction between line speed, (E) and the benzophenone concentration, D on the average tensile stress at break.

Figure 5-6 indicates that at both the low and high levels of benzophenone concentration, increasing line speed causes the average tensile stress at break to decrease. However, at low line speed, increasing the benzophenone concentration causes the average tensile stress at break to increase. At high line speed, increasing the benzophenone concentration causes the average tensile stress at break to decrease.

Table 5-5 also indicates that the effect of the interaction between line speed, benzophenone concentration and the screen is -0.35 at a P-value of 0.0325. This means that it is significant at the 95% and the 90% confidence levels.

The effects listed in Table 5-5 were used to construct a model (Equation 4) to describe the effect of processing and radiation on the tensile stress at break of LLDPE films.

$$\hat{y}_i = \hat{\beta}_0 + \hat{\beta}_C x_C + \hat{\beta}_{BC} x_{BC} + \hat{\beta}_{ABC} x_{ABC}$$

Equation 4: Effect of processing and radiation on the tensile stress at break

The ANOVA table for this model is shown in Table 5-6 while the model diagnostics are listed in Table 5-7.

44

Table 5-6: ANOVA Table for effects model for tensile stress at break

Source	Sum of Squares	Degrees of Freedom	Mean Square	F_0	P-value
Model	36.55	3	12.18	168.57	1.44E-07
E	34.76	1	34.76	480.90	1.97E-08
DE	1.31	1	1.31	18.16	0.0028
CDE	0.48	1	0.48	6.67	0.0325
Residual	0.95	12	0.08	-	-
Lack of Fit	0.37	4	0.09	1.30	0.349
Pure Error	0.58	8	0.07	-	
Total	37.50681	15	2.50		

Table 5-7: Diagnostic checks on effects model for the tensile stress at break

Diagnostic	Value
R^2	0.9746
R^2_{adj}	0.9711
PRESS	3.81
R^2_{pred}	0.8984

Table 5-6 indicates that the p-value of the model is 1.44×10^{-7}. It also indicates that the p-value of the lack of fit is 0.349. This indicates that the lack of fit is statistically insignificant.

This conclusion is complemented by model diagnostics listed in Table 5-7. The coefficient of variation for the model is 0.9746. This indicates that the model explains 97% of the variability in the experimental data. This value drops by only 0.3% when the coefficient of variation is adjusted for the number of parameters in the model. Finally, the model would predict almost 90% of variability in new data.

Taken together, the diagnostics in Table 5-7 provide strong evidence that variations in the tensile stress at break can be understood as being caused by variations in the line speed, in the interaction between line speed and benzophenone concentration and in the interaction between line speed, benzophenone concentration and the illumination pattern.

5.1.2 Conclusion

The purpose of the factor screening test was to investigate how the processing variables (line speed and benzophenone concentration) affect the mechanical properties of the films and how they interact with the radiation variables (radiation intensity, radiation time and illumination pattern).

The results indicate that the most significant factor affecting the mechanical performance of the LLDPE films is the line speed. In general, increasing line speed causes the tensile properties of the film to decrease. The amount of decrease is dependent on the tensile property being examined. The modulus of elasticity drops by 95 MPa while the tensile stress at break drops by 2.95 MPa.

Furthermore, the tests show that while there is significant interaction between the processing variables and the radiation variables, the effect of this interaction is dependent on the tensile property being examined. These differences are summarized below:

1. The effect of the interaction between line speed and benzophenone concentration on the elastic modulus is statistically insignificant while on the tensile stress at break it is -0.57 MPa

2. The effect of the interaction between line speed and radiation intensity on the elastic modulus is -11.26 MPa while its effect on the tensile stress at break is statistically insignificant

3. The effect of the interaction between radiation intensity and illumination pattern (screen) on the elastic modulus is -9.66 MPa.

4. The effect of the interaction between line speed, benzophenone concentration and illumination pattern on the elastic modulus is statistically insignificant while its effect on the tensile stress at break is -0.35 MPa.

5. Finally, the factor screening test suggests that the optimum compounding settings at which to study the effect of radiation are the low level of line speed and the high level of benzophenone concentration. The resin corresponding to this setting is PE 1B. The following section will report on the results of carrying out an exhaustive mechanical and rheological analysis of this resin at different radiation conditions.

Study of the effect of radiation treatment variables on the mechanical and rheological properties of LLDPE films

5.1.3 Mechanical Properties

The factor screening experiment suggested that the best setting to run further experiments was low line speed and high benzophenone concentration. This section reports on the effect of the radiation treatment variables (radiation intensity [A], radiation time [B] and illumination pattern [C]) on the mechanical properties of the LLDPE films. The mechanical properties considered in this study include the modulus of elasticity, the stress at yield, the ultimate tensile stress and the tensile strain at break. Each of these properties was studied in the machine and in the transverse direction of the films.

The effects as well significance levels of each of the radiation parameters on the elastic modulus are listed in Table 5-8.

Table 5-8: Effects and P-values of factors influencing modulus of elasticity of LLDPE films in machine direction and transverse direction

Factors	Machine Direction			Transverse Direction		
	Effect (MPa)	95% Confidence Interval	p-value	Effect (MPa)	95% Confidence Interval	p-value
A	22.32	32.15	0.07	45.45	26.97	0.004
B	-12.41	32.15	0.29	7.06	26.97	0.56
C	-15.50	32.15	0.19	-29.12	26.97	0.04
AB	-12.73	32.15	0.28	11.65	26.97	0.35
AC	21.76	32.15	0.07	-17.16	26.97	0.18
BC	4.73	32.15	0.68	2.76	26.97	0.82
ABC	15.20	32.15	0.20	-1.78	26.97	0.88

Table 5-8 indicates that in the machine direction only the radiation intensity and the interaction between intensity and illumination pattern (screen) are significant below a 10% significance level. In the transverse direction only the radiation intensity and the screen are statistically significant.

Furthermore, Table 5-8 reveals that while the radiation intensity and the screen affect the films in qualitatively similar manner, the magnitude of the effect is different in each case. In the machine direction, radiation intensity has an effect of 22.32 MPa while in the transverse direction; it has an effect of 45.45 MPa. Similarly, in the machine direction, the effect of the screen is -15.50 MPa while in the transverse direction, it is -29.12 MPa.

Marginal means plots for the effect of radiation intensity and for the interaction between intensity and the screen on the elastic modulus in the machine direction are presented in Figure 5-7.
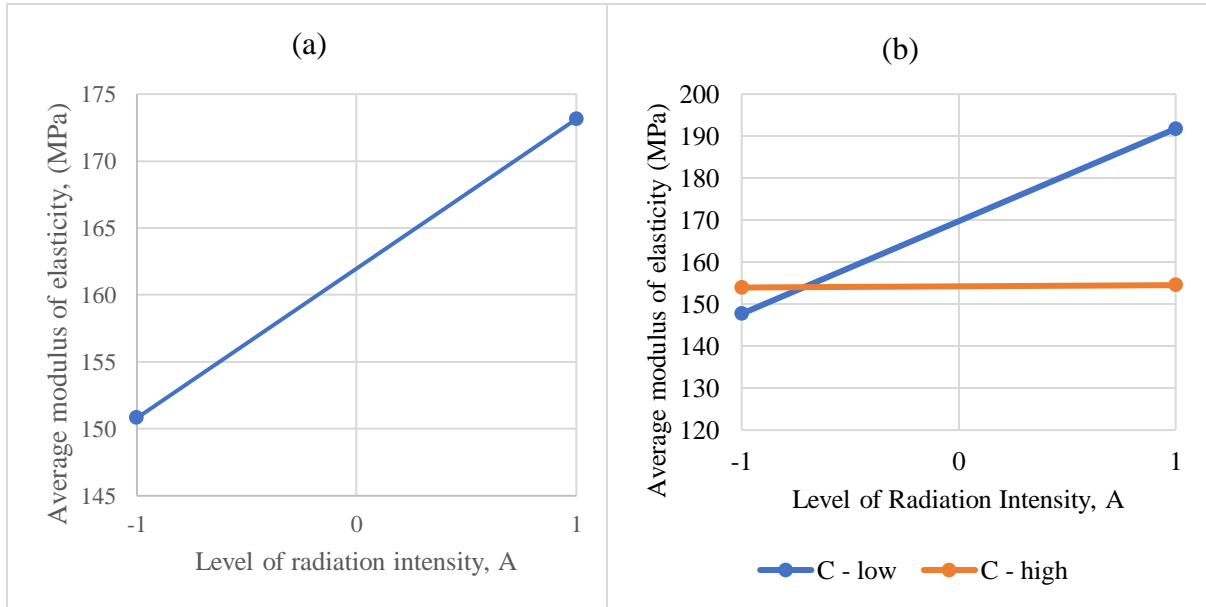
Figure 5-7: Marginal means plot showing the main factors and interactions affecting the elastic modulus in the machine direction.

Figure 5-7 (a) shows that increasing the level of radiation intensity causes the average modulus of elasticity to increase from 150.81 MPa to 173.14 MPa. Figure 5-7 (b) shows that the effect of the screen is quite sensitive to the level of radiation intensity. When the screen is absent (C-low), increasing the intensity causes the average modulus of elasticity to increase by 44.08 MPa. When the screen is present (C-High), increasing the radiation intensity has a negligible (less than 1MPa increase) effect on the modulus of elasticity in the longitudinal direction.

Figure 5-8 presents the marginal means plots for the effects of radiation intensity and the screen on the average modulus of elasticity in the transverse direction.

49
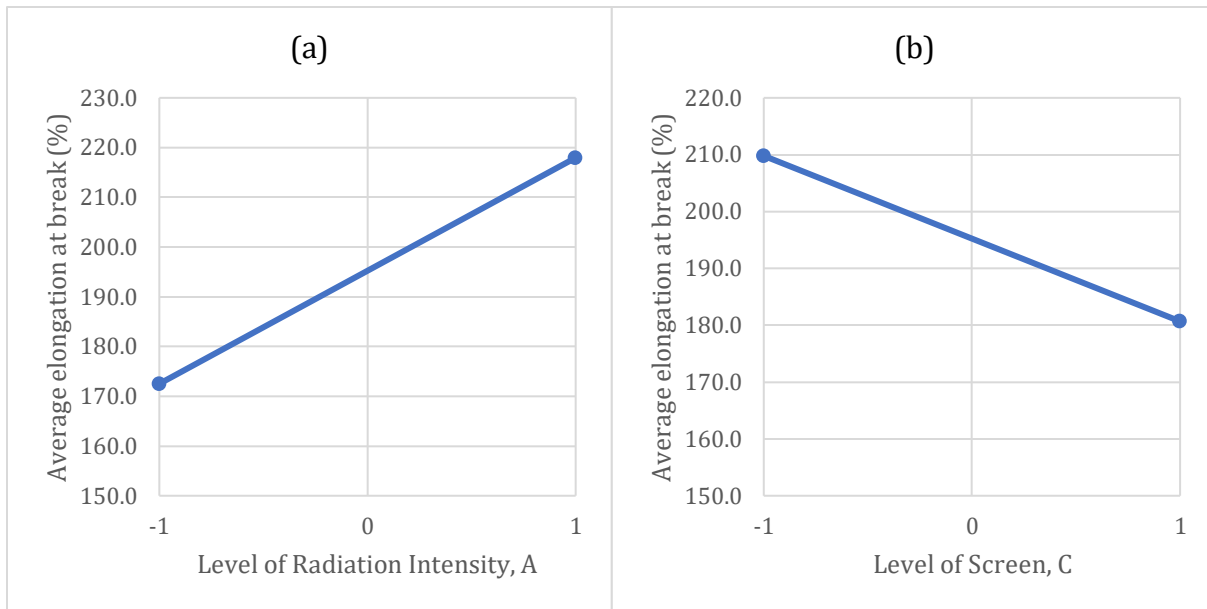
Figure 5-8: Marginal means plots showing the main factors and interactions affecting the average elastic modulus of LLDPE films in the transverse direction

Figure 5-8 (a) indicates that increasing the level of radiation intensity causes the average modulus of elasticity in the transverse direction to increase from 172.51 MPa to 217.96 MPa while Figure 5-8 (b) indicates that increasing the level of the screen causes the average modulus of elasticity to decrease from 209.79 MPa to 180.68 MPa.

In addition to illustrating the effect of radiation intensity and illumination pattern as processing variables, Figure 5-7 and Figure 5-8 suggest that these two variables give rise to different, but perhaps related structures in the films. The effect of radiation alone is to increase the stiffness of the material, an effect that has been associated with crosslinking [26], [27].

When the screen is introduced, the illumination incident on the films changes from uniformly bright to a series of alternating bring and dark bands. A sketch of the illumination pattern is shown in Figure 5-9.
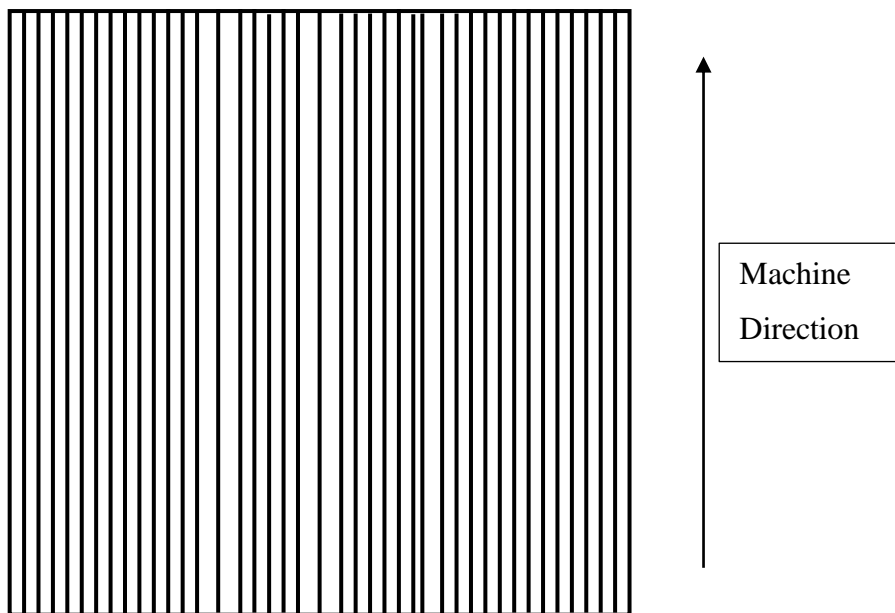
Figure 5-9: Sketch of illumination pattern on sample surface when irradiation is carried out under a screen.

The effect of this pattern could be to further constrain the location of crosslinking events by limiting the sites on the film where the reaction can occur. This could potentially lead to a pattern of crosslinks forming on the film which decrease the stiffness of the material overall. Evidence of this possibility shall be explored in the section dedicated to the rheology of the films.

While the elastic modulus is a measure of the stiffness of a material, the stress at yield is an indication of the maximum load that a material can withstand before permanent deformation begins. The effects of the radiation variables on the tensile stress at yield of the LLDPE films are listed in Table 5-9.

Table 5-9: Effects and significance levels of radiation variables on the tensile stress at yield of LLDPE films in both the machine and transverse direction

Factor	Machine Direction			Transverse direction		
	Effect (MPa)	95% Confidence Interval	p-value	Effect (MPa)	95% Confidence Interval	p-value
A	0.64	0.62	0.04	1.61	0.77	0.001
B	-0.71	0.62	0.03	0.44	0.77	0.23
C	-0.10	0.62	0.73	-0.77	0.77	0.05
AB	-0.66	0.62	0.04	0.22	0.77	0.54
AC	-1.13	0.62	0.003	-0.79	0.77	0.05
BC	-0.05	0.62	0.87	-0.14	0.77	0.69
ABC	0.27	0.62	0.34	-0.18	0.77	0.61

Table 5-9 shows that the effect of the radiation variables on the yield stress is dependent on the orientation of the film. In the machine direction, the radiation intensity has a positive effect while radiation time and the screen have negative effects. In the transverse direction, the radiation time and intensity have positive effects while the screen has a negative effect. Furthermore, in the machine direction, the radiation time and intensity have effects which are significant at the 5% significance level while the screen does not. In the transverse direction, it is the radiation intensity and the screen that are significant at the 5% significance level while the effect of the radiation time is not statistically significant.

Figure 5-10 shows the marginal means plots for those factors and interactions whose effects on the yield stress in the machine direction are statistically significant.
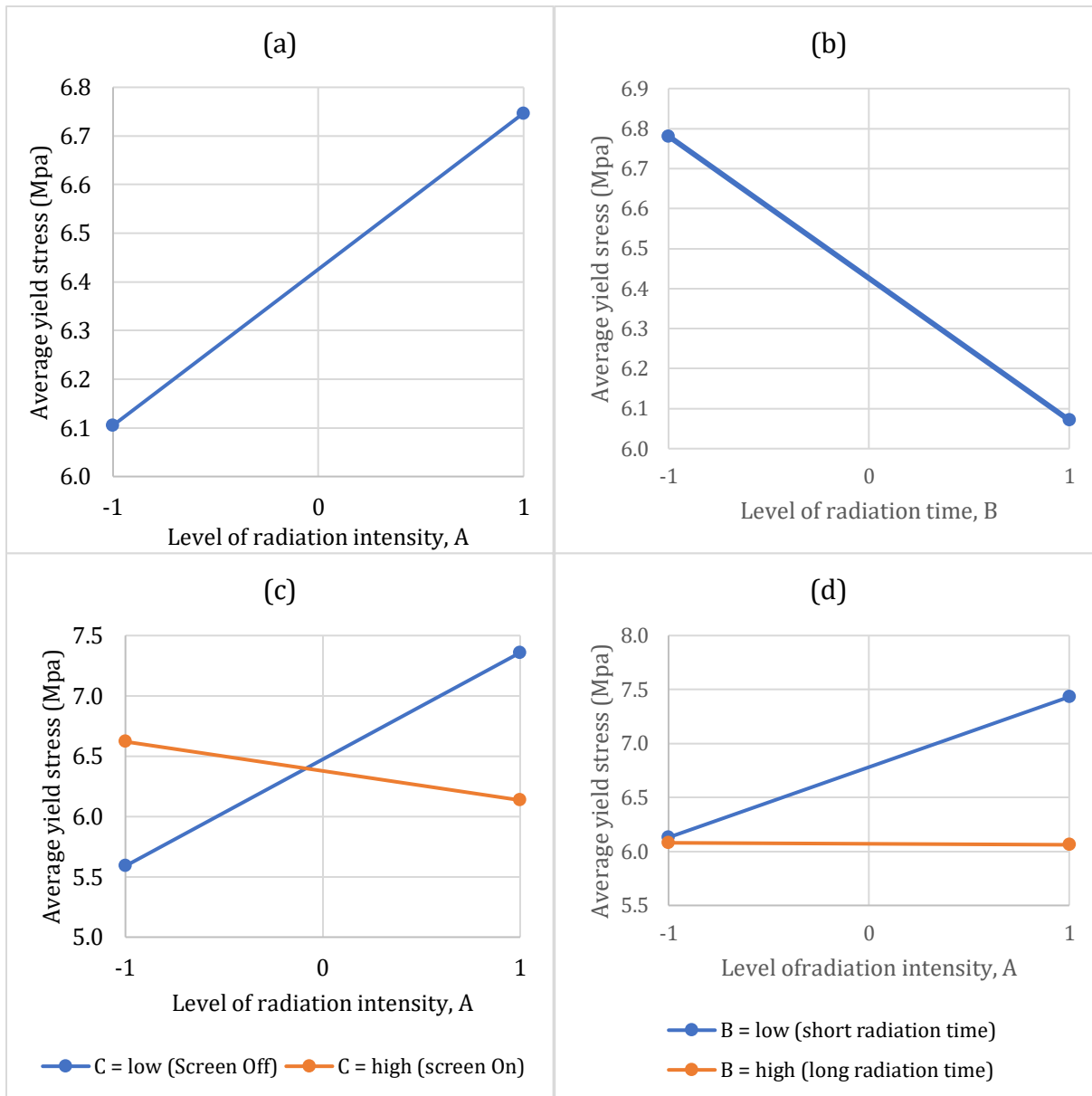
Figure 5-10: Marginal means plots showing effects of radiation variables on the yield stress in the machine direction of LLDPE films

Figure 5-10 shows that increasing radiation intensity causes the average yield stress in the machine direction to increase from 6.11 MPa to 6.75 MPa while increasing the level of the radiation time causes it to decrease from 6.78 MPa to 6.07 MPa. Furthermore, Figure 5-10 (c) shows that the effect of the screen is dependent on the level of radiation intensity. When the level of radiation intensity is low, increasing the level of the screen causes the average yield stress to increase from 5.59 MPa to 6.62 MPa. When the level of radiation intensity is at the high level,

increasing the level of the screen causes the average yield stress to decrease from 7.36 MPa to 6.14 MPa.

While the results presented in Table 5-9 and in Figure 5-10 (b) show that the radiation time has a significant negative effect on the yield stress, Figure 5-10 (d) reveals that the effect of radiation time is actually affected by the level of the radiation intensity. When the radiation time is at the high level, changing the radiation intensity has negligible effect on the average yield stress; however, when the radiation time is at the low level, increasing the level of radiation intensity causes the average yield stress to increase from 6.08 MPa to 7.43 MPa.

Figure 5-11 present marginal means plots for the significant factors and interactions affecting the yield stress in the transverse direction. Figure 5-11 (a) shows that increasing the radiation intensity causes the average yield stress in the transverse direction to increase from 7.60 MPa to 9.22 MPa while Figure 5-11 (b) shows that increasing the level of the screen causes the average yield stress to decrease from 8.79 MPa to 8.02 MPa.

Figure 5-11 (c) provides more insight into the effect of the interaction between the screen and the radiation intensity. In general, it shows that increasing the level of intensity causes the average yield stress to increase, regardless of the level of the screen. This observation is consistent with the results reported in Figure 5-11(a). Nevertheless, Figure 5-11 (c) reveals that when the level of radiation intensity increases from the low level to the high level, the average yield stress increases more rapidly at the low level of the screen than at the high level of the screen. Furthermore, at the high level of radiation intensity, the average yield stress is higher when the screen is at the low level than at the high level.

Since the low level of the screen corresponds to a situation where the screen is absent, the results presented in Figure 5-11 (b) an (c) both suggest that changing the illumination pattern incident on the films causes a change that is different in kind from the effect of radiation intensity by itself. In this case, increasing the radiation intensity causes the yield stress to increase while changing the illumination pattern causes the yield stress to decrease.
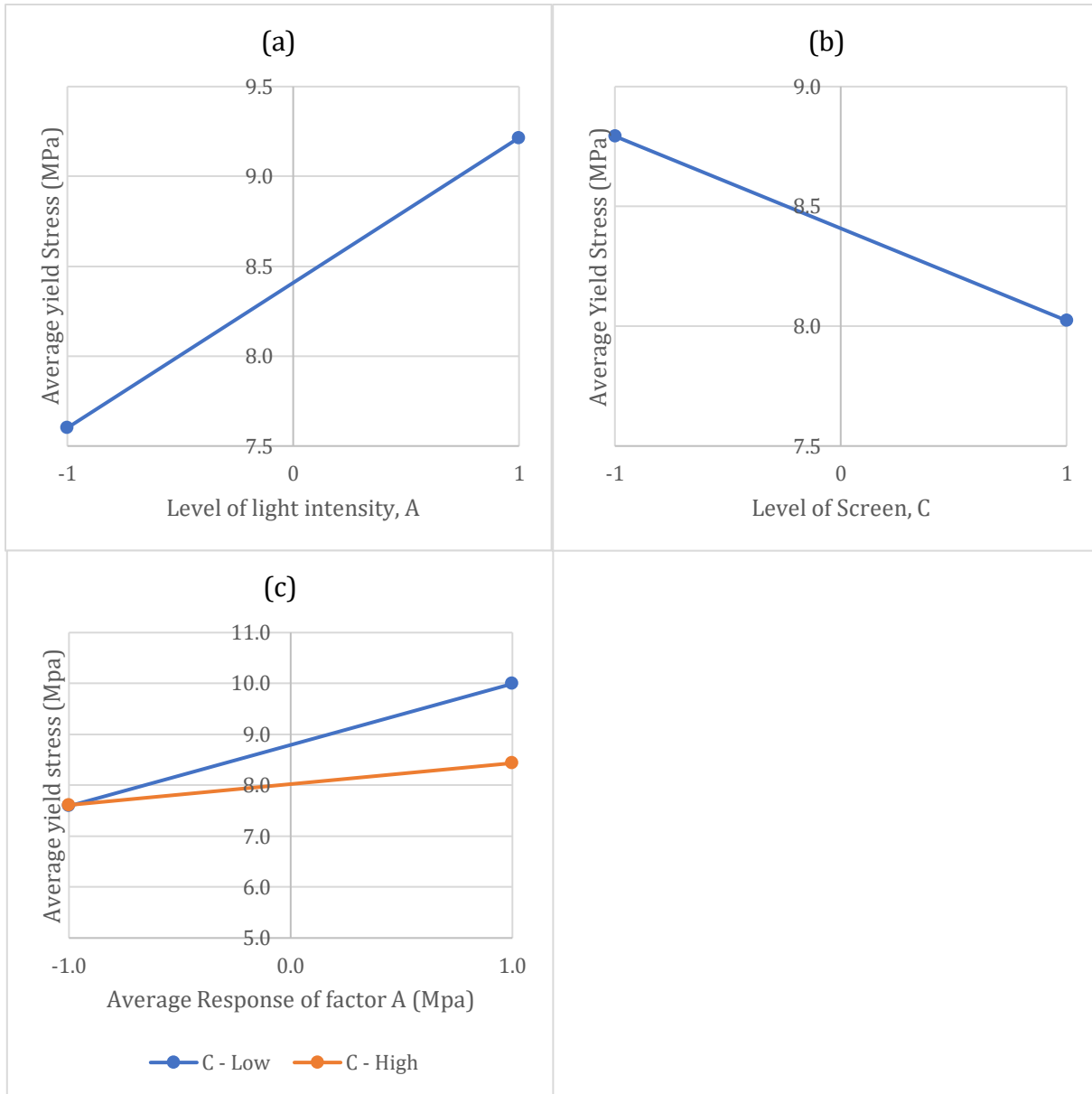
Figure 5-11: Marginal means plots showing the effects of radiation variables on the yield stress of LLDPE films in the transverse direction

The tensile stress at break is an important measure of the strength of a material and determines its sphere of usefulness. Table 5-10 lists the effects of the radiation variables on the tensile stress at break of the LLDPE films.

Table 5-10: Effects and significance levels of radiation variables on the tensile stress at break of LLDPE films in both the machine and transverse direction

Factor	Machine direction			Transverse direction		
	Effect (MPa)	95% Confidence Interval	P-value	Effect (MPa)	95% Confidence Interval	P-value
A	-3.65	1.80	0.002	-0.88	2.46	0.43
B	-5.05	1.80	0.0002	-4.10	2.46	0.005
C	4.90	1.80	0.0002	3.69	2.46	0.009
AB	2.13	1.80	0.03	1.54	2.46	0.19
AC	-2.74	1.80	0.008	-0.36	2.46	0.74
BC	-0.90	1.80	0.29	-1.37	2.46	0.24
ABC	1.43	1.80	0.10	-1.00	2.46	0.38

Table 5-10 indicates that the effects of the variables on the tensile stress at break in the machine and transverse directions are similar in quality but different in magnitude. In general, tensile stress at break in the machine direction is more sensitive to the treatments than the tensile stress at break in the transverse direction. This is evinced by both the absolute value of the effects as well as the magnitude of the p-values. In the machine direction, 5of the 7 factors are significant at the 5% significance level while in the transverse direction, 2 of the 7 factors are significant.

The marginal means plots for each of the statistically significant factors and interactions are presented in Figure 5-12.
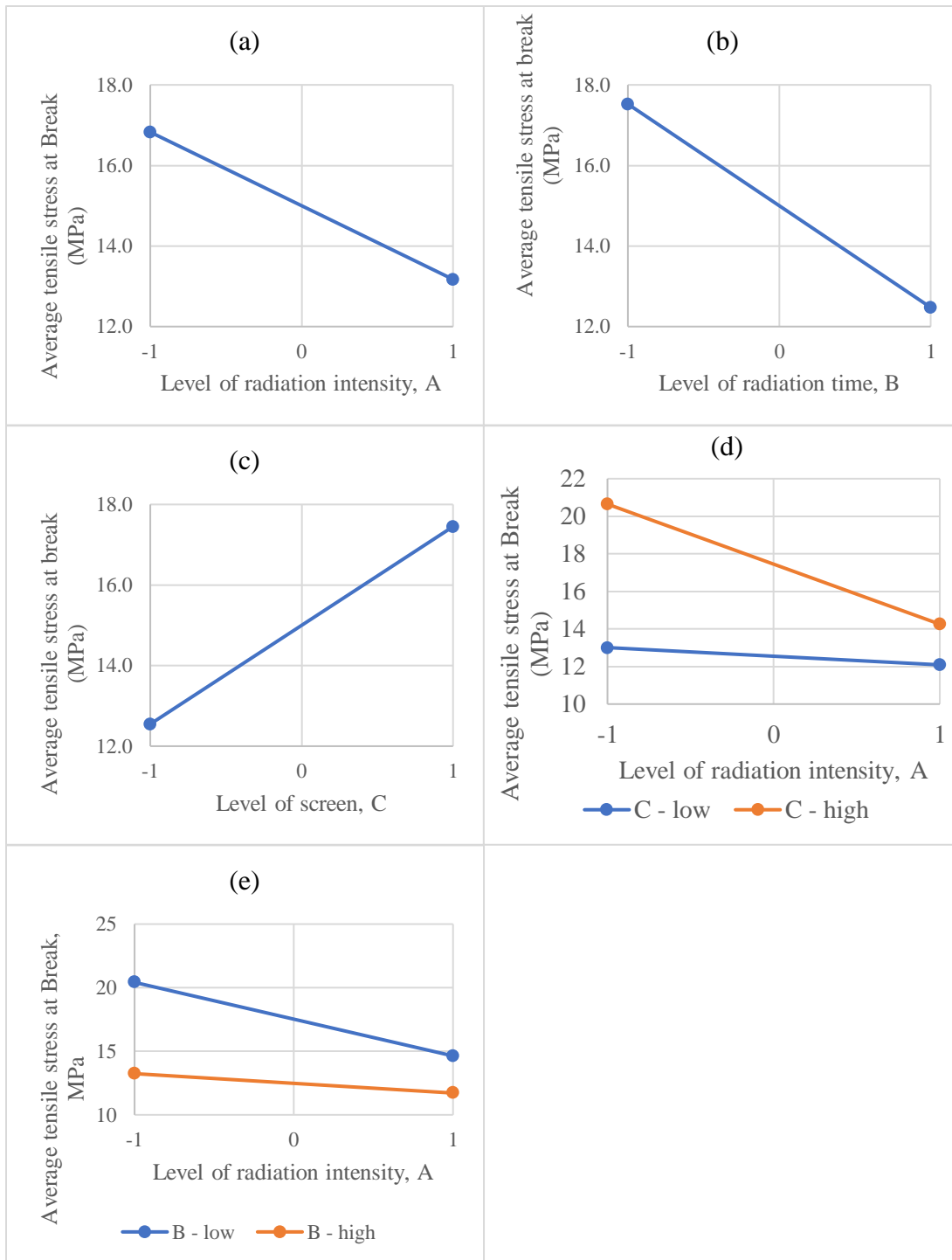
Figure 5-12: Marginal means plots showing the effects of radiation variables on the tensile stress at break of LLDPE films in the machine direction. (a) Effect of radiation intensity; (b): Effect of radiation time; (c) Effect of the level of the screen (d) Effect of the interaction between radiation intensity and level of the screen; (e) Effect of the interaction between the level of radiation intensity and the level of radiation time.

Figure 5-12 shows that increasing the level of radiation intensity causes the average tensile stress at break to decrease from 16.83 MPa to 13.17 MPa while increasing the level of radiation time causes the average tensile stress at break to decrease from 17.52 MPa to 12.48 MPa. When the level of the screen is increased from off to on, the tensile stress at break increases from 12.55 MPa to 17.45 MPa. This provides further evidence that the effect of changing the illumination pattern is different in kind from the effect of radiation by itself.

In addition to the main factor effects, Figure 5-12 illustrates the effects of two significant interactions: the interaction between radiation intensity and the illumination pattern and the interaction between radiation time and radiation intensity. Figure 5-12 (d) shows that the average tensile stress at break is generally higher when the screen is on; however, it decreases quite sharply when the level of radiation intensity increases from the low level to the high level. When the level of the screen is low, the average tensile stress at break is relatively insensitive to the level of radiation intensity.

Figure 5-12 (e) shows that regardless of the level of radiation intensity, the tensile stress at break is higher at low levels of radiation time. This is expected because prolonged exposure to UV radiation is known to cause degradation of polyethylene. This degradation is reflected in a decrease in the average tensile stress at break and in the elongation at break [28]. When the level of radiation intensity is increased, the average tensile stress at break decreases more rapidly at the low level of radiation time than at the high level of radiation time.

In the transverse direction, the most significant factors are radiation time and illumination pattern. The marginal means plots for these two factors are show in Figure 5-13.
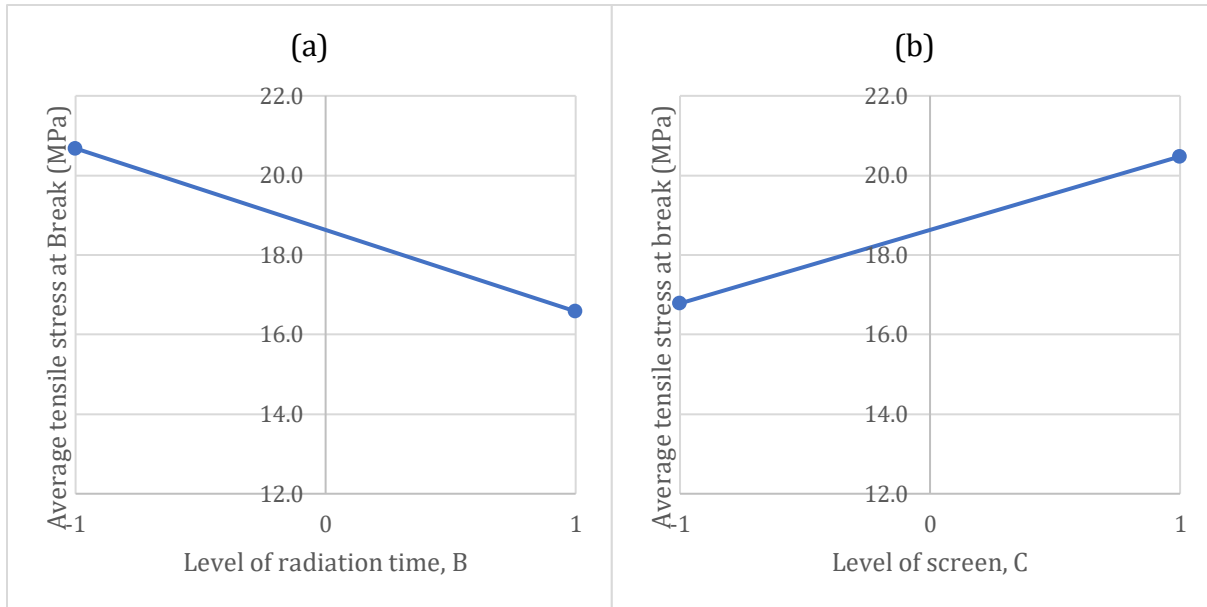
Figure 5-13: Marginal means plot showing the effect of radiation time, (B) and screen level (C) on the average tensile stress at break of LLDPE films

Figure 5-13 (a) shows that increasing the level of radiation time causes the average tensile stress at break to decrease from 20.68 MPa to 16.58 MPa. On the other hand, increasing the level of the screen causes the average tensile stress at break to increase from 16.78 MPa to 20.48 MPa. These results coincide with those reported in Figure 5-12 for the machine direction.

The elongation at break is a measure of the ductility of a material. This is important because it describes the ability of a material to withstand changes in shape before rupturing. Table 5-11 lists the effects of the radiation variables on the tensile stress at break of the LLDPE films.

Table 5-11: Effects and p-values of radiation treatment variables on the tensile strain at break of LLDPE films in both the machine and transverse directions

Factor	Machine Direction			Transverse direction		
	Effect (%)	95% CI	p-value	Effect (%)	95% CI	p-value
A	-124.06	150.61	0.0007	-106.86	57.47	0.003
B	-151.42	150.61	0.0002	-167.85	57.47	0.0002
C	141.84	150.61	0.0003	104.06	57.47	0.003
AB	55.26	150.61	0.04	28.32	57.47	0.29
AC	-53.64	150.61	0.05	-7.04	57.47	0.78
BC	38.62	150.61	0.13	-30.05	57.47	0.26
ABC	48.83	150.61	0.07	4.33	57.47	0.87

Table 5-11 illustrates that the all three main factors and two binary interactions significantly affect the tensile strain at break in the machine direction while only the main factors affect the elongation at break in the transverse direction. It also shows that with the exception of the interaction between radiation time and the screen (BC), the radiation variables affect the tensile strain at break in the same way in both orientations. Interestingly, of the main factors, only the screen level has a positive effect.

Figure 5-14 shows marginal means plots for all statistically significant factors and interactions in the machine direction. In general, the effects of the radiation variables on the average elongation at break parallel their effects on the average stress at break. Increasing the radiation intensity Figure 5-14 (a) and the radiation time Figure 5-14 (b) causes the average elongation at break to decrease while increasing the level of the screen causes the average elongation at break to increase from 570.07 MPa to 711.91 MPa.

In addition to illustrating the effect of the main factors, Figure 5-14 reveals the effects of the main interactions on the average elongation at break. Figure 5-14 (d) shows that the extent to which increasing the radiation intensity causes the elongation at break to decrease is affected by

the level of radiation intensity. When the level of radiation time is low, increasing the level of radiation intensity causes the average elongation at break to decrease from 806.36 MPa to 627.04 MPa while when the level of radiation time is high, the average elongation at break decreases from 599.68 MPa to 530.88 MPa.
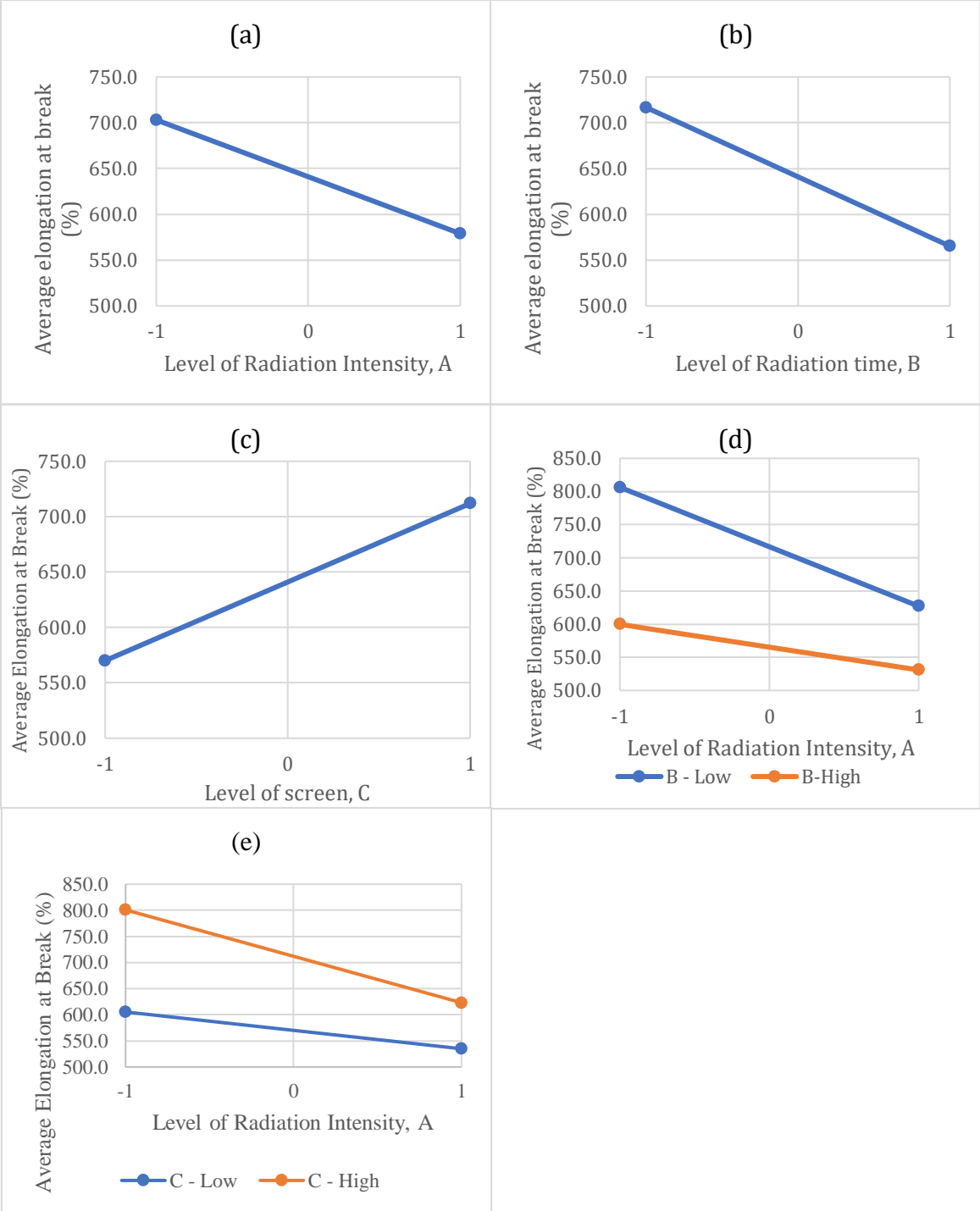
Figure 5-14: Marginal means plot showing the effect of radiation variables on the elongation at break of LLDPE films in the machine direction. (a) Effect of the level of radiation intensity; (b) Effect of the level of radiation time; (c) Effect of the level of the screen; (d) Effect of the interaction between the level of radiation intensity and the level of radiation time; (e) Effect of the interaction between the level of radiation intensity and the level of the screen.

Figure 5-14 (e) shows that the effect of the screen is affected by the level of radiation intensity. At both the high and low levels of the screen, increasing the level of radiation intensity causes the average elongation at break to decrease; however, the rate of decrease as well at the extent of decrease is affected by the level of the screen. At the high level of the screen, increasing the level of radiation intensity causes the average elongation at break to decrease from 800.76% to 623.05% while at the low level of the screen, increasing the level of radiation intensity causes the average elongation at break to decrease from 605.28 % to 534.86%.

Figure 5-15 presents the effects of the radiation variables on the elongation at break in the transverse direction. Figure 5-15 (a) shows that increasing the level of radiation intensity causes the average elongation at break to decrease from 745.01 % to 638.15 %. Figure 5-15 (b) shows that increasing the radiation time cause the average elongation at break to decrease from 775.51 % to 607.66 %. Finally, increasing the level of the screen causes the average elongation at break to increase from 639.55 % to 743.61 %.
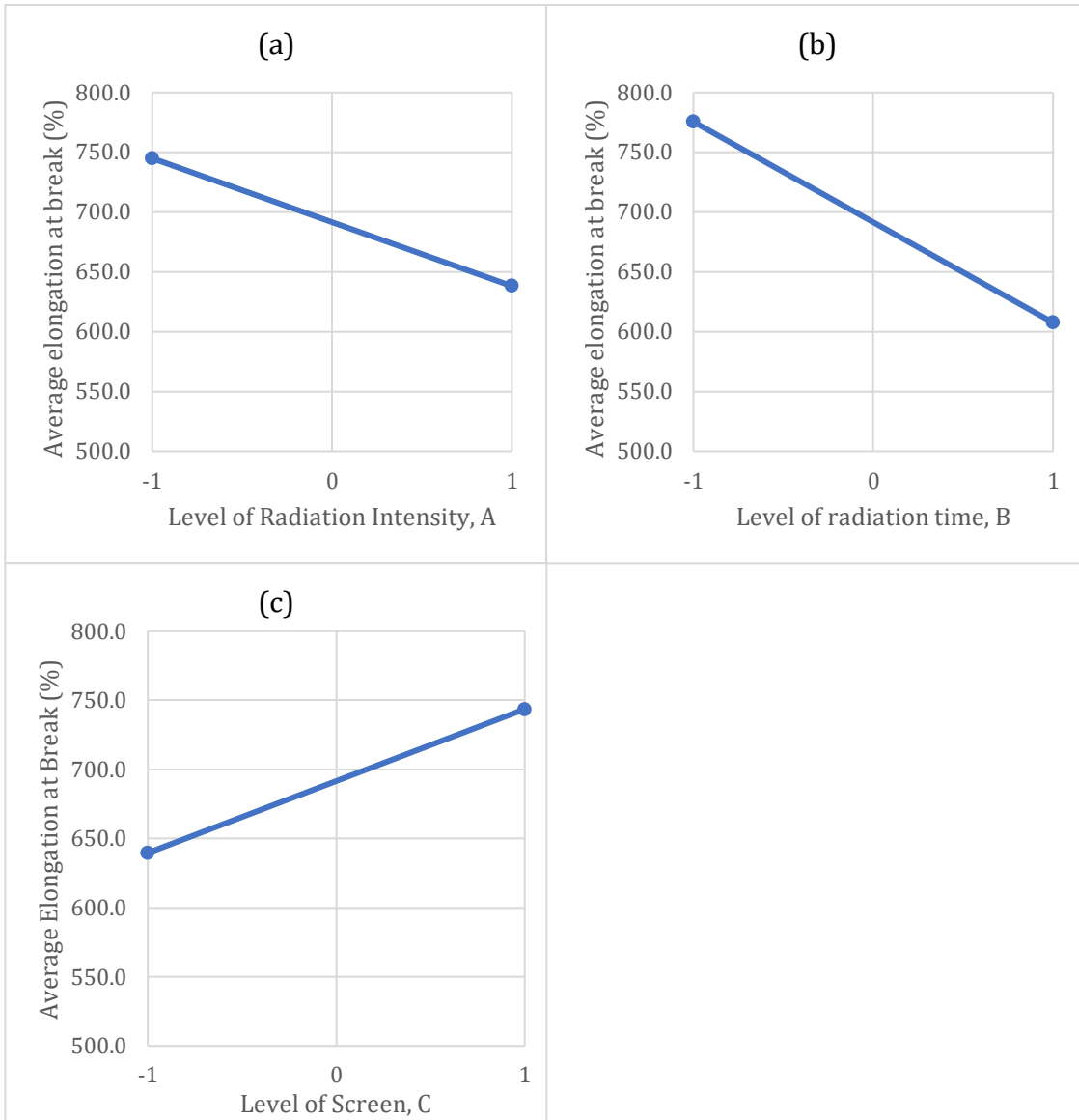
Figure 5-15: Marginal means plots showing the effects of radiation variables on the elongation at break of LLDPE films in the transverse direction.(a) Effect of radiation intensity; (b) effect of radiation time; (c) Effect of the screen

5.1.3.1 Conclusion

Table 5-12 and Table 5-13 summarize the effects of each radiation variable on the mechanical properties of the LLDPE films in both the machine and transverse direction..

Table 5-12: Summary of effects of radiation variables on the mechanical properties of LLDPE films in the machine direction

Factor	Effects			
	Elastic Modulus (MPa)	Yield Stress (MPa)	Tensile Stress at Break (MPa)	Tensile strain at break (%)
A	22.32	0.64	-3.65	-124.06
B	-12.41	-0.71	-5.05	-151.42
C	-15.50	-0.10	4.90	141.84
AB	-12.73	-0.66	2.13	55.26
AC	-21.76	-1.13	-2.74	-53.64
BC	4.73	-0.05	-0.90	38.63
ABC	15.20	0.27	1.43	48.83

Table 5-13:Summary of effects of radiation variables ono the mechanical properties of LLDPE films in the transverse direction

Factor	Elastic Modulus (MPa)	Yield Stress (MPa)	Tensile Stress at Break (MPa)	Tensile strain at break (%)
A	45.45	1.61	-0.88	-106.86
B	7.06	0.44	-4.10	-167.85
C	-29.12	-0.77	3.69	104.06
AB	11.65	0.22	1.54	28.32
AC	-17.16	-0.79	-0.36	-7.04
BC	2.76	-0.14	-1.37	-30.05
ABC	-1.78	-0.18	-1.00	4.33

Comparing only the main effects, Table 5-12 and Table 5-13 reveal that increasing the level of radiation intensity causes the modulus of elasticity and the yield stress to increase and the tensile stress at break and the tensile strain at break to decrease.

While the effect of radiation intensity appears to be independent of the orientation of the films, Table 5-12 and Table 5-13 show the effect of radiation time anisotropic. In the machine direction, increasing the level of radiation time causes all of the tensile properties to decrease while in the transverse direction, the effect of radiation time is similar to the effect of radiation intensity.

It is interesting to note that the effect of the screen is isotropic and opposite to the effect of radiation intensity. Increasing the level of the screen causes the elastic modulus and the yield stress to decrease while the tensile stress at break and the tensile strain at break increase.

5.1.4   Rheological Properties

The rheological properties of polymers are highly sensitive to their molecular structure [29]. Linear viscoelastic behaviour in particular provides a rich source of information from which details of the effect of processing variables on the structure of a polymer can be inferred [30], [31], [32]. Accordingly, in this section, the effect of radiation processing on some rheological properties of the LLDPE films will be presented. The properties that shall be investigated include the complex viscosity and the linear viscoelastic properties.

5.1.4.1   The effect of radiation processing on shear viscosity

The main factors which affect the viscosity of molten plastics include the molecular weight, the molecular weight distribution and the degree and type of long chain branching [32] [29]. In general, if the molecular weight distribution and degree of branching are held constant, the effect of increasing molecular weight is to increase the zero-shear viscosity of a molten thermoplastic. On the other hand, molecular weight distribution affects the shear thinning behaviour of plastics. Broadening the molecular weight distribution causes a material to be more shear-thinning. This behaviour is reflected in the increase of the slope of viscosity-shear rate curve in the shear thinning region [29].

The effect of long chain branching on the viscosity of plastics is more complex and has features which coincide with the effect of molecular weight as well as the effect of molecular weight distribution. Furthermore, the effect of long chain branching is sensitive to the type of polymer being studied. For example, for metallocene polyolefins, the zero-shear viscosity increases with branching level for the same weight average molecular weight [29]. Furthermore, in these polyolefins, long chain branching substantially increases the degree of shear thinning [29].

From the foregoing, it can be noted that while viscosity data is indeed quite sensitive to changes in the molecular architecture of molten plastics, it needs to be used in conjunction with other data in order to pin-point the cause of the observed changes.

Figure 5-16 presents plots of the viscosity of samples treated at different combinations of radiation time, intensity and illumination pattern.

67

(a)

(b)
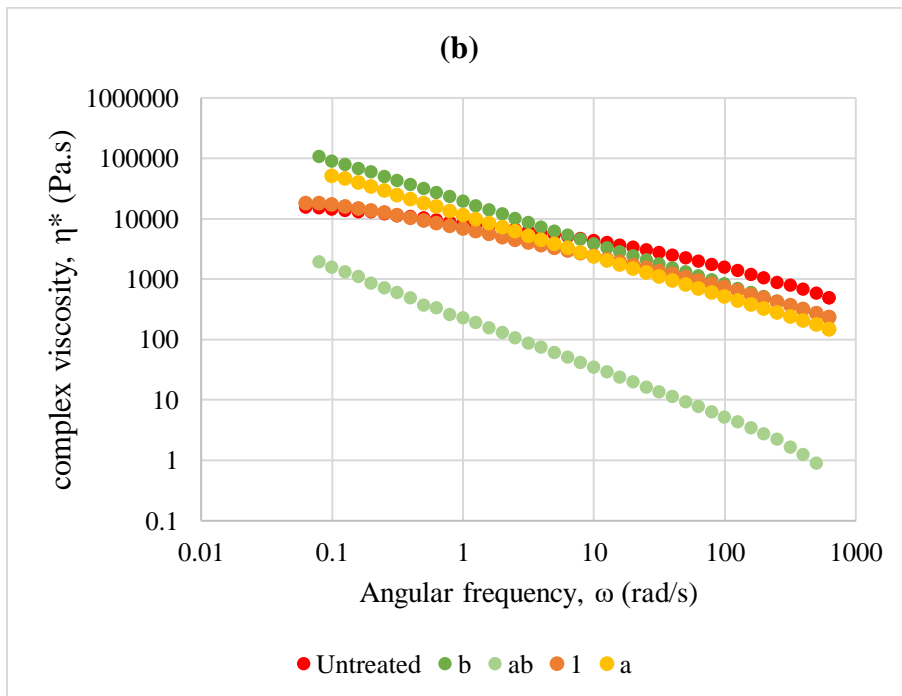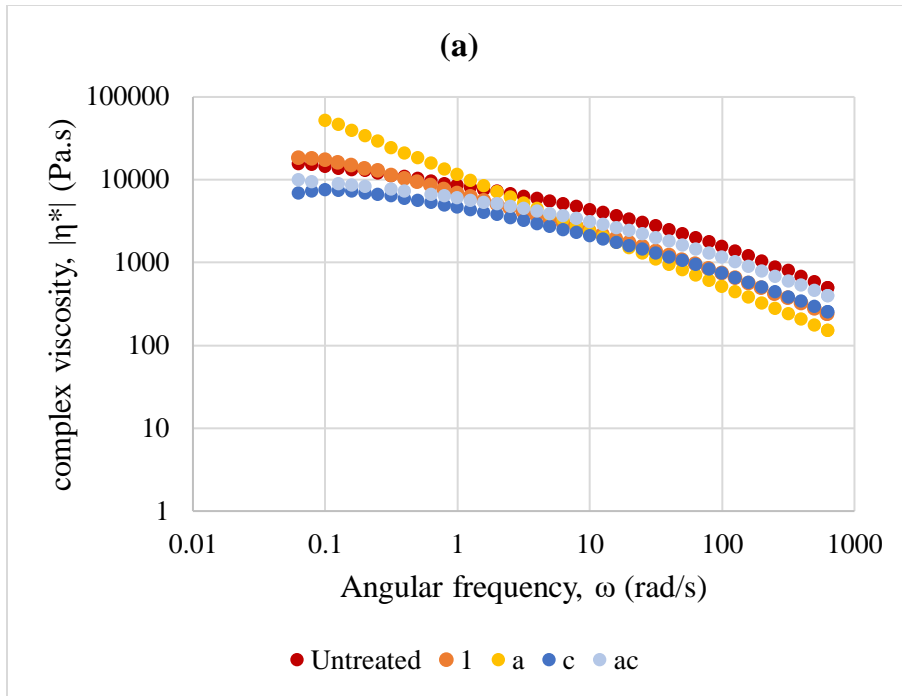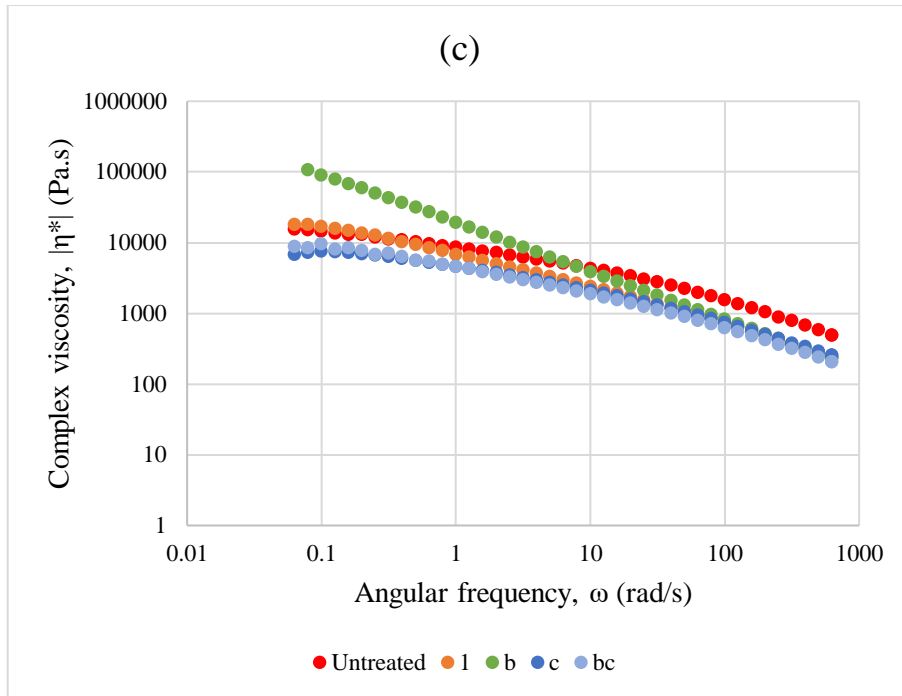
Figure 5-16: Effect of radiation variables on the viscosity of LLDPE films. (a.) Effect of radiation intensity and screen on viscosity; (b). Effect of radiation time and radiation intensity; (c) Effect of radiation time and screen on viscosity;

Figure 5-16 (a) suggests that the radiation intensity and the screen have significantly different effects on the viscosity of the irradiated LLDPE films. The untreated the film approaches a Newtonian Plateau at a shear rate of 0.1 rad/s. This behaviour is also present at both the high and low levels of radiation intensity when samples are irradiated under the screen; however, the zero-shear viscosity increases with increasing intensity.

In the absence of the screen, the viscosity at low shear rates is significantly more sensitive to the level of the radiation intensity. At the low level of radiation intensity, LLDPE still demonstrates an approach to the Newtonian Plateau at around 0.1 rad/s but the viscosity at this shear rate is 3 times higher than the viscosity of the untreated sample. When the radiation intensity is at the high level, a Newtonian Plateau is no longer visible at 0.1 rad/s and the viscosity at this shear rate is 10 times higher than the untreated sample.

Figure 5-16 (a) also shows that radiation intensity and the screen have different effects on the shear thinning behaviour of the LLDPE films. In general, radiation intensity causes the films to

become less shear thinning than the untreated sample. However, the effect of the screen on the shear thinning behaviour of the films depends on the level of radiation intensity.

Sample ac, which corresponds to a combination of high radiation intensity and high screen level, is less shear thinning than sample c which corresponds to a low level of intensity and high level of the screen. In the absence of the screen, increasing the level of radiation intensity causes the film to become more shear thinning.

Figure 5-16 (b) shows that in the absence of a screen, increasing the level of radiation time causes the viscosity in the low shear rate region to increase. Increasing the level of radiation time from zero (untreated) to the low level causes the viscosity at 0.1 rad/s to increase from 5720 Pa.s to 17180 Pa.s. When the radiation time is increased to the high level, the viscosity reaches 90500 Pa.s at 0.1 rad/s. When the screen is introduced, increasing the radiation time has a negligible effect of the viscosity. This can be seen because curves c and bc nearly overlap.

Comparing sample 1 and b, it can be seen that as the shear rate increases, the viscosity draws closer together. This suggests that increasing the radiation time increases the range over which the transition from low shear rate behaviour to high shear rate behaviour occurs. For polyethylene, broadening of this transition region has been linked with both long chain branching and broadening of the molecular weight distribution [32] [29]. When the screen is introduced, this effect is not present. The viscosity of samples c and bc overlap throughout the range of shear rates studied in this work.

Figure 5-16 (c) indicates that the effect of radiation intensity is dependent on the level of radiation time. At low radiation time (30 seconds), increasing the relative radiation intensity causes the shear rate at 0.1 rad/s to increase from 5720 Pa.s (0% intensity) to 51870 Pa.s at 100 % relative intensity. At high radiation time, increasing the radiation intensity from 0% to 100% causes the viscosity to decrease from 5720 Pa.s to 1602 Pa.s.

Figure 5-16 also shows that both the intensity and radiation time affect the shear thinning behaviour of the samples relative to the untreated resin. Comparing the trajectory of the viscosity of the untreated sample at 10 rad/s with the viscosity of the treated samples, it can be seen that the untreated samples are more shear thinning. This suggests that the untreated samples have a broader molecular weight distribution than the treated samples. Furthermore, comparing the

treated samples with each other, it can be seen that increasing the radiation intensity from 47% to 100% not only causes the viscosity at 0.1 rad/s to increase but also lowers the viscosity of the sample at shear rates higher than 10 rad/s.

On the other hand, Figure 5-16 (c) shows that, at the low level of radiation intensity, increasing the radiation time increases the viscosity at 0.1 rad/s from 5720 Pa.s to 90500 Pa.s. This is higher than the effect of increasing the radiation intensity. It also shows that the viscosity of the sample treated at high radiation time converges with the viscosity of the sample treated at low radiation time at a shear rate of 100 rad/s. This suggest that rather than increasing the shear thinning behaviour of the LLDPE films, increasing radiation time broadens the range over which the transition from low shear to high shear behaviour occurs.

Earlier, it was observed that the untreated samples and samples 1, c and ac demonstrated an approach to Newtonian behaviour (that is, the viscosity becoming independent of the shear rate) as the shear rate approached 0.1 rad/s. In order to quantify the effect of the radiation treatments on the zero shear viscosity and on the shear-thinning behaviour of the films, the data presented in Figure 5-16 were fit to the Cross Model [33], [29], Equation 5.

$$\eta = \frac{\eta_0}{1 + (|\lambda|\gamma)^{1-n}}$$

Equation 5: Cross Model

Where η_0 Zero-shear viscosity

λ Characteristic time at which transition from Newtonian to shear thinning behaviour occurs

n   Shear-thinning index

Because some of the samples did not exhibit a Newtonian Plateau in the shear rate window reported herein, care must be exercised in using the parameters derived from fitting the Cross model to these data [29]. They have been included because it was felt that the model results, especially the zero- shear viscosity and the shear thinning index, fit the general trend observed

from the plots shown in Figure 5-16. Estimates of the Cross-model parameters are listed in Table 5-14.

Table 5-14: Cross model parameters for radiation treated LLDPE films

Treatment	η_0 (Pa.s)	λ (s)	n
Untreated	22,869	2.96	0.56
1	34,243	10.7	0.44
a	159,455	25.3	0.18
b	603,608	105.5	0.27
ab	744,597	215.0	0.11
c	9,239	0.9	0.44
ac	12,679	1.2	0.53
bc	12,934	2.7	0.46
abc	47,788	26.6	0.28

The effects of the radiation variables on the zero-shear viscosity and on the shear thinning index of the films are listed in Table 5-15.

Table 5-15: Effects and p-values of radiation variables on the zero shear viscosity and shear-thinning index of LLDPE films

Factor	Effect of zero-shear viscosity, η_0			Effect on shear-thinning index		
	Effect (Pa.s)	90% Confidence Interval	p-value	Effect	90% Confidence Interval	p-value
A	17,632	170,551.84	0.852	-0.12	0.06	1.51E-03
B	194,159	170,551.84	0.0671	-0.11	0.06	2.92E-03
C	-266,526	170,551.84	0.0197	0.13	0.06	8.38E-04
AB	-65,098	170,551.84	0.4979	0.01	0.06	0.78
AC	19,430	170,551.84	0.8375	0.09	0.06	7.32E-03
BC	-157,107	170,551.84	0.125	0.02	0.06	0.46
ABC	100,440	170,551.84	0.305	-0.06	0.06	4.35E-02

Table 5-15 indicates that only radiation time and the screen have a significant effect on the zero-shear viscosity. The effect of radiation time is 194,159 Pa.s while the effect of the screen in -266,526 MPa.

It is curious that the effect of radiation intensity is not statistically significant. This is unexpected because all the results obtained thus far indicate that the intensity of radiation significantly affects the mechanical properties of the films. A potential reason for this contradiction could be that a true Newtonian plateau for is not observed in the frequency range studied herein. Thus, an additional level of error is introduced by extrapolation of the data to low shear rate values [29].

Table 5-15 shows that the shear thinning parameter is quite sensitive to the radiation variables. Both the radiation time and the radiation intensity cause the shear-thinning index to decrease (by 0.11 and 0.12 respectively) while the irradiation under a screen causes the shear-thinning parameter to increase by 0.13. These results suggest that the radiation time and the radiation

intensity cause the molecular weight distribution or the level of long chain branching to decrease while the screen causes the molecular weight distribution to become broader.

Table 5-15 also reveals the effect of the interaction between the level of the screen and the level of radiation intensity on the shear thinning index is significant. This interaction is illustrated in Figure 5-17.
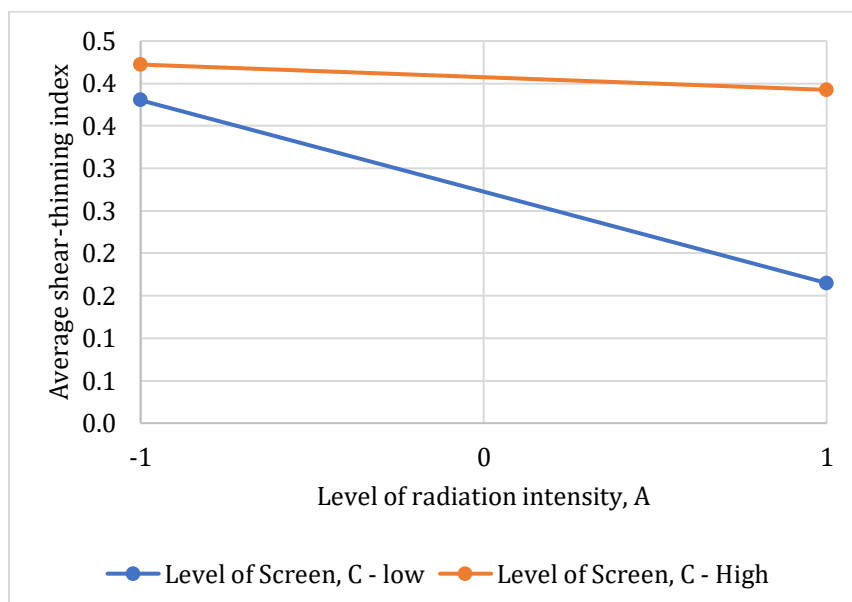
Figure 5-17: Effect of interaction between the level of radiation intensity and the level of the screen on the shear- thinning index of LLDPE films

Figure 5-17 clarifies that the effect of radiation intensity is dependent on the level of the screen. When the screen is at the low level, increasing the level of radiation intensity causes the average shear thinning index to decrease from 0.38 to 0.16. When the screen is at the high level, increasing the level of radiation intensity causes the average shear-thinning index to decrease from 0.42 to 0.39. Hence, it can be concluded that the screen reduces the effect of radiation intensity on the shear thinning index.

5.1.4.2   *Effect of Radiation Processing on the Linear Viscoelastic Properties of LLDPE films*

The previous section established that radiation processing induces some important differences in the viscosity of LLDPE films. In particular, it showed that the screen introduces some changes in the low shear and high shear behaviour of the films. In the low shear region, the screen reduces

the zero-shear viscosity. In the high shear region, it was observed at the high level of radiation intensity the screen decreases the extent of shear thinning.

It is desirable to correlate these changes with changes in the molecular architecture of the films. Earlier it was noted that the linear viscoelastic properties in general and the storage modulus in particular are highly sensitive to the changes in the structure of polyolefins. Accordingly, these changes shall be explored by analysing the cross-over modulus, the storage modulus and the loss tangent.

Figure 5-18 presents plots of dynamic moduli against frequency for samples irradiated at different combinations of radiation intensity, radiation time and illumination pattern (screen).
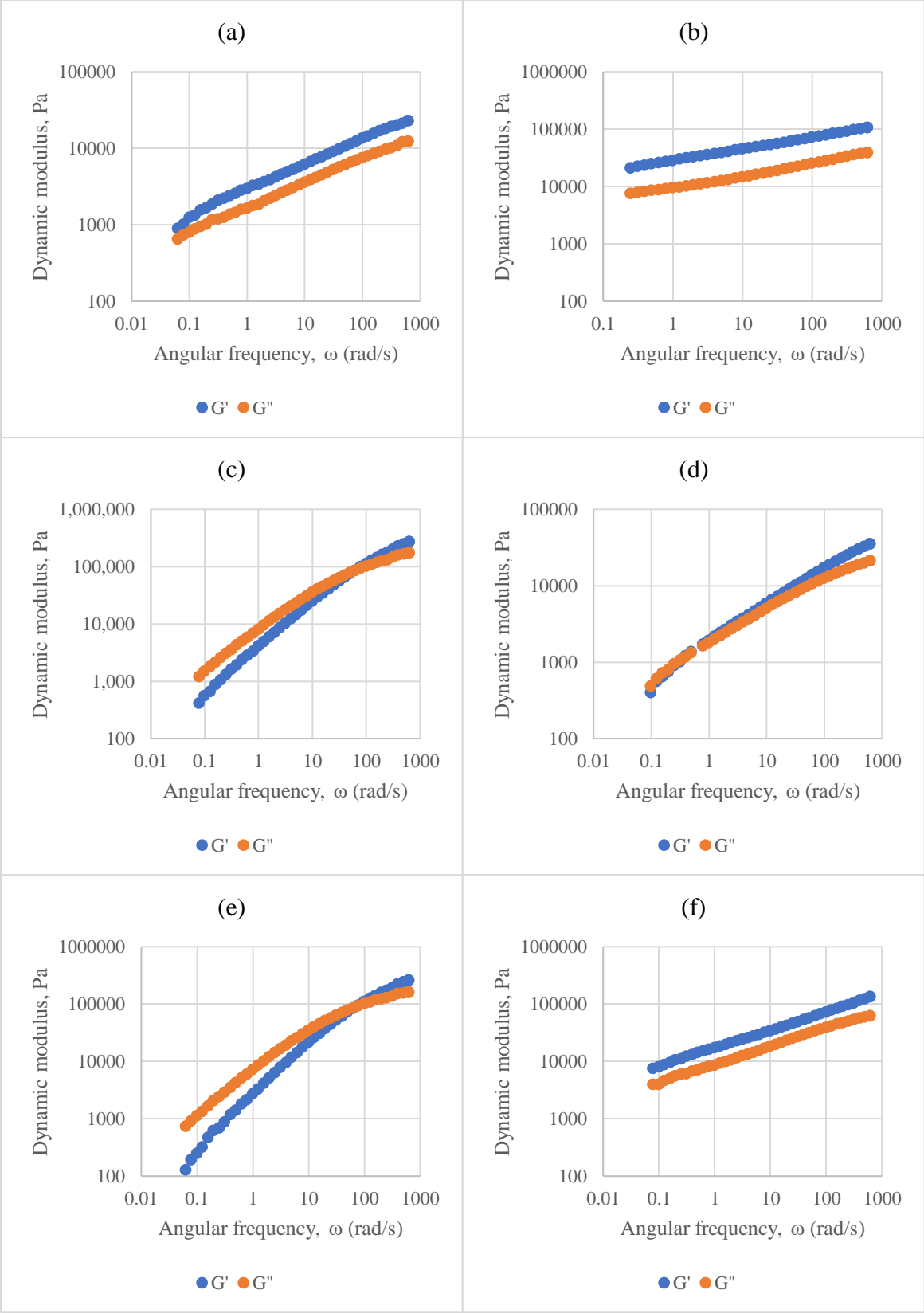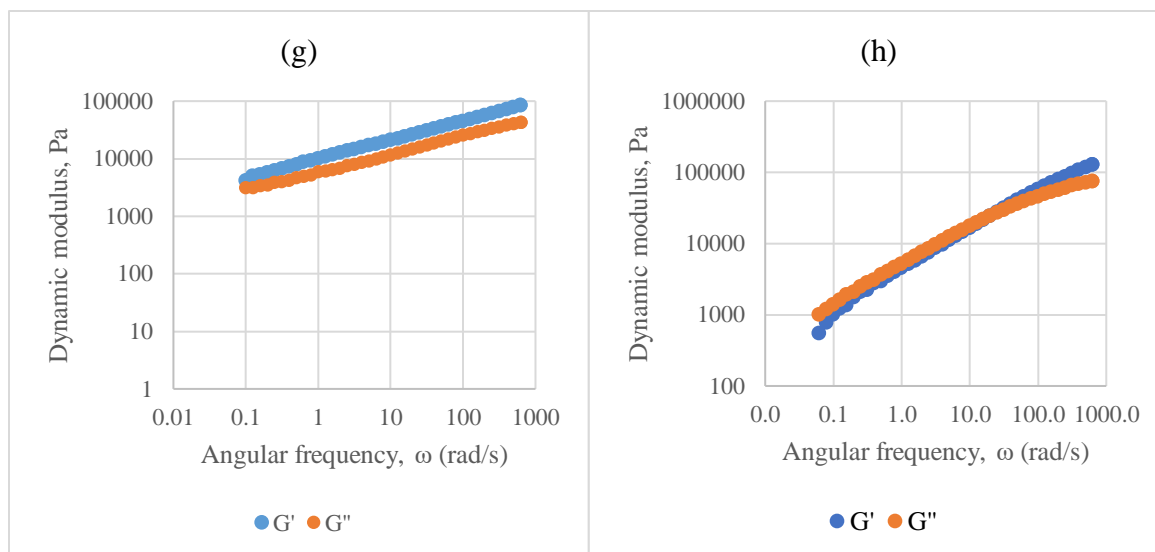
Figure 5-18: Plots of dynamic moduli against frequency for LLDPE films irradiated at different combinations of radiation intensity, radiation time and illumination pattern. (a) high intensity, high time and screen on [abc]; (b) high intensity + high time + screen off [ab]; (c)low intensity + low time + screen on [c]; (d) low intensity + high time + screen on [bc]; (e) high intensity + low time + screen on [ac]; (f) low intensity + high time + screen off [b]; (g) high intensity + low time + screen off [a]; (h) low intensity + low time + screen off.

Comparing, Figure 5-18 (c), (e), (g) and (h), it can be seen that radiation treatment shifts the cross-over modulus to lower frequency and modulus value. Sample a does not exhibit a crossover modulus in the frequency range tested.

Figure 5-18 (f) and (g) show that in the absence of the screen, when radiation time is increased from 30 seconds to 180 seconds, no crossover modulus is observed, and the elastic modulus rises above the loss modulus for all the frequencies observed. This suggests that when the sample is irradiated for 180 seconds, it becomes highly crosslinked.

In addition to the above, Figure 5-18(c) and (d) indicate that the presence of the screen modifies the effect of radiation time. At the low level of radiation time, the effect of the screen is to shift the crossover point (frequency and modulus) up and to the right. At the high level of radiation time, the screen causes the crossover point to shift down and to the left.

The cross over modulus, G_c, is obtained from a plot of storage and loss modulus against the frequency. It is defined as the point at which both moduli are equal. Estimates of this parameter

were obtained by fitting the curves in the vicinity of the cross-over point with simple linear equations. An example of this procedure is shown in Figure 5-19.
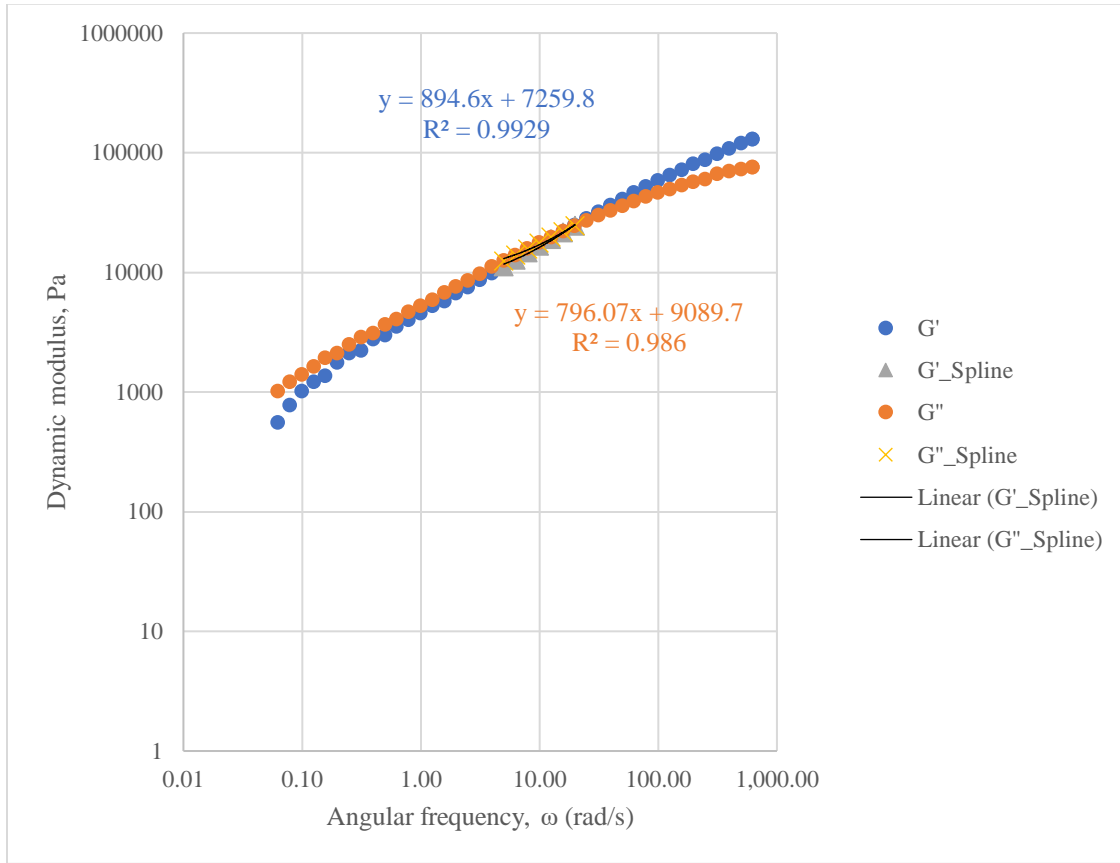
Figure 5-19: Example of a plot used to determine the cross-over modulus of irradiated LLDPE films

The estimates of the cross-over modulus were then used to determine the rheological polydispersity index according to Equation 6 [30]:

$$PI(Z) = \frac{10^5}{G_c(Pa)}$$

Equation 6: Rheological Polydispersity Index

Though the PI (Z) was initially developed for polypropylene [34], Shroff and Mavridis found that it can be used in both linear and branched polyethylene [35]. A caution that they give is that it exhibits diminished sensitivity to changes in polydispersity in branched systems.

The values of the crossover modulus and the rheological polydispersity index for the irradiated samples are listed in Table 5-16.

Table 5-16: Values of the crossover modulus and the rheological polydispersity index for samples irradiated at various combinations of radiation intensity, radiation time and illumination pattern

Sample	Cross-over modulus (Pa)	Cross over frequency (rad/s)	PI(Z)
Untreated	87,119	60.05	1.15
1	23,874	18.57	4.19
a	-	-	-
b	-	-	-
ab	-	-	-
c	89,874	71.016	1.11
ac	88,129	65.102	1.13
bc	2,618	0.4338	38.20
abc	-	-	-

According to Table 5-16, the crossover modulus of the untreated film is 87,119 Pa, corresponding with a PI (Z) of 1.15. When the film is irradiated at low intensity for short time without the screen present (sample 1), the cross-over modulus decreases to 23,874 Pa while the PI (Z) decreases to 4.19. A larger value of the polydispersity index suggests a broader molecular weight distribution while a smaller value suggests a narrower molecular weight distribution [29], [30], [35]. Accordingly, it can be seen from Table 5-16 that in the absence of the screen, increasing the radiation intensity from 0% (untreated) to 47% (1) causes the molecular weight distribution of the films to increase. This can be attributed to either crosslinking or long chain branching [35] [36].

When the radiation intensity is increased further, the cross-over modulus moves out of the frequency window studied in this work. Furthermore, it can be seen from Figure 5-18 (g) that for the sample treated at the high level of radiation intensity (a), the storage modulus dominates the loss modulus for all values of frequency. A study published by Murray et al [37] found that these observations correlated with samples that were crosslinked to gel content greater than 80%. Hence, it can be inferred that the sample treated at a high level of radiation was similarly highly crosslinked.

In contrast, increasing the radiation intensity while the screen is present has a less noticeable effect on the rheological polydispersity. In this case, increasing the level of radiation intensity causes the PI (Z) to increase from 1.11 to 1.13. This value is comparable to the polydispersity of the untreated film. This could mean that the screen significantly attenuates the intensity of the radiation that is incident on the film. As a result, crosslinking/long chain branching proceeds less quickly when the screen is present.

Evidence of the attenuating effect of the screen can be seen by considering the effect of increasing radiation time. At the low level of radiation intensity, increasing the radiation time from 30s to 180s causes the polydispersity to increase from 1.11 to 38.20. From this, it can be inferred that the rate of photo-chemical reactions when the screen is present is slower than when the screen is absent. From this, it would follow that increasing the radiation time would allow more time for the crosslink density or degree of long chain branching to increase.

Another useful measure of polydispersity is the "ER", introduced by Shroff and Mavridis [35]. It is defined in Equation 7.

$$ER = C_1 . G'|_{at\ G''_{ref}}$$

Equation 7: Definition of "ER" polydispersity index

Where C_1 - normalization constant with a value of $1.781*10_{-3}$

G''_{ref} – 500 Pa

The value of the normalization constant, C_1 in Equation 7 is dependent on the polymer being studied. The value used here was suggested by Shroff and Mavridis [35] in their original paper for high density polyethylene and linear low-density polyethylene in the melt.

The advantage conferred by this polydispersity index is that it is quite sensitive to changes in the polydispersity of the high molecular weight end of the molecular weight distribution.

ER is calculated from a plot of the storage modulus against the loss modulus. This kind of plot is also known as a modified Cole-Cole plot. A sample plot is shown in Figure 5-20.
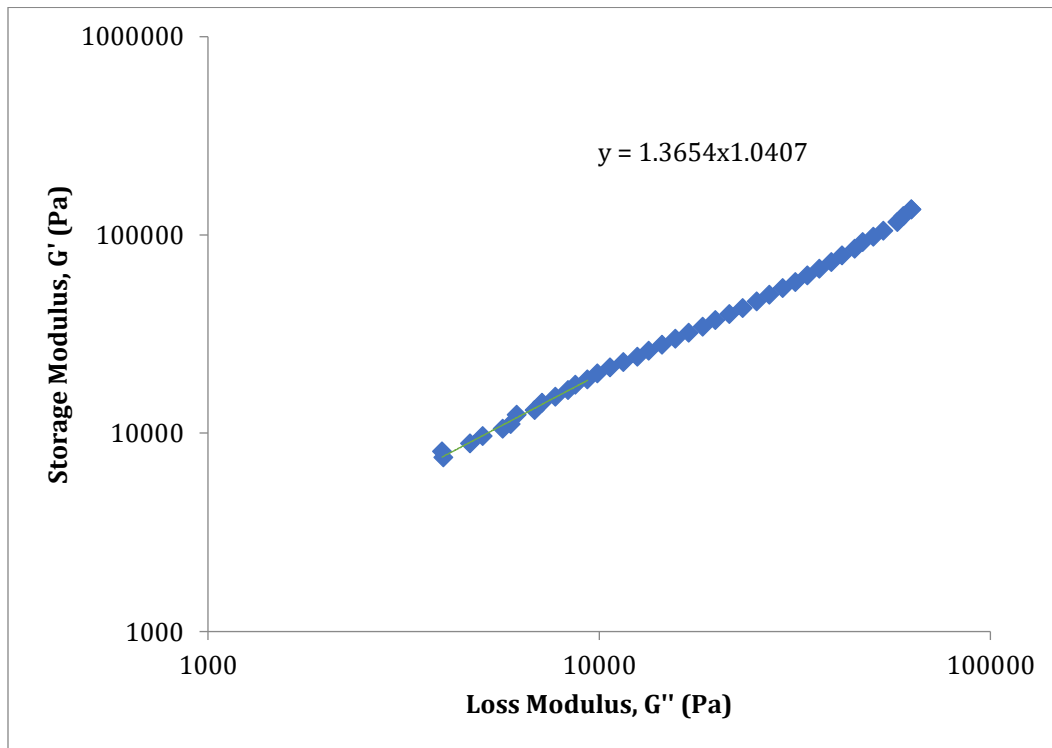
Figure 5-20: Example of plot used to calculate the ER

Since the data obtained in this study did not extend to a G''_{ref} of 500 Pa, it was necessary to extrapolate the data. Shroff and Mavridis suggest that this can be done by fitting the data in the last two decades of frequency to a straight line [35]. Since the data here is in a log-log scale, a straight line is obtained by fitting the data in the last two decades to a power function. This function is also shown in Figure 5-20.

Table 5-17 lists the ER values for LLDPE samples treated at different combinations of radiation intensity, radiation time and illumination pattern. These values are listed alongside the PI (Z) values to facilitate comparison.

Table 5-17: ER and PI (Z) values of samples irradiated at different conditions of radiation intensity, time and illumination pattern

Treatment	ER	PI(Z)
Untreated	0.17	1.15
1	0.17	4.19
a	1.34	-
b	1.57	-
ab	1.35	-
c	0.30	1.11
ac	0.19	1.13
bc	0.42	38.20
abc	1.06	-

In general, a lower ER value indicates either a narrower distribution of the high molecular weight chains or degradation while a higher ER value indicates a broader distribution of high molecular weight chains [36].

Considering the effect of radiation intensity alone, Table 5-17 shows that increasing the radiation intensity from 47% (1) to 100% (a), causes the ER to increase. This indicates that the distribution of molecular weights has become broader and suggests that either branching or network formation has occurred. This is also reflected in the PI (Z) which goes from 4.19 to being undetected in the frequency range examined in this study. The reason why the crossover modulus is undetected is because it has shifted to the low frequency region. A shift of the crossover modulus to lower frequencies is associated with broadening of the molecular weight distribution [29].

When the screen is present, increasing the radiation intensity from 47% (c) to 100% (ac) causes the ER to decrease. This suggests that the distribution of high molecular weight chains has become narrower. It is interesting to note that the PI (Z) indicates that the polydispersity of these two samples is comparable. This echoes the results of Shroff and Mavridis who found that the PI (Z) was not sensitive to long chain branching in samples of HDPE with the same molecular weight distribution [35]. Given the similarity between their results and those reported here for samples c and ac, it is hypothesized that increasing the radiation intensity while the screen is present causes chain scission of the higher molecular weight chains.

Considering the effect of radiation time, Table 5-17 shows that when the radiation time is increased from 30 seconds (1) to 180 seconds (b), the ER increases significantly. When the screen is present, increasing radiation time from 30 seconds (c) to 180 seconds (bc) causes the ER to increase but not as significantly as in the absence of the screen.

The effect of the radiation treatments on the topology of the films can be further elucidated using plots of the storage modulus and the loss angle. These are presented in Figure 5-21 , Figure 5-22, Figure 5-23 and Figure 5-24.
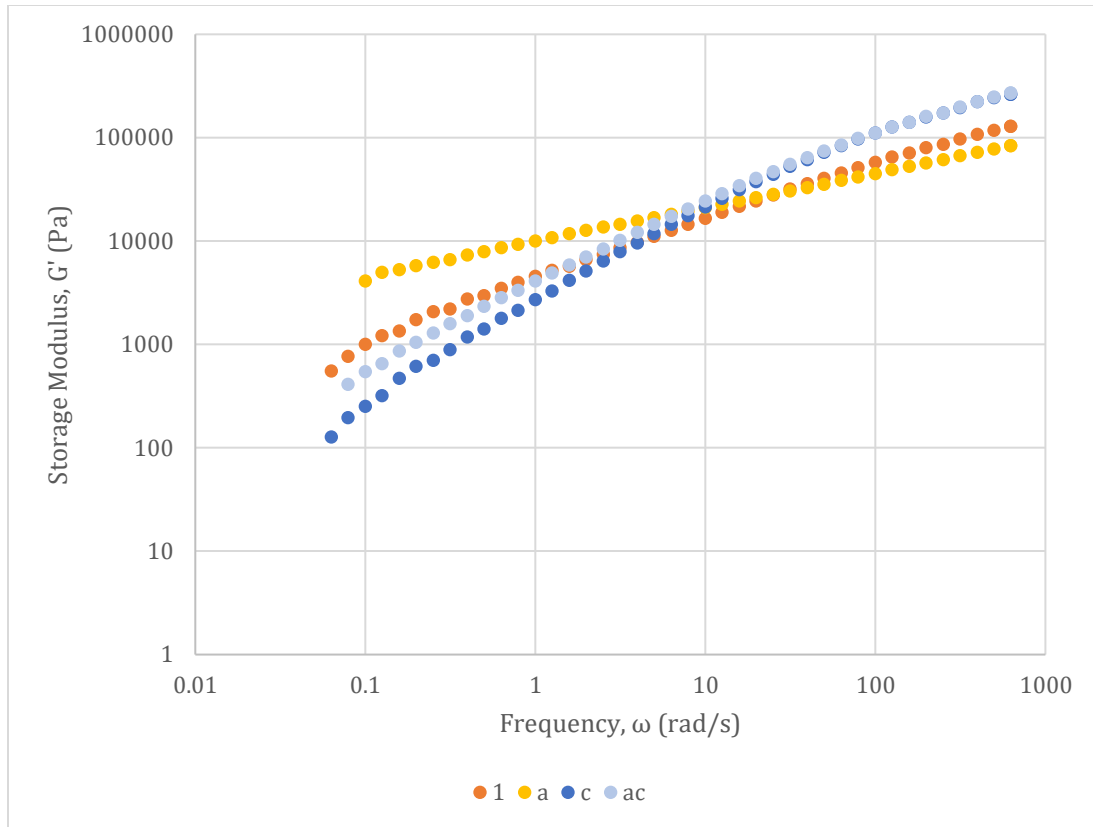
Figure 5-21: Effect of radiation intensity and level of screen on the elastic modulus of LLDPE films. 1: 47% radiation intensity + no screen; a: 100% radiation intensity + no screen; c: 47% radiation intensity + screen; ac: 100% radiation intensity + screen

Figure 5-21 shows that radiation treatment has a stronger effect on the elastic modulus in the low shear rate region than at the high shear rate region. This is expected because as the frequency approaches the low frequency limit, the storage modulus becomes proportional to the steady state compliance as shown in Equation 8 [35]

$$\lim_{\omega \to 0} G'(\omega) = \eta_0^2 J_e^0 \omega^2$$

Equation 8: Relation between storage modulus and steady-state compliance

Where: $\eta 0$ = zero shear viscosity

        J_{e0} = stead-state compliance

        ω = angular frequency

In turn, the storage modulus in the limit of zero frequency can be connected to the crosslink density according to equation 9 [38].

$$M_c = \frac{\rho RT}{G_{\omega=0}}$$

Equation 9: Relationship between modulus and cross-link density.

Where: M_c = average molecular weight between crosslinks

ρ = polymer density at the experimental temperature

R = Universal Gas Constant

T = experimental temperature

G = value of the modulus at an extrapolated frequency of zero

Taken together, Equation 8 and Equation 9 show that comparisons of the storage modulus at low shear rates provide a good indication of the elasticity and of the crosslink density of the films.

When the screen is off, the storage modulus in the low shear rate region increases with increasing radiation intensity. Furthermore, while the storage modulus increases with increasing shear rate, the elastic modulus of the sample that was treated at 47% intensity increases more sharply than that of the sample treated at 100% intensity. This indicates that as the radiation intensity increases, the storage modulus becomes less sensitive to the shear rate and approaches ideally elastic behaviour.

When the screen is introduced, Figure 5-21 shows that the storage modulus in the low shear region becomes less sensitive to the level of radiation intensity. This can be seen in that the storage modulus of sample ac (100% intensity + screen) is lower than the storage modulus of sample 1 (47% intensity + no screen). Furthermore, Figure 5-21 shows that the storage moduli of samples c and ac are increase more rapidly with increasing shear rate than samples 1 and a. This suggests that these samples have less elastic behaviour than the samples treated without a screen
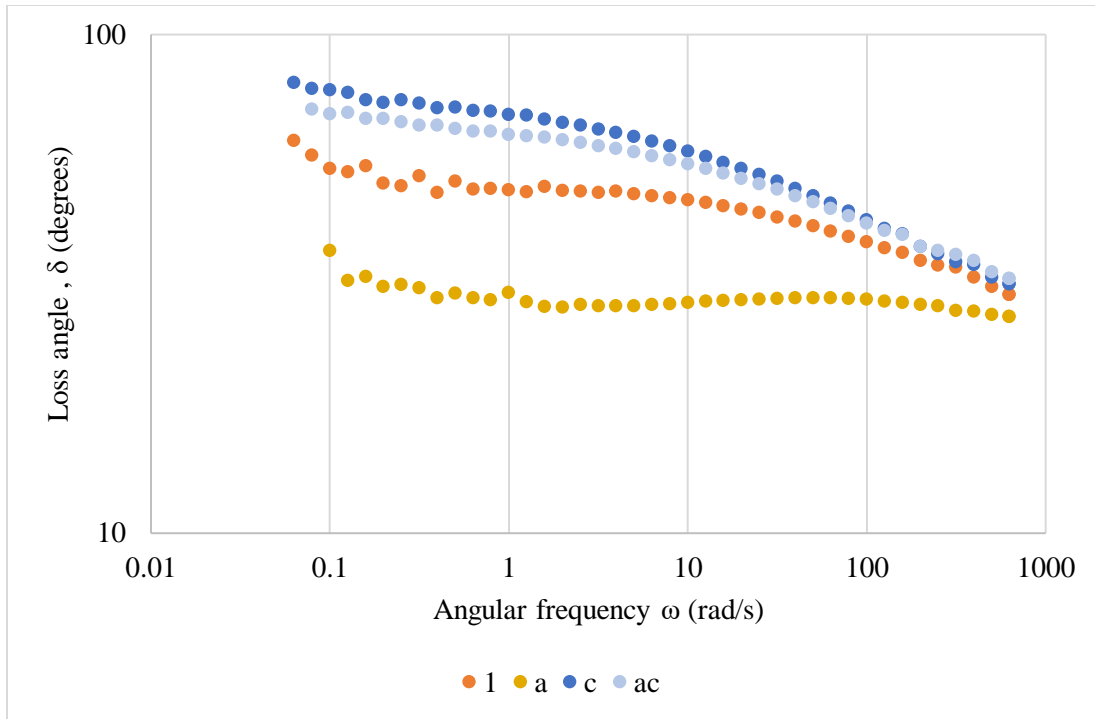
Figure 5-22: Effect of radiation intensity and level of screen on the loss angle of LLDPE films. 1: 47% radiation intensity + no screen; a: 100% radiation intensity + no screen; c: 47% radiation intensity + screen; ac: 100% radiation intensity + screen

In general, purely elastic behaviour would be characterized by a loss angle of zero while purely viscous behaviour would be characterized by a loss angle of 90 degrees [37]. Figure 5-22 shows that the sample (a) has the lowest loss angle and that this loss angle is nearly independent of the shear rate. This is further evidence that this sample is highly crosslinked. As the radiation intensity decreases from 100% to 47%, the loss angle increases and begins to drop with increasing shear rate. When the screen is introduced the loss angle increases further, with the highest value reported for sample c. These results suggest that the screen decreases the bulk degree of crosslinking of the sample.
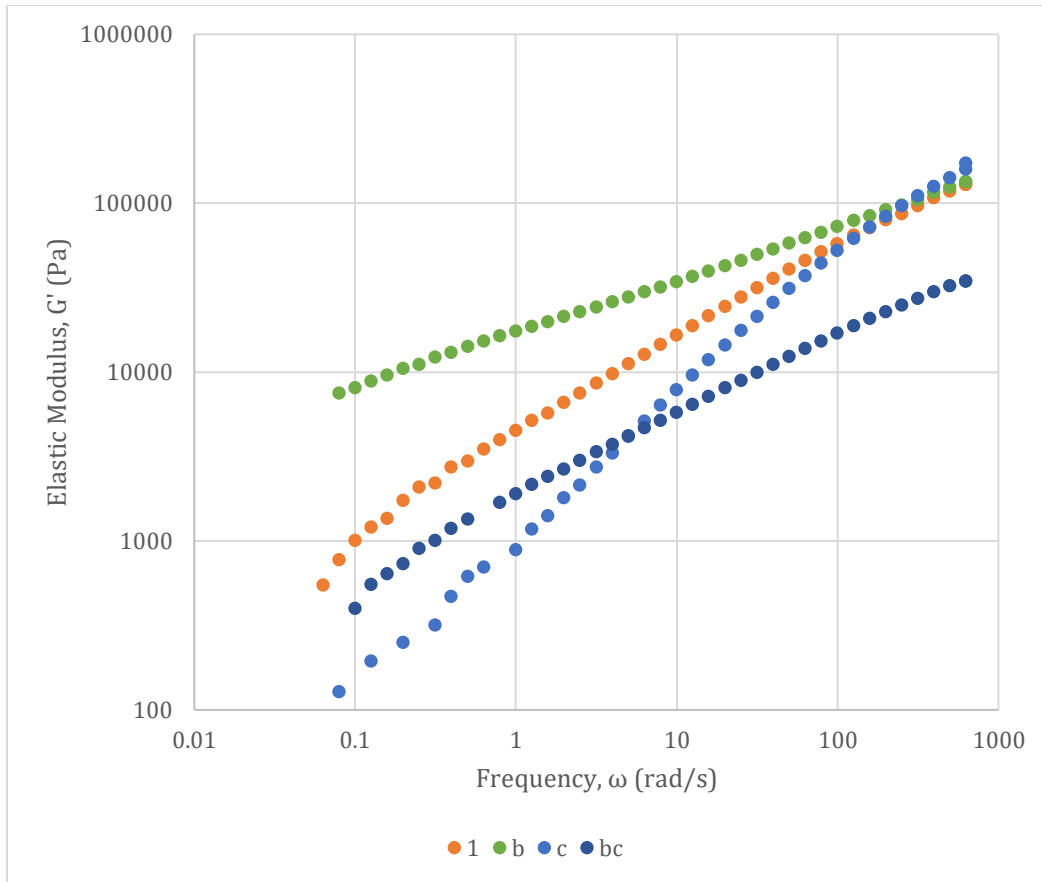
Figure 5-23: Effect of radiation time and screen on the storage modulus of LLDPE films. 1: 30 sec + no screen; b: 180 sec + no screen; c: 30 seconds + screen; bc: 180 sec + screen

Figure 5-23 indicates that radiation time mostly affects the elastic modulus in the low shear rate region. In the absence of a screen, increasing the radiation time from 30 seconds to 180 seconds causes the storage modulus in the low shear rate region to increase. In general, introducing the screen causes the modulus to decrease; however, the effect radiation time on the low shear modulus is the same as before.

It is interesting to note that while the samples radiated in the absence of the screen converge toward the same value in the high shear rate region, the samples irradiated with the screen present do not converge. Increasing the radiation time with the screen present causes the high shear modulus to decrease.
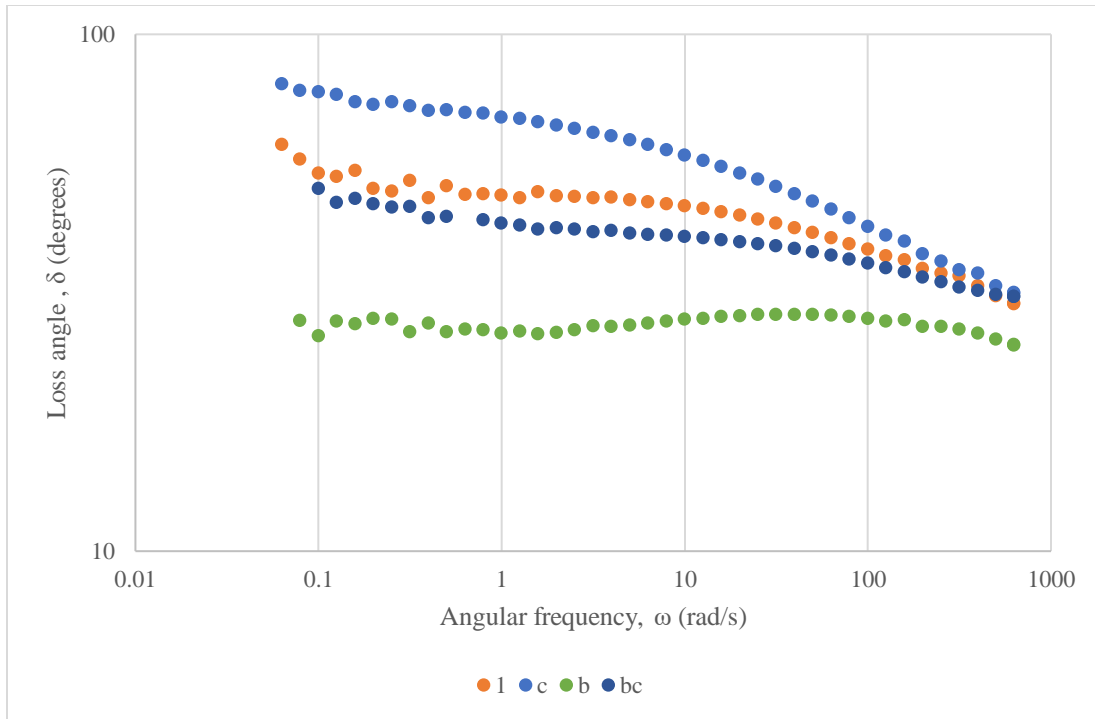
Figure 5-24: Effect of radiation time and screen on the loss angle of LLDPE films. 1: 30 sec + no screen; b: 180 sec + no screen; c: 30 seconds + screen; bc: 180 sec + screen

Figure 5-24 shows that increasing the radiation time cause the loss angle of the films to decrease and to become less sensitive to the shear rate. In general, a loss angle closer to zero indicates a material with more elastic behaviour while a loss angle closer to 90 suggests that the material has more viscous behaviour in the melt [37]. Accordingly, Figure 5-24 shows that increasing the radiation time increases the elasticity of the films. One possible cause of this increase in elasticity is the formation of crosslinks.

In this connection, it is interesting to note that the samples which were irradiated with the screen present have a higher loss angle compared to samples irradiated without a screen for the same duration of time. This suggests that while crosslinks are present in all the films, the screen might affect the crosslink density of the films. One way that this could happen is by constraining the location where crosslinks form by limiting the irradiated area on the films.

Effect of processing and radiation treatment on HDPE films

Given their ubiquity in the packaging industry, it is desirable to study the effect of the same radiation treatment variables on the mechanical and rheological properties of films made from high density polyethylene. The films considered in this study were formed using a method that results in the formation of a row nucleated lamellar microstructure. This morphology gives rise to materials that exhibit unusually high elongation, high modulus and high elastic recovery from high strains [39]. Additionally, micropores can form between the stacked lamellae, enabling these materials to be used for separation applications [40].

The study published herein will proceed in two stages. The first stage will explore the effect of compounding and processing variables on some macroscopic properties of HDPE films. The properties considered include: the tensile elongation at break, the tensile stress at break, the puncture resistance and the Gurley permeation rate.

The next stage of the study will explore the effect of adding 5 wt. % benzophenone to the precursor films. Similar to the study on LLDPE films, this section will consider the effect of radiation on the mechanical and the rheological properties of these films.

5.1.5 The effect of processing and radiation on HDPE films without photosensitizer

Table 5-18 re-introduces the variables that shall be reviewed in this study.

Table 5-18: Compounding and Radiation Variables

Factor	Letter Code	Low level	High Level
Concentration of HDPE (%)	A	95	100
Degree of stretch	B	Low	High
Screen	C	OFF	Screen 2
Radiation time (sec)	D	30	120
Radiation Intensity (%)	E	47	100

The effect of these variables on HDPE films will be studied by considering, in turn, their effect on the mechanical and barrier properties of the films.

Since the films that were considered in this study are used for separation processes, their resistance to mechanical failure is of crucial importance. The mechanical properties that are indicative of this resistance are the tensile stress at break, the elongation at break and the

puncture resistance. The tensile properties were studied in the machine and the transverse direction.

Table 5-19 lists the effect of the compounding variables on the tensile stress at break in the machine direction and transverse directions.

Table 5-19: Effect of radiation and compounding variables on the tensile stress at break in both the machine and transverse direction

	Machine Direction				Transverse Direction		
Factor	Effect (MPa)	95% Confidence Interval (MPa)	p-value	Factor	Effect	95% Confidence Interval (MPa)	p-value
A	-498.50	1754.81	1.42E-06	A	132.99	69.88	
B	265.51	1754.81	3.17E-03	B	10.29	69.88	
C	-58.43	1754.81	-	C	-64.87	69.88	
D	25.81	1754.81	-	D	30.21	69.88	
E	-53.63	1754.81	-	E	-7.19	69.88	
AB	133.90	1754.81	-	AB	-63.36	69.88	
AC	-70.48	1754.81	-	AC	-161.70	69.88	0.03
AD	15.05	1754.81	-	AD	17.72	69.88	
AE	104.95	1754.81	-	AE	21.02	69.88	
BC	27.44	1754.81	-	BC	9.60	69.88	
BD	-197.74	1754.81	0.02	BD	129.30	69.88	
BE	-123.06	1754.81	-	BE	106.26	69.88	
CD	-35.58	1754.81	-	CD	94.88	69.88	
CE	13.34	1754.81	-	CE	113.80	69.88	

DE	-17.85	1754.81	-	DE	-40.76	69.88	
ABC	-87.92	1754.81	-	ABC	-431.69	69.88	9.98E-07
ABD	31.04	1754.81	-	ABD	-3.74	69.88	
ABE	-20.24	1754.81	-	ABE	-55.81	69.88	
ACD	-171.82	1754.81	-	ACD	-11.67	69.88	
ACE	-30.78	1754.81	-	ACE	-20.21	69.88	
ADE	7.34	1754.81	-	ADE	190.32	69.88	0.01
BCD	41.48	1754.81	-	BCD	174.62	69.88	0.02
BCE	15.10	1754.81	-	BCE	28.15	69.88	
BDE	-28.06	1754.81	-	BDE	2.42	69.88	
CDE	-134.40	1754.81	-	CDE	117.42	69.88	
ABCD	-24.81	1754.81	-	ABCD	95.49	69.88	
ABCE	48.46	1754.81	-	ABCE	-37.43	69.88	
ABDE	-96.54	1754.81	-	ABDE	218.30	69.88	3.49E-03
ACDE	-90.09	1754.81	-	ACDE	23.79	69.88	
BCDE	112.54	1754.81	-	BCDE	26.38	69.88	
ABCDE	77.65	1754.81	-	ABCDE	102.81	69.88	

Since these treatments were un-replicated, it was not possible to directly obtain the error. Normal probability plots were used to identify the factors which had the highest probability of being statistically significant. The sums of squares of the rest of the factors were pooled in order to give an estimate of the error. Since they were used to estimate the error, it was not possible to determine the p-values of the effects of these factors. Figure 5-25 illustrates the use of normal probability plots to identify significant effects.
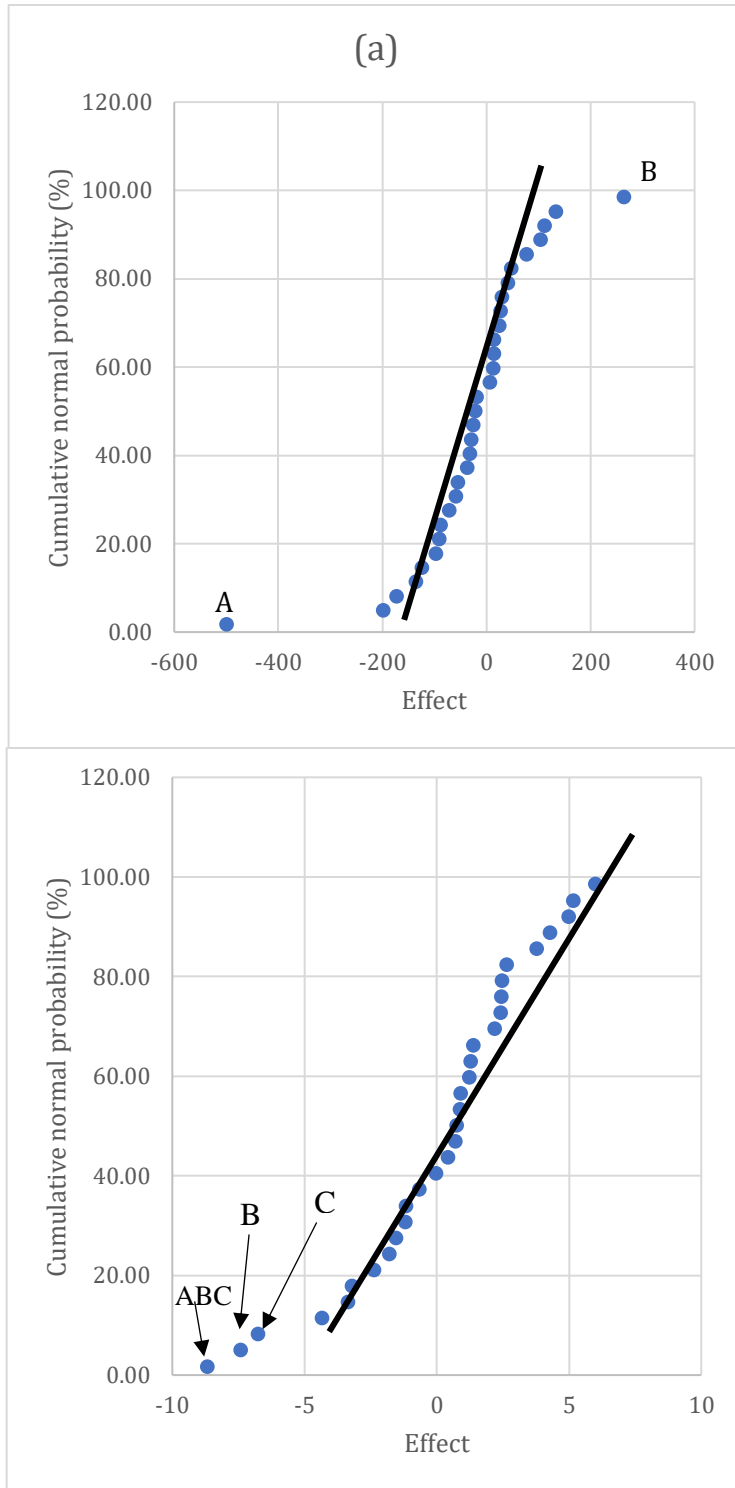
Figure 5-25: Normal Probability plots used to determine which factors have the highest probability of being significant. (a) Machine Direction (b). Transverse Direction

Table 5-19 shows that the tensile stress in the machine direction is affected by 4 variables while the tensile stress in the transverse direction is affected by 3 variables. This suggests that the tensile stress in the transverse direction is less sensitive to the compounding and radiation variables than the tensile stress in the machine direction. Furthermore, the magnitude of the effect of the variables is much higher in the machine direction than in the transverse direction. This can be attributed to the strength imparted to the films as a result of the orientation of the crystals in the machine direction [39] [40].

It is interesting to note that the manner in which the compounding and radiation variables affect the tensile stress of the film is affected by their orientation. For example, the degree of stretch has a positive effect on the tensile stress at break in the machine direction but a negative effect in the transverse direction. Similarly, the level of the screen is a significant main factor with a negative effect in the transverse direction while it is not a significant main factor in the machine direction. Finally, neither the radiation intensity nor the radiation time significantly affects the tensile stress in the transverse direction whereas the interaction between the radiation time and the degree of stretch is significant in the machine direction.

Table 5-19 indicates that the interaction between stretching and radiation time is significant in the machine direction. Figure 5-26 illustrates this interaction using a marginal means plot.
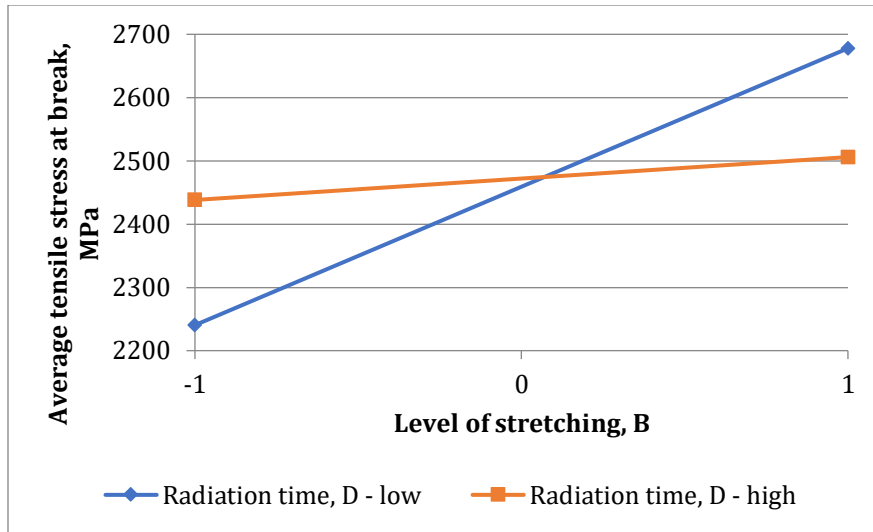
Figure 5-26: Interaction between the effect of degree of stretching and radiation time on the average tensile stress at break of HDPE films.

Figure 5-26 shows that the effect of radiation time is highly dependent on the level of stretching. In the precursor films (low degree of stretching), increasing the radiation time causes the average tensile stress at break to increase from 2240.4 MPa to 2438.2 MPa. When the films are stretched, increasing the radiation time causes the average tensile stress at break to decrease from 2677.9 MPa to 2506.0 MPa.

This behaviour may be attributed to the effect of stretching on the morphology of the films. In general, stretching causes the films to become even more crystalline and oriented in the direction of the stretch [39] [40]. Since the crosslinking reaction occurs in the amorphous region of the polymer, this means that fewer chains are available for crosslinking in the stretched films, resulting in a material with smaller crosslink density than the precursor film.

One other salient observation from Figure 5-26 is that at high radiation time, the average tensile stress at break is relatively insensitive to the degree of stretching while at low radiation time, the average tensile stress at break increases with increased stretching.

Table 5-20 lists the effects and significance levels of the processing and radiation variables on the tensile stress at break

94

Table 5-20: Effects and significance levels of radiation and compounding variables on the tensile strain at break of HDPE films

	Machine Direction				Transverse Direction		
Factor	Effect (%)	95% Confidence Interval	p-value	Factor	Effect (%)	95% Confidence Interval	p-value
A	5.73	30.28	4.35E-04	A	132.99	1726.84	
B	-3.69	30.28	0.02	B	10.29	1726.84	
C	-1.12	30.28		C	-64.87	1726.84	
D	-1.91	30.28		D	30.21	1726.84	
E	-1.42	30.28		E	-7.19	1726.84	
AB	-4.37	30.28	0.01	AB	-63.36	1726.84	
AC	-2.20	30.28		AC	-161.70	1726.84	0.025
AD	-1.58	30.28		AD	17.72	1726.84	
AE	-0.60	30.28		AE	21.02	1726.84	
BC	0.25	30.28		BC	9.60	1726.84	
BD	1.31	30.28		BD	129.30	1726.84	
BE	1.41	30.28		BE	106.26	1726.84	
CD	2.25	30.28		CD	94.88	1726.84	
CE	-0.60	30.28		CE	113.80	1726.84	
DE	0.80	30.28		DE	-40.76	1726.84	
ABC	0.41	30.28		ABC	-431.69	1726.84	9.98E-07
ABD	2.90	30.28		ABD	-3.74	1726.84	
ABE	2.06	30.28		ABE	-55.81	1726.84	
ACD	0.50	30.28		ACD	-11.67	1726.84	

ACE	-1.00	30.28		ACE	-20.21	1726.84	
ADE	-0.99	30.28		ADE	190.32	1726.84	0.01
BCD	-3.53	30.28	0.02	BCD	174.62	1726.84	0.016
BCE	0.70	30.28		BCE	28.15	1726.84	
BDE	-0.67	30.28		BDE	2.42	1726.84	
CDE	-1.01	30.28		CDE	117.42	1726.84	
ABCD	-3.32	30.28	0.03	ABCD	95.49	1726.84	
ABCE	3.12	30.28		ABCE	-37.43	1726.84	
ABDE	-0.05	30.28		ABDE	218.30	1726.84	3.49E-03
ACDE	-1.55	30.28		ACDE	23.79	1726.84	
BCDE	0.75	30.28		BCDE	26.38	1726.84	
ABCDE	0.17	30.28		ABCDE	102.81	1726.84	

Similar to Table 5-19, Table 5-20 shows that the factors which affect the tensile strain at break in the machine direction are different from those factors which affect the tensile strain at break in the transverse direction. In the machine direction, two main factors, concentration of HDPE and degree of stretch affect the tensile strain at break while in the transverse direction; no main factors have a significant effect. Furthermore, the radiation intensity does not significantly affect the tensile strain at break in the machine direction while in the transverse direction it does when in combination with other factors. These observations suggest that the films are highly anisotropic.

Table 5-20 indicates that a significant interaction between the concentration of HDPE and the degree of stretching exists in the machine direction. The effect of this interaction is illustrated in Figure 5-27
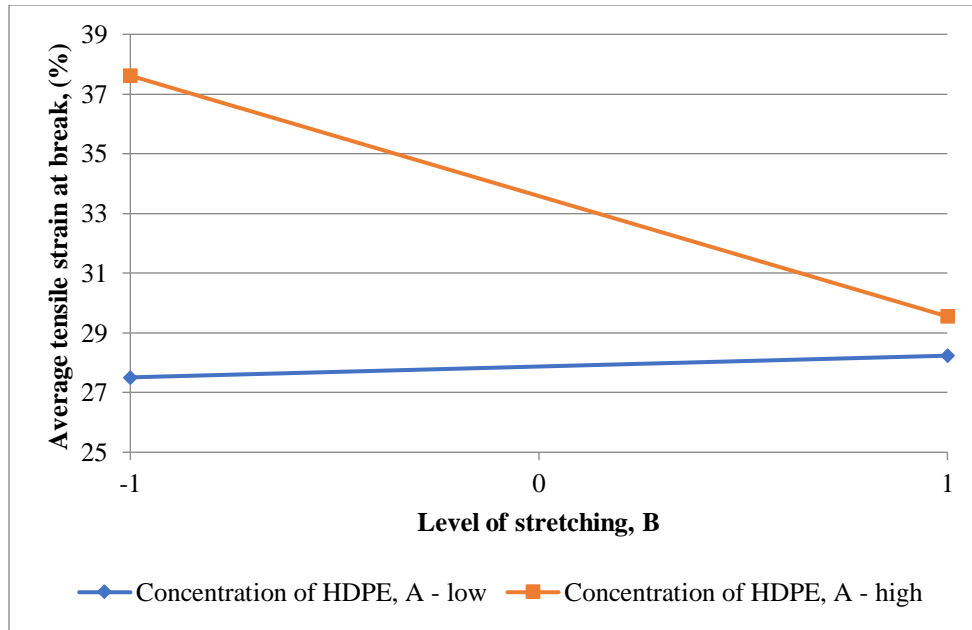
Figure 5-27: Effect of the interaction between degree of stretching and concentration of HDPE on the tensile strain at break of HDPE films.

Figure 5-27 indicates that the effect of stretching the films is highly dependent on the concentration of HDPE. When the concentration of HDPE is at the low level (95 wt. %), stretching the film causes the tensile strain at break to increase slightly. When the concentration of HDPE is at the high level (100 wt. %), stretching the films causes the average tensile strain at break to decrease from 37.62 % to 29.55 %. Nonetheless, Figure 5-27 shows that regardless of the level of stretching, films with 100% HDPE exhibit a higher tensile strain at break.

In the transverse direction, a significant interaction exists between the concentration of HDPE and the illumination pattern (Table 5-20). This interaction is illustrated in Figure 5-28.
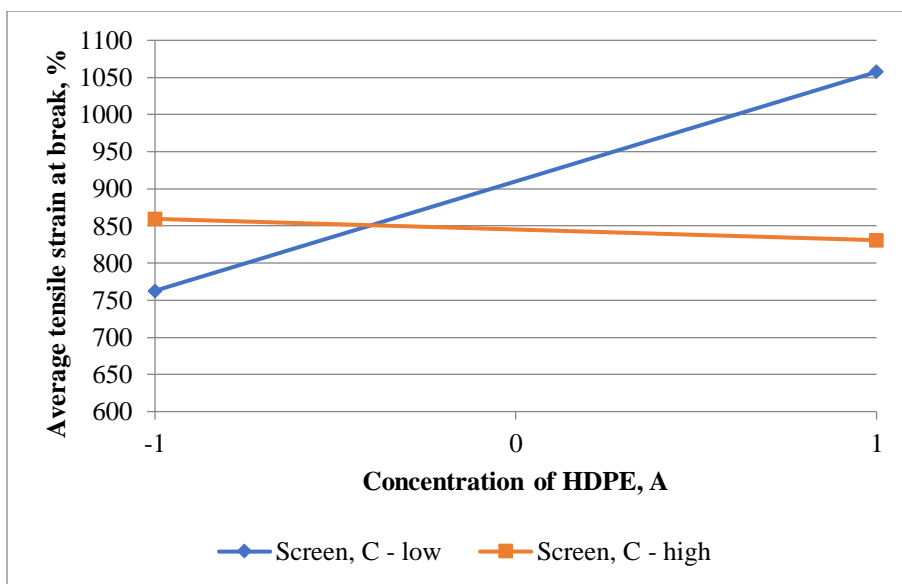
Figure 5-28: Effect of the interaction between concentration of HDPE and the level of the screen on the tensile strain at break in the transverse direction of HDPE films

Figure 5-28 indicates that radiation under a screen modifies the effect of changing the concentration of HDPE in the films. When the screen is off, increasing the concentration of HDPE causes the tensile strain at break to increase from 762.73 % to 1057.43%. When the screen is on, and the sample is illuminated, increasing the concentration of HDPE causes the tensile strain at break to decrease slightly.

It is instructive to note the effect of introducing a screen on the tensile strain at break in the transverse direction. At a low concnentration of HDPE, increasing the level of the screen from off to on causes the average tensile strain at break to increase by 96.84%. Conversely, at a high concentration of HDPE, increasing the level of the screen causes the tensile strain at break to decrease by 226.57 %.

The observations made above imply that the effect of the illumination pattern is dependent on the composition of the film. A possible explanation can be advanced by noting that the samples with a low concentration of HDPE are actually blends of 95 wt.% HDPE with 5 wt.% LLDPE. It is hypothesised that this small amount of LLDPE decreases the crystallinity of the resin, enabling it to form crosslinks more easily when it is irradiated. In the absence of LLDPE, the crystallinity of the resin increases, causing the efficiency of crosslink formation to decrease. Since in air, the

crosslinking reaction competes with chain scission by oxidation, the tensile strain at break decreases with increasing HDPE concentration.

The puncture resistance is a property used to measure the ability of a film to resist intrusion by a foreign object. Along with the tensile properties described above, it is a useful measure of the robustness of the films. For this reason, it is important to understand how the compounding and radiation variables examined in this study affect the puncture resistance. Table 5-21 lists the effects and p-values of the variables that were found to significantly affect this property.

Table 5-21: Effects and p-values of statistically significant factors and interactions on the puncture resistance of HDPE films

Factor	Effect (MPa)	95% Confidence Interval (MPa)	p-value
A	7.85	94.73	0.05
B	-11.21	94.73	0.006
C	-1.96	94.73	-
D	1.03	94.73	-
E	8.23	94.73	0.038
AB	-3.65	94.73	-
AC	-6.38	94.73	-
AD	0.34	94.73	-
AE	4.24	94.73	-
BC	2.79	94.73	-
BD	4.33	94.73	-
BE	-7.98	94.73	-
CD	3.90	94.73	-
CE	-12.03	94.73	0.004
DE	-2.74	94.73	-

ABC	13.18	94.73	0.002
ABD	-0.86	94.73	-
ABE	-5.76	94.73	-
ACD	0.69	94.73	-
ACE	-5.74	94.73	-
ADE	0.97	94.73	-
BCD	-4.05	94.73	-
BCE	10.03	94.73	0.013
BDE	-0.14	94.73	-
CDE	-0.06	94.73	-
ABCD	-2.76	94.73	-
ABCE	4.91	94.73	-
ABDE	1.08	94.73	-
ACDE	11.38	94.73	0.006
BCDE	1.49	94.73	
ABCDE	-12.18	94.73	0.004

Table 5-21 indicates that both the concentration of HDPE and the degree of stretching significantly affect the puncture resistance of the films. Increasing the concentration of HDPE causes the average puncture resistance of the films to increase by 7.850 MPa while stretching the films causes the puncture resistance to decrease by 11.213 MPa. The loss in puncture resistance as a result of stretching can be felt even in how the stretched films handle. They tear very easily and are require great care when cutting.

It is interesting to note from Table 5-21 that increasing the radiation intensity causes the puncture resistance to increase by 8.225 MPa but that the interaction between radiation intensity and the

screen exerts a negative effect on the films. This interaction is explored with the aid of Figure 5-29.
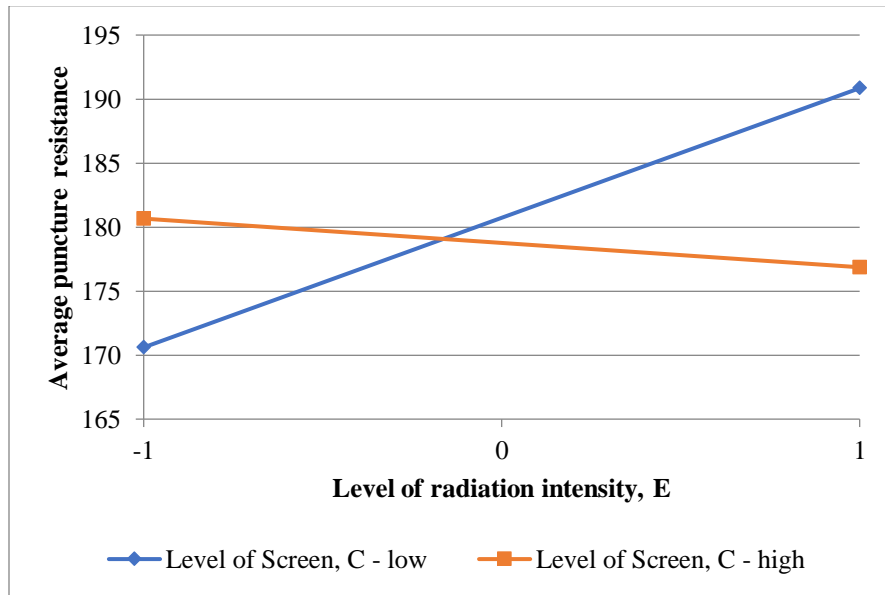
Figure 5-29: Effect of the interaction between radiation intensity and the level of the screen on the average puncture resistance of HDPE films.

Figure 5-29 shows that the effect of radiation intensity on the puncture resistance of the films is conditioned by the level of the screen. When the screen is off, increasing the radiation intensity causes the puncture resistance to increase by 20.3 MPa; however, when the screen is on, increasing the radiation intensity causes the puncture resistance to decrease by 3.8 MPa.

Alternatively, it can be seen from Figure 5-29 that at the low level of radiation intensity, increasing the level of the screen increases the average puncture resistance while at the high level of radiation intensity, increasing the level of the screen causes the average puncture resistance to decrease.

The permeability of the films to air was measured in Gurley seconds. A Gurley second is a unit which describes the air permeability as a function of the time required for 100 cm_3 of air to pass through 1.0 $inch_2$ of a given material [41]. When analysis of variance was applied to the effects of the radiation and processing variables, it was found that only the concentration of HDPE significantly affects the permeability of the films. The effect of HDPE concentration was found to be -357.0 seconds with a p-value of 5×10^{-7} this means that when the concentration of

HDPE was increased from 95 to 100 wt. %, the time taken for 100 cm₃ of air to pass through the films decreased by 357.0 seconds, indicating that the films became significantly more permeable.

It is well known that a condition of forming a "row-nucleated lamellar" morphology is a high degree of crystallinity in the base resin [39] [40]. Furthermore, it has been established that the permeability of films with this morphology comes from slit-like pores which form between stacked lamellae. It can thus be inferred that the addition of LLDPE diminishes the ability of the base HDPE to attain to the desired morphology and thus reduces the permeability of the film overall. When this solute is removed, the resin's porosity increases because its microstructure becomes more regular.

It is reasonable that radiation would not significantly affect the permeability of the films. Crosslink formation is known to occur mostly in the amorphous region as it is here that macro-radicals would have sufficient mobility to interact with each other by forming crosslinks [42]. On the other hand, the permeability of the films is due to the formation of pores between lamellae in the crystalline region. These two processes can therefore be understood as occurring in different regions of the same film and cannot interact with each other.

5.1.6   Exploring the effect of adding benzophenone as a photosensitizer

Benzophenone is known to act as a photosensitizer in the UV crosslinking of polyethylene [22] [19]. Accordingly, the present study of the response of HDPE films to radiation treatment was extended by examining the mechanical and rheological properties of precursor films bearing a 1 wt. % loading of benzophenone.

Investigations carried out by Qu et al [22] found that the mechanism through which benzophenone improves the crosslinking density of UV radiated polyethylene begins with the absorbance of a quantum of ultraviolet radiation the benzophenone molecule. The efficiency of this process can be improved by matching the output wavelength of the radiation source to the absorbance wavelength of benzophenone, which is 260 nm.

The UV lamp used in the study thus far had a peak wavelength at 365 nm. Since it is desirable to match the output of the radiation source to the absorbance of the main chromophore, a new lamp with a peak wavelength of 278nm was installed. Since UV lamps output radiation in broad frequency range, it is expected that shifting the peak wavelength closer to the absorbance of

benzophenone would have the concomitant effect of increasing the radiative flux at this frequency.

This section will examine the effect of radiation intensity, time and screen on the mechanical properties of HDPE films. To maintain continuity with the study reported above, the mechanical properties that shall be considered in this section include the tensile stress at break and the tensile strain at break.

Table 5-22 lists the effects and p-values of the radiation variables on the tensile stress at break in both the machine and transverse direction.

Table 5-22: Effect of radiation variables on the tensile stress at break of HDPE precursor films in the machine and transverse directions

Machine Direction				Transverse Direction			
Factor	Effect (MPa)	95% Confidence Interval	p-value	Factor	Effect	95% Confidence Interval	p-value
A	-8.32	2.86	0.0008	A	0.30988	1.22	0.47
B	-2.69	2.86	0.04	B	1.84663	1.22	0.01
C	9.55	2.86	0.0004	C	-0.79538	1.22	0.11
AB	0.52	2.86	0.60	AB	0.43416	1.22	0.32
AC	-0.08	2.86	0.93	AC	-0.36230	1.22	0.40
BC	-0.80	2.86	0.43	BC	-0.86732	1.22	0.089
ABC	-0.19	2.86	0.84	ABC	-0.29035	1.22	0.49

It is interesting to note from Table 5-22 that the main factors have different effects in the machine and transverse direction. In the machine direction, increasing the level of radiation intensity causes the tensile stress at break to decrease by 8.32 MPa while in the transverse direction; radiation intensity does not significantly affect the tensile stress at break. Similarly, increasing the radiation time causes the tensile stress at break in the machine direction to

decrease by 2.69 MPa while in the transverse direction, it increases by 1.85 MPa. Finally, in the machine direction, using a screen causes the tensile stress at break to increase by 9.55 MPa while in the transverse direction; its effect is not statistically significant. These observations suggest that the anisotropy of the films plays a significant role in determining how they respond to radiation treatments.

Table 5-22 indicates that the effect of the interaction between radiation time and the screen is significant at the 10% significance level. This interaction is shown in Figure 5-30.
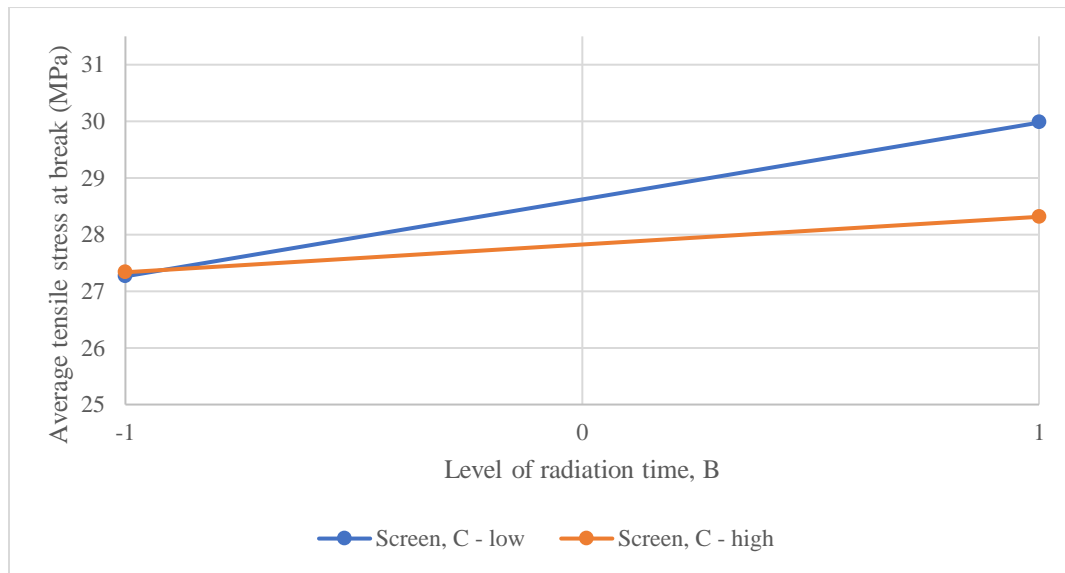
Figure 5-30: Effect of interaction between level of radiation time and level of screen on the tensile stress at break in the transverse direction of HDPE films loaded with 10 wt. % benzophenone

Figure 5-30 shows that the screen modifies the rate and extent to which increasing radiation time causes the average tensile stress at break to increase. In the absence of a screen, increasing the radiation time causes the average tensile stress at break to increase by 2.71 MPa. When radiation is carried out in the presence of the screen, increasing the radiation time from 30 seconds to 120 seconds causes the average tensile stress at break to increase by 0.98 MPa.

The tensile strain at break is a measure of the amount of deformation that a material can sustain before rupture. Since the kind of radiation treatment being explored in this study would be incorporated into a post-processing operation, it is important to understand how it affects the

tensile strain at break. Accordingly, Table 5-23 lists the effect of the radiation treatment variables on the elongation at break in both the machine and transverse directions.

Table 5-23: Effects of radiation treatment variables on the tensile strain at breakoff HDPE films in the machine and transverse directions

Machine Direction				Transverse Direction			
Factor	Effect (%)	95% Confidence Interval	p-value	Factor	Effect (%)	95% Confidence Interval	p-value
A	-12.56	3.19	0.0002	A	-0.47	0.15	0.0007
B	5.39	3.19	0.0058	B	0.04	0.15	0.44
C	9.27	3.19	0.0008	C	0.10	0.15	0.12
AB	3.20	3.19	0.03	AB	0.49	0.15	0.0005
AC	-6.87	3.19	0.0024	AC	0.03	0.15	0.56
BC	-7.62	3.19	0.0016	BC	0.10	0.15	0.12
ABC	-0.91	3.19	0.41	ABC	0.03	0.15	0.58

Table 5-23 exhibits the same kind of trend as Table 5-22 in that the effect and significance of the radiation variables is dependent on the orientation of the film. In the machine direction, all of the main factors and all of the binary interactions are significant while in the transverse direction; one main factor (radiation intensity) and one binary interaction are significant.

Nevertheless, Table 5-23 indicates that the effects of the main factors are qualitatively similar in both orientations. For example, increasing the level of radiation intensity from 47% to 100% causes the average tensile strain at break to decrease by 12.56 MPa in the machine direction and -0.47 MPa in the transverse direction. Similarly, increasing the radiation time causes the tensile strain at break to increase by 5.39 MPa in the machine direction and 0.04 MPa in the transverse direction (though this effect is not statistically significant).

The binary interactions in the machine direction are illustrated in Figure 5-31.
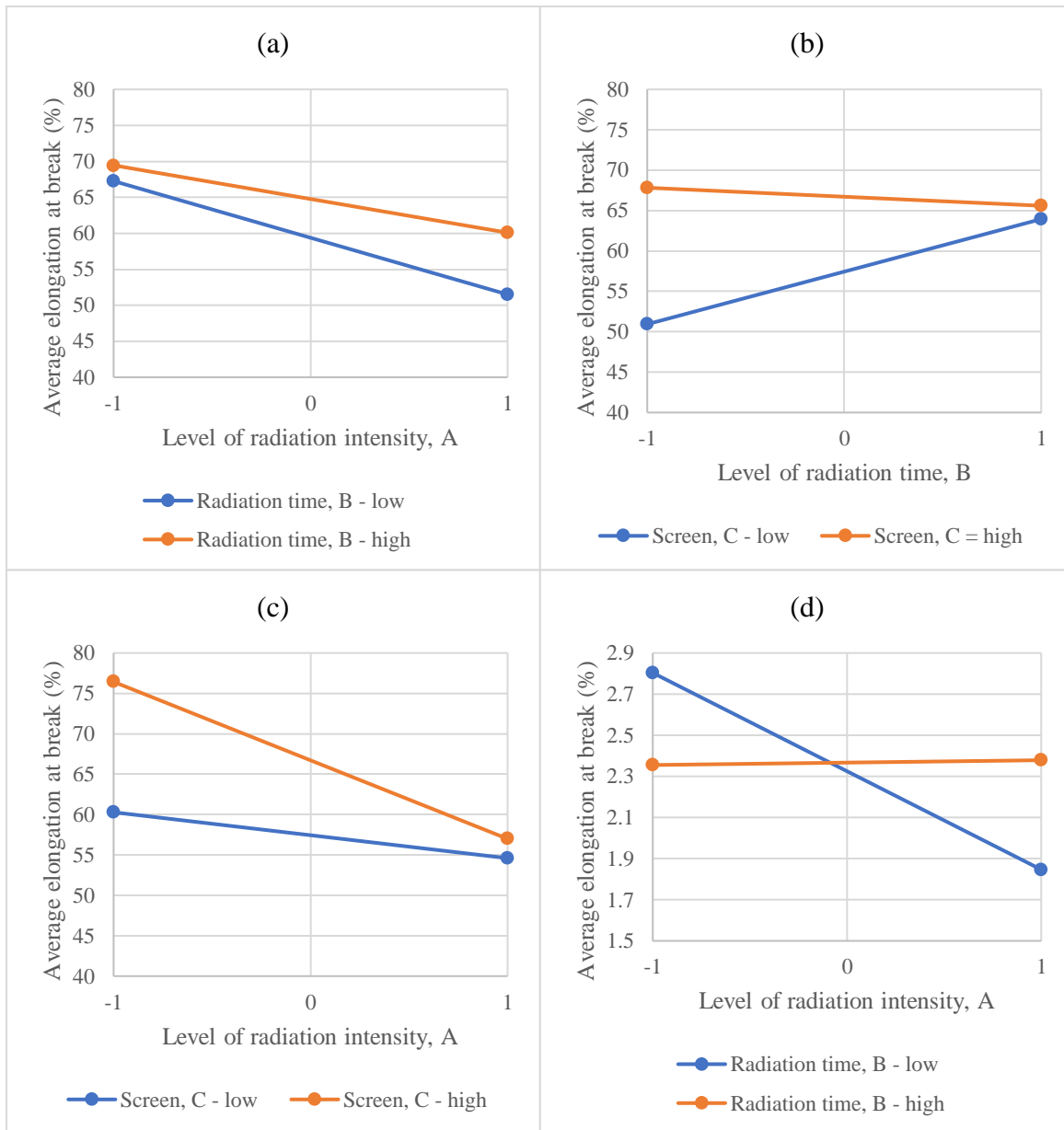
Figure 5-31: Effect of binary interactions on the elongation at break of HDPE films in the machine (a – c) and transverse (d) directions.

Figure 5-31 (a) and (c) illustrate that both the radiation time and the screen modify the effect of increasing the level of radiation intensity. In Figure 5-31 (a), the tensile strain at break decreases more rapidly with increasing intensity when the level of radiation time is low. Increasing the level of radiation time decreases the extent to which the tensile strain at break decreases with increasing radiation intensity.

Figure 5-31 (b) and (c) show that the screen significantly modifies the effect of radiation time and intensity on the tensile stress at break in the machine direction. Figure 5-31 (c) indicates that when the screen is on, the tensile strain at break decreases more sharply with increasing radiation intensity than when the screen is off. Figure 5-31 (b) indicates that when the screen is off, increasing the level of radiation time causes the average elongation at break to increase by 13.00%. When the screen is on, increasing the level of radiation time causes the average elongation at break in the machine direction to decrease by 2.23MPa.

The tendency of the screen to modify the effect of radiation intensity on the tensile strain at break is also apparent in the transverse direction. Figure 5-31 (d) illustrates that when the screen is off; increasing the level of radiation intensity causes the average elongation at break to decrease by 0.96 % whereas, when the screen is on, increasing the radiation intensity causes the average elongation at break to increase by 0.02 %.

5.1.6.1 Conclusion

Table 5-24 lists the effects of the radiation variables on the tensile properties of the photosensitized HDPE films.

Table 5-24: Summary of effects of radiation variables on the tensile properties of photosensitized HDPE films in the machine and transverse directions

Factor	Effects			
	Machine Direction		Transverse Direction	
	Tensile stress at break (MPa)	Tensile strain at break (%)	Tensile stress at break (MPa)	Tensile strain at break (%)
A	-8.32	-12.56	0.31	-0.47
B	-2.69	5.39	1.85	0.04
C	9.55	9.27	-0.80	0.10
AB	0.52	3.20	0.43	0.49
AC	-0.08	-6.87	-0.36	0.03
BC	-0.80	-7.62	-0.87	0.10
ABC	-0.19	-0.91	-0.29	0.03

Comparing the effects of the main factors alone, Table 5-24 illustrates that the effect of radiation intensity, radiation time and screen are dependent on the orientation of the films. In the machine direction, increasing the level of radiation intensity causes both the tensile stress at break and the

tensile strain at break to decrease. However, in the transverse direction, increasing the level of radiation intensity causes the tensile stress at break to increase and the tensile strain at break to decrease. Similarly, increasing the level of radiation time causes the tensile stress at break in the machine direction to decrease while the tensile stress at break in the transverse direction increases. Finally, increasing the level of the screen causes the tensile stress and strain at break to increase in the machine direction while it causes the tensile stress at break to decrease in the transverse direction and the tensile strain at break to increase.

Comparing the results presented in Table 5-12, Table 5-13 and Table 5-24 it can be observed that for the LLDPE films, only the effect of radiation time was dependent on the orientation of the films while for the HDPE films all of the main factor effects were dependent on orientation. This could be a result of the greater orientation of the HDPE films due to the special technique used to fabricate them.

In addition to revealing the effect of anisotropy, Table 5-12, Table 5-13 and Table 5-24 show that the effect of the screen is consistently opposite in sign to the effect of radiation intensity. This suggests that the effect of introducing a screen is distinct from the effect of radiation intensity.

5.1.7 Effect of radiation treatment on the rheological properties of HDPE films

Examining the mechanical and barrier properties of the HDPE films enabled insights into the effect of radiation treatment on their macroscopic behaviour. Now, attention will be given to examining the effect of radiation on the molecular architecture of the films. This will be done by the aid of rheological measurements since they are quite sensitive to the molecular architecture of the films.

The properties that shall be examined here are the cross-over modulus and the complex viscosity. Furthermore, the scope of the study was extended to compare the effect of radiation treatment under two screens. The properties of these screens are listed in Table 5-25.

Table 5-25: Properties of photo-masking screens

	Screen 1	Screen 2
Hole diameter (inches)	0.0156	0.0330
Centre to centre distance	0.055	0.055
Thickness (inches)	0.0225	0.0225
Orientation of centres	60° staggered centre	Straight line centres

As can be seen in Table 5-25, the key differences between the two screens is the diameter of the holes and the orientation of the centres. It is expected that these properties affect the open area of the screen as well as the illumination pattern under them.

Plots of the dynamic moduli of the films under different illumination conditions are presented in Figure 5-32. It can seen in (a) that a crossover modulus exists in the untreated film and occurs at about 0.39 rad/s with a modulus value of 1370 Pa. After radiation treatment, no crossover modulus is observed for any of the samples (b) to (c). The disappearance of the cross-over modulus has been correlated with a high degree of crosslinking [43]. Therefore, it can be inferred that all of the irradiated samples are highly crosslinked. This can be attributed to the better matching of the emission spectrum of the UV lamp to the absorbance spectrum of benzophenone as well as to the concentration of benzophenone in the films.
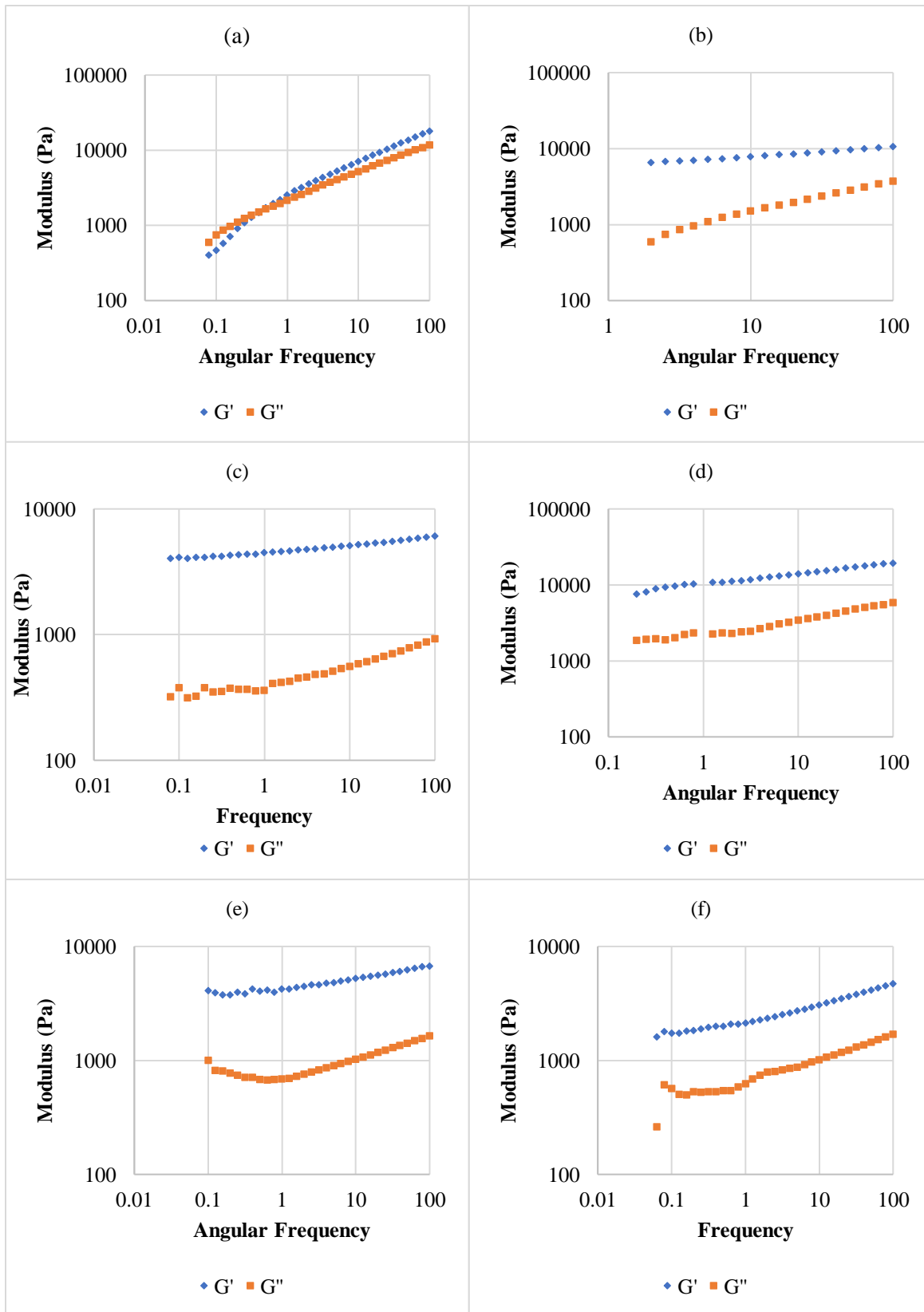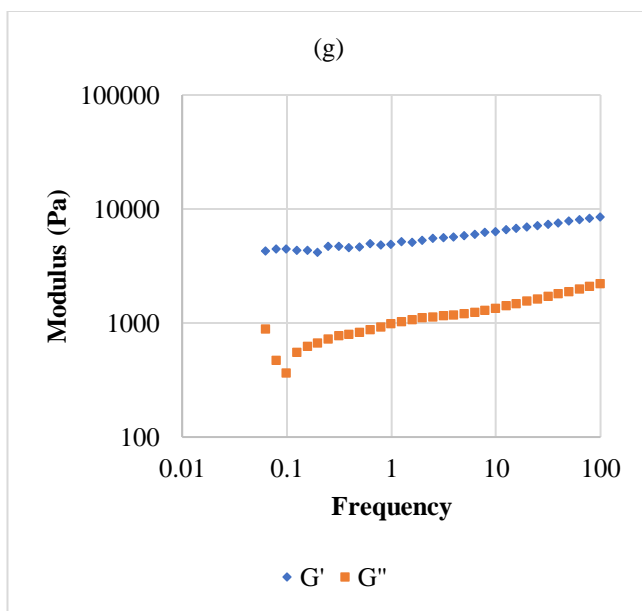
Figure 5-32 Effect of radiation treatment variables on the crossover modulus of HDPE films. (a) Untreated film, (b): 47% light intensity + no screen; (c): 100% light intensity + no screen; (d) 47% light intensity + screen 1; (e): 100% light intensity + screen 1; (f): 47% light intensity + screen 2; (g): 100% light intensity + screen 2

The distinction between the screens can be better appreciated by examining their effect on the viscosity of the films (Figure 5-33). The untreated film approaches a Newtonian Plateau as the shear rate approaches 0.07 rad/s. All of the treated films have a higher viscosity than the untreated film in this region and exhibit shear-thinning behaviour. This shift in viscosity to higher values in the low shear rate region is a sign of increased molecular weight [44]

It is interesting to observe the difference between samples treated at the low level of radiation intensity but with different screens (c_1 and c_2). Sample c_2 shows a smaller increase in the low shear rate viscosity than sample c_1. This suggests that sample c_1 has a higher molecular weight than sample c_2 even though they have been irradiated using light of the same intensity and for the same duration of time. What is even more striking is that the sample c_1 has a higher viscosity than even the sample treated at high intensity without a screen (a).

The screens also appear to affect the shear thinning behaviour of the films. This can be observed by examining the samples treated at a high level of radiation intensity (a, ac_1 and ac_2). The viscosity of these samples is very similar in the low shear rate region; however, as the shear rate increases, differences in their shear thinning behaviour can be observed.

111
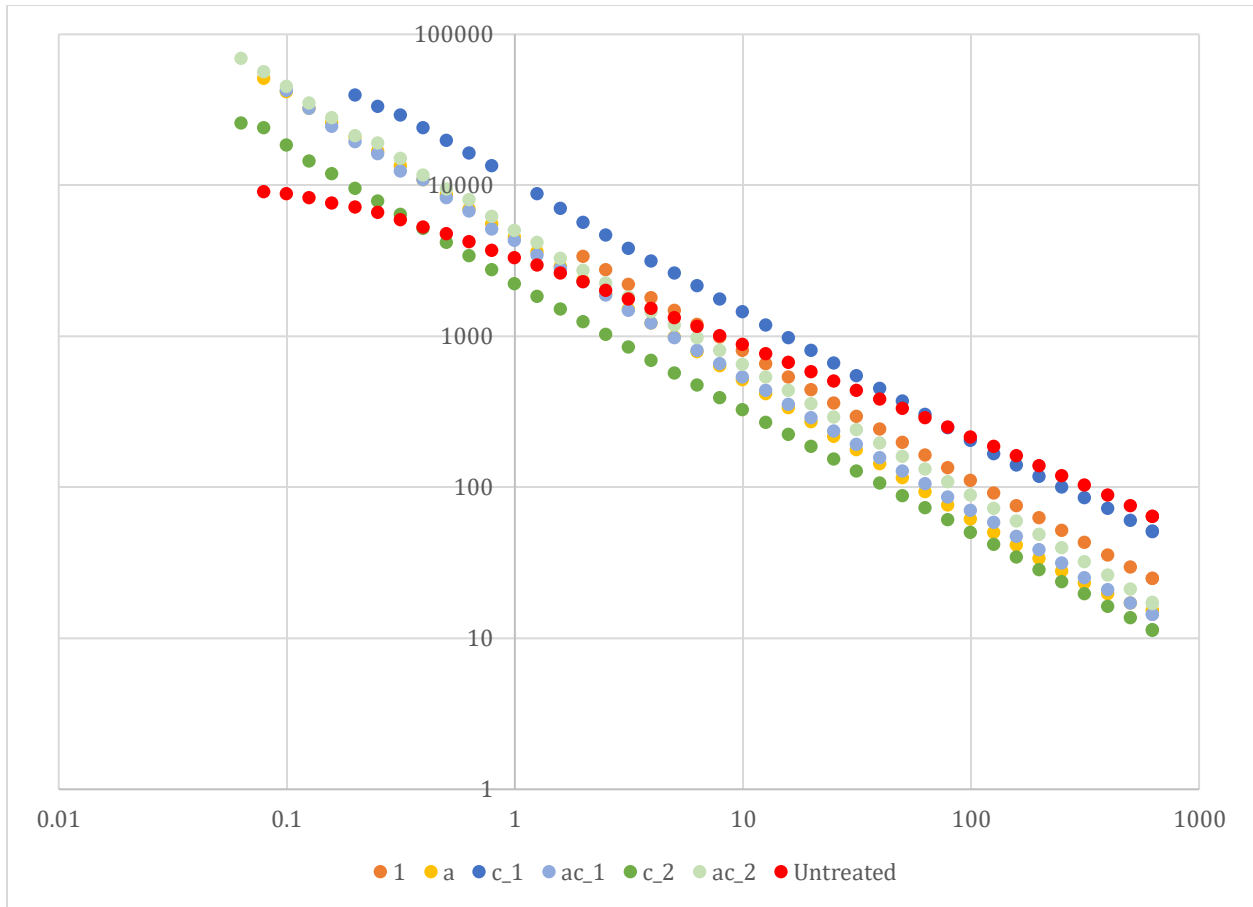
Figure 5-33: Effect of radiation variables on the complex viscosity of HDPE films. (1): 47% light intensity + no screen; (a): 100 % light intensity + no screen; (c_1): 47% light intensity + screen 1; (ac_1): 100% light intensity + screen 1; (c_2): 47% light intensity + screen 2; (ac_2): 100% light intensity + screen 2

Sample a exhibits the greatest degree of shear thinning followed closely by sample ac_1 and then by sample ac_2. Since the shear thinning behaviour is related to the molecular weight distribution [44], it can be inferred that the screen have a subtle effect on the molecular weight distribution of the films. Comparing ac_2 and ac_1, it is inferred that illumination under screen 1 broadens the molecular weight distribution of the HDPE films more relative to screen 1.

6   CONCLUSIONS AND RECOMMENDATIONS

Conclusions

The primary objective of this work was to examine the effect of UV irradiation variables on the mechanical and rheological properties of HDPE and LLDPE films. The reason for investigating their mechanical properties is because these often determine the end use of films. The rheological properties were investigated because they provide rich insight into the effect of irradiation on the molecular architecture of the films. By combining these two sources of information, a deeper understanding of the structure-property relationships of the films could be achieved. The radiation variables that were studied include: radiation time, radiation intensity and illumination pattern. The illumination pattern was altered using two different photo-masking screens.

The properties that were investigated varied according to the resin. For the LLPE films, an exhaustive study of tensile properties was conducted, followed by an investigation on the rheological and linear viscoelastic properties. For the HDPE films, two tensile properties were investigated, complemented by a study of the puncture resistance and the air permeability. Following this study, the HDPE resin was loaded with 1 wt. % benzophenone and an examination of the mechanical and rheological properties of the photosensitized films was conducted.

The key results from this investigation are as follows:

1. The radiation variables affect different mechanical properties differently. For example, only the intensity and the screen affect the modulus of elasticity while all three variables (radiation intensity, time and illumination pattern) affect the tensile stress at break and the elongation at break. In general, it was found that the photo-masking screen caused the elastic modulus to decrease but caused the elongation and stress at break to increase.

2. For the HDPE samples that were not loaded with benzophenone, the effect of radiation intensity was found to be dependent on the level of the screen. When the screen was absent, increasing intensity caused the puncture resistance to increase. When the screen is present, increasing the intensity causes the puncture resistance to decrease.

3. It was found that the radiation treatment variables did not significantly affect the permeability of the HDPE films.

4. For the LLDPE films, the screen modified both the viscosity and the linear viscoelastic behavior of the films.

   a. The effect of the screen on viscosity was to modify the rate at which the zero-shear viscosity of the films increased with an increase in radiation intensity. Since the zero-shear viscosity is related to the molecular weight of the films, it may be inferred that the screen affected the rate at which the films weight average molecular weight increased with increasing intensity.

   b. The rheological polydispersity of the films was studied using two different indices: the polydispersity index PI(Z) and the ER. It was found that for the same level of radiation intensity, samples irradiated with the screen had a smaller polydispersity than samples irradiated without a screen. Since the rheological polydispersity index is an indirect measured of the molecular weight distribution, it was found that the samples irradiated with the screen present had a narrower molecular weight distribution than samples irradiated without a screen.

   c. Finally, by studying plots of the loss tangent of the films, hypotheses about the distribution of crosslinks in the film were advanced. It was suggested that the screen affects the crosslink density of the films by constraining the locations in which they form.

5. The effect of two screen types on the rheological properties of the photosensitized HDPE films was investigated.

   a. With respect to the linear viscoelastic properties of the photosensitized films, radiation treatment caused the cross-over modulus to shift outside of the range of experimental observation. This was an indication that all of the samples were highly crosslinked.

   b. Plots of the viscosity showed that the screens affect the viscosity of the film both the zero-shear viscosity and the shear thinning behavior of the films. For the same level of radiation intensity, samples irradiated under a screen with narrower holes and a $60°$ staggering angle (screen 1) had a higher zero-shear viscosity than

samples irradiated under a screen with wider holes and a 0° staggering angle (screen 2). Samples irradiated under screen 1 were also more shear thinning.

Recommendations

Though much ground was covered in this study, there is scope for more work to be done.

First, due to time constraints, the effect of changing the wavelength of radiation was not explored. Accordingly, it would be desirable to study the effect of the mercury-lead lamp on the rheological and mechanical properties of the LLDPE films. This would allow a comparison of the effect of wavelength to be made.

A complementary direction for future work would be to extend the rheological investigations by using temperature-time superposition to extend the observation window so that the zero-shear viscosity can be properly determined for each film. This would increase the confidence with which inferences on the effect of the radiation variables on the zero-shear viscosity of the films could be made. This work could be combined with GPC measurements on these films so that the effect of the radiation treatments on the molecular weight distribution of the films can be precisely determined.

An additional source of insight into the molecular architecture of the films would be swelling experiments and gel tests. These would allow insights into the effect of the radiation treatments on the density of crosslinks to be determined.

Finally, the distribution of crosslinks on the surface of the films could be investigated using optical microscopy [16]. These studies would aim to verify how changes to the illumination pattern on the films correlate with structures formed on the films themselves.

Having mapped the basic effects of wavelength, illumination pattern, radiation time and illumination intensity, attention would need to be focused on applying these variables to rationally modify the properties of films. Effects that could be sought would include strengthening the tensile properties in the transverse direction while maintaining these properties in the machine direction and tuning the puncture resistance.

BIBLIOGRAPHY

[1] M. U. Farooq, "Modification of Metallocene Alpha-Olefin Copolymer by UV-Irradiation, MASc. Thesis," University of Waterloo, Department of Chemical Engineering, University of Waterloo, 2016.

[2] D. Hamdi-Akriche, "Choosing between HDPE versus LLDPE for your next containment project," SOLMAX, 13 June 2019. [Online]. Available: https://www.solmax.com/en/blog/choosing-between-hdpe-versus-lldpe-for-your-next-containment-project. [Accessed 2020 June 30].

[3] A. Charlesby, "Crosslinking of polyethylene by Pile Radiation," *Proceedings of the Royal Society, A,* vol. 214, pp. 187 - 214, 1952.

[4] F. Gugumus, "Mechanisms of photooxidation of polyolefins," *Die Angewandte Makromolekulare Chemie,* vol. 176, no. 1, pp. 27 - 42, 1990.

[5] P. Sardashti, C. Tzoganakis, M. Polak and A. Penlidis, "Radiation Induced Long Chain Branching in High-Density Polyethylene through a Reactive Extrusion Process," *Macromolecular Reaction Engineering,* vol. 8, no. 2, pp. 100 - 111, 2013.

[6] A. L. Andrady and M. A. Neal, "Applications and societal benefits of plastics," *Philosophical Transactions of Royal Society B,* vol. 364, no. 1526, pp. 1977 - 1984, 2009.

[7] R. Geyer, J. R. Jambeck and K. L. Law, "Production, use, and fate of all plastics ever made," *Science Advances,* vol. 3, pp. 1 - 5, 2017.

[8] D. Jubinville, E. Esmizadeh, S. Saikrishnan , C. Tzoganakis and T. Mekonnen, "A Comprehensive review of global production and recycling methods of polyolefins (PO) based products and their post-recycling applications," *Sustainable Materials and Technologies,* vol. 25, pp. 1 - 34, 2020.

[9] O. Horodystka, F. Valdés and A. Fullana, "Plastic flexible films waste management - A state of art review," *Waste Management,* vol. 77, pp. 413 - 425, 2018.

[10] P. Cinelli, M. Schmid, E. Bugnicourt, M. B. Coltelli and A. Lazzeri, "Recylability of PET/WPI/PE Multilayer Films by Removal of Whey Protein Isolate-Based Coatings with Enzymatic Detergents," *Materials,* vol. 9, no. 6, p. 473, 2016.

[11] S. L. Favaro, A. R. Freitas, T. A. Ganzerli, A. G. Pereira, A. L. Cardozo, E. C. Muniz, E. M. Girotto and E. Radovanovic, "PET and aluminium recycling from multilayer food packaging using supercritical ethanol," *The Journal of Supercritical Fluids,* vol. 75, pp. 138 - 143, 2013.

[12] D. S. Achilias, A. Giannoulis and G. Z. Papageorgiou, "Recycling of polymers from plastic packaging materials using the dissolution-reprecipitation technique," *Polymer Bulletin,* vol. 63, pp. 449 - 465, 2009.

[13] G. Ciamician, "The Photochemistry of the future," *Science,* vol. 36, pp. 385 - 394, 1912.

[14] S. Chatani, C. J. Kloxin and C. N. Bowman, *The power of light in polymer science: Photochemical processes to manipulate polymer formation, structure, and properties,* vol. 5, Royal Society of Chemistry, 2014, pp. 2187-2201.

[15] N. Corrigan, J. Yeow, P. Judzewitsch, J. Xu and C. Boyer, "Seeing the Light: Advancing Materials Chemistry through Photopolymerization," *Angewandte Chemie,* vol. 131, no. 16, pp. 5224-5243, 8 4 2019.

[16] J. E. Poelma, B. P. Fors, G. F. Meyers, J. W. Kramer and C. J. Hawker, "Fabrication of complex three-dimensional polymer brush nanostructures through light-mediated living radical polymerization," *Angewandte Chemie - International Edition,* vol. 52, no. 27, pp. 6844-6848, 1 7 2013.

[17] C. P. Kabb, C. S. O'Bryan, C. C. Deng, T. E. Angelini and B. S. Sumerlin, "Photoreversible Covalent Hydrogels for Soft-Matter Additive Manufacturing," *ACS Applied Materials and Interfaces,* vol. 10, no. 19, pp. 16793-16801, 16 5 2018.

[18] M. L. Allegrezza, Z. M. Demartini, A. J. Kloster, Z. A. Digby and D. Konkolewicz, "Visible and sunlight driven RAFT photopolymerization accelerated by amines: Kinetics and

mechanism," *Polymer Chemistry,* vol. 7, no. 43, pp. 6626-6636, 21 11 2016.

[19] K. N. Long, T. F. Scott, H. J. Qi, C. N. Bowman and M. L. Dunn, "Photomechanics of light-activated polymers," *Journal of the Mechanics and Physics of Solids,* vol. 57, pp. 1103 - 1121, 2009.

[20] B. P. Fors and C. J. Hawker, "Control of a Living Radical Polymerization of Methacrylates by Light," *Angewandte Chemie,* vol. 51, no. 35, pp. 8850 - 8853, 2012.

[21] F. A. Carey and R. J. Sundberg, "Photochemistry," in *Advanced Organic Chemistry Part A: Structure and Mechanisms*, New York, Springer , 2007, pp. 1073 - 1080.

[22] N. R. Draper and H. Smith, "Transformation of the Response Variable," in *Applied Regression Analysis*, New York, John Wiley and Sons, 1998, pp. 277 - 298.

[23] G. Oster, G. K. Oster and H. Moroson, "Ultraviolet induced crosslinking and grafting of solid high polymers," *Journal of Polymer Science,* vol. 34, no. 127, pp. 671-684, 1 1959.

[24] S. Author, :. A. Charlesby, C. S. Grace and F. B. Pilkington, "Crosslinking of Polyethylene and Paraffins by Ultra-Violet Radiation in the Presence of Sensitizers," 1962.

[25] R. H. Partridge, "Near-ultraviolet absorption spectrum of polyethylene," *The Journal of Chemical Physics,* vol. 45, no. 5, pp. 1679-1684, 1966.

[26] B. Qu, Y. Xu, L. Ding and B. Rånby, "New mechanism of benzophenone photoreduction in photoinitiated crosslinking of polyethylene and its model compounds," *Journal of Polymer Science, Part A: Polymer Chemistry,* vol. 38, no. 6, pp. 999-1005, 15 3 2000.

[27] Y.-C. Hsu, M. P. Weir, R. W. Truss, C. J. Garver, T. M. Nicholson and P. J. Halley, "A fundamental study on photo-oxidative degradation of linear low density polyethylene films at embrittlement," *Polymer,* vol. 53, pp. 2385 - 2393, 2012.

[28] J. Lacoste and D. J. Carlsson, "Gamma-, photo-, and thermally-initiated oxidation of linear low density polyethylene: A quantitative comparison of oxidation products," *Journal of Polymer Science Part A: Polymer Chemistry,* vol. 30, no. 3, pp. 493-500, 1992.

[29] UV Process Supply, Inc., "Three-Dimensional Ultraviolet Curing of Liquid and Powder Coatings," 2000. [Online]. Available: http://www.uvprocess.com/manuals/manual_3D-Curing.pdf. [Accessed August 2019].

[30] R. Chen, Y. Bin, Y. Nakano, K. Naoko and M. Matsuo, "Effect of chemical crosslinking on mechanical and electrical properties of ultrahigh-molecular-weight polyethylene-carbon fiber blends prepared by gelation/crystallization from solutions," *Colloid Polymer Science,* vol. 228, pp. 307 - 316, 2010.

[31] L. Mészáros, Y. Kara, T. Fekete and K. Molnár, "Development of self-reinforced low-density polyethylene using γ-irradiation cross-linked polyethylene fibres," *Radiation Physics and Chemistry,* vol. 170, pp. 1 - 6, 2020.

[32] Y.-C. Hsu, M. P. Weir, R. W. Truss, C. J. Gavrvey, T. M. Nicholson and P. J. Halley, "A fundamental study on photo-oxidative degredation of linear low density polyethylene films at embrittlement," *Polymer,* vol. 53, pp. 2385 - 2393, 2012.

[33] J. M. Dealy and W. Jian, "Rheology and Molecular Structure," in *Melt Rheology and its Applications in the Plastics Industry*, Netherlands, Springer Netherlands, 2013, pp. 181 - 204.

[34] Y. Amintowlieh, C. Tzoganakis, S. G. Hatzikiriakos and A. Penlidis, "Effects of processing variables on polypropylene degradation and long chain branching with UV irradiation," *Polymer Degradation and Stability,* vol. 104, no. 1, pp. 1-10, 2014.

[35] P. M. Wood-Adams, J. M. Dealy, A. W. DeGroot and O. D. Redwine, "Effect of molecular structure on the linear viscoelastic behavior of polyethylene," *Macromolecules,* vol. 33, no. 20, pp. 7489-7499, 3 10 2000.

[36] P. M. Wood-Adams, "The effect of long chain branches on the shear flow behavior of polyethylene," *Journal of Rheology,* vol. 45, no. 1, pp. 203-210, 1 2001.

[37] M. M. Cross, "RHEOLOGY OF NON-NEWTONIAN FLUIDS: A NEW FLOW EQUATION FOR PSEUDOPLASTIC SYSTEMS".

[38] G. R. Zeichner and P. D. Patel, "A comprehensive study of polypropylene melt rheology," in *Proceedings of the 2nd World Congress of Chemical Engineering*, Montreal, 1981.

[39] R. Shroff and H. Mavridis, "New Measures of Polydispersity from Rheological Data on Polymer Melts," *Journal of Applied Polymer Science,* vol. 57, pp. 1605 - 1626, 1995.

[40] Y. Amintowlieh, "Rheological Modification of Polypropylene by Incorporation of Long Chain Branches Using UV Radiation, PhD Thesis," Department of Chemical Engineering, University of Waterloo, Waterloo, 2014.

[41] K. A. Murray, J. E. Kennedy, B. McEvoy, O. Vrain, D. Ryan, R. Cowman and C. L. Higginbotham, "The effects of high energy electron beam irradiation in air on accelerated aging and on the structure property relationships of low density polyethylene," *Nuclear Instruments and Methods in Physics Research B,* vol. 297, pp. 64 - 74, 2013.

[42] T. Bremner and A. Rudin, "Peroxide Modification of Linear Low-Density Polyethylene: A Comparison of Dialkyl Peroxides," *Journal of Applied Polymer Science,* vol. 49, pp. 785 - 798, 1993.

[43] R. T. Chen, C. K. Saw, M. G. Jamieson, T. R. Aversa and R. W. Callahan, "Structural Characterization of Celgard Microporous Membrane Precursors: Melt-Extruded Polyethylene Films," *Journal of Applied Polymer Science,* vol. 53, pp. 471 - 483, 1994.

[44] T. Sarada, L. Sawyer and M. Ostler, "Three dimensional structure of Celgard microporous membranes," *Journal of Membrane Science,* vol. 15, no. 1, pp. 97 - 113, 1983.

[45] I. M. Hutten, Handbook of Nonwoven Filter Media, Oxford: Elsevier, 2007.

[46] L. Mészáros, K. Yahya, T. Fekete and K. Molnár, "Development of self-reinforced low-density polyethylene using γ-irradiation cross-linked polyethylene fibres," *Radiation Physics and Chemistry,* vol. 170, pp. 1 - 6, 2020.

[47] K. A. Murray, J. E. Kennedy, B. McEvoy, O. Vrain, D. Ryan, R. Cowman and C. L. Higginbotham, "THe effects of high energy electron beam irradiation in air on accelerated aging and on the structure property relationships of low density polyethylene," *Nuclear*

Instruments and Methods in Physics Research B, vol. 297, pp. 64 -74, 297.

[48] J. Dealy and W. Jian, "Rheology and Molecular Structure," in *Melt Rheology and its Applications in the Plastics Industry*, Springer, 2013, pp. 181 - 204.

APPENDICES

FULL ANOVA TABLES FOR TWO-LEVEL FACTORIAL EXPERIMENTS

Table 26: Full ANOVA table for elastic modulus in them machine direction for LLDPE films

Factor	SS	df	MS	F_0	p-value	95% CI
A	2990.06	1.00	2990.06	3.84	0.07	32.15
B	923.63	1.00	923.63	1.19	0.29	32.15
C	1442.35	1.00	1442.35	1.85	0.19	32.15
AB	972.20	1.00	972.20	1.25	0.28	32.15
AC	2840.48	1.00	2840.48	3.65	0.07	32.15
BC	134.46	1.00	134.46	0.17	0.68	32.15
ABC	1386.22	1.00	1386.22	1.78	0.20	32.15
Total	23133.01	23.00				
Error	12443.59	16.00	777.72			

Table 27: Full ANOVA table for elastic modulus in the transverse direction for LLDPE films

Factor	Effect	SS	df	MS	F_0	p-value	95% CI
A	45.45	8261.52	1.00	8261.52	15.10	0.005	26.97
B	7.06	199.13	1.00	199.13	0.36	0.563	26.97
C	-29.12	3391.15	1.00	3391.15	6.20	0.038	26.97
AB	11.65	542.85	1.00	542.85	0.99	0.348	26.97
AC	-17.16	1177.25	1.00	1177.25	2.15	0.181	26.97
BC	2.76	30.54	1.00	30.54	0.06	0.819	26.97
ABC	-1.78	12.66	1.00	12.66	0.02	0.883	26.97
Total		17993.18	15.00	1199.55			
Error		4378.10	8.00	547.26			

Table 28: Full ANOVA table for tensile stress at yield in machine direction

Factor	SS	df	MS	F_0	p-value	Effect (MPa)	CI
A	1.65	1.00	1.65	5.74	0.04	0.64173	0.62
B	2.02	1.00	2.02	7.03	0.03	-0.70980	0.62
C	0.04	1.00	0.04	0.13	0.73	-0.09630	0.62
AB	1.74	1.00	1.74	6.08	0.04	-0.66007	0.62
AC	5.08	1.00	5.08	17.70	0.00	-1.12661	0.62
BC	0.01	1.00	0.01	0.03	0.87	-0.04572	0.62
ABC	0.30	1.00	0.30	1.03	0.34	0.27161	0.62
Total	13.12	15.00					
Error	2.29	8.00	0.29				

Table 29: Full ANOVA table for tensile stress at yield in transverse direction

Factor	SS	df	MS	f probe	p-value	Effect	95% CI
A	10.42	1.00	10.42	23.29	0.001	1.61	0.77
B	0.77	1.00	0.77	1.71	0.227	0.44	0.77
C	2.37	1.00	2.37	5.29	0.050	-0.77	0.77
AB	0.19	1.00	0.19	0.42	0.537	0.22	0.77
AC	2.49	1.00	2.49	5.58	0.046	-0.79	0.77
BC	0.07	1.00	0.07	0.17	0.693	-0.14	0.77
ABC	0.12	1.00	0.12	0.27	0.615	-0.18	0.77
Total	20.01	15.00	1.33				
Error	3.58	8.00	0.45				

Table 30: Full ANOVA table for tensile stress at break in the machine direction

Factor	Effect	SS	df	MS	f probe	p-value	95% CI
A	-3.65	53.42	1.00	53.42	21.86	0.00	1.80
B	-5.05	101.92	1.00	101.92	41.71	0.00	1.80
C	4.90	96.12	1.00	96.12	39.33	0.00	1.80
AB	2.13	18.16	1.00	18.16	7.43	0.03	1.80
AC	-2.74	29.93	1.00	29.93	12.25	0.01	1.80
BC	-0.90	3.21	1.00	3.21	1.31	0.29	1.80
ABC	1.43	8.18	1.00	8.18	3.35	0.10	1.80
Total		330.49	15.00	22.03			
Error		19.55	8.00	2.44			

Table 31: Full ANOVA table for tensile stress at break in the transverse direction

Factor	Effect	SS	df	MS	f probe	p-value	95% CI
A	-0.88	3.10	1.00	3.10	0.68	0.4336	2.46
B	-4.10	67.10	1.00	67.10	14.72	0.0050	2.46
C	3.69	54.58	1.00	54.58	11.98	0.0086	2.46
AB	1.54	9.51	1.00	9.51	2.09	0.1865	2.46
AC	-0.36	0.53	1.00	0.53	0.12	0.7425	2.46
BC	-1.37	7.51	1.00	7.51	1.65	0.2353	2.46
ABC	-1.00	3.99	1.00	3.99	0.88	0.3768	2.46
Total		182.76786	15				
Error		36.45920	8	4.55740			

Table 32: Full ANOVA table for tensile strain at break in the machine direction for LLDPE films

Factor	Effect	SS	df	MS	f probe	p-value	95% CI
A	-124.06	61563.49	1.00	61563.49	28.87	0.0007	150.61
B	-151.42	91713.59	1.00	91713.59	43.00	0.0002	150.61
C	141.84	80472.23	1.00	80472.23	37.73	0.0003	150.61
AB	55.26	12216.39	1.00	12216.39	5.73	0.0436	150.61
AC	-53.64	11510.51	1.00	11510.51	5.40	0.0487	150.61
BC	38.63	5967.69	1.00	5967.69	2.80	0.1329	150.61
ABC	48.83	9536.91	1.00	9536.91	4.47	0.0674	150.61
Total		290042.49	15.00				
Error		17061.67	8.00	2132.71			

Table 33: Full ANOVA for tensile strain at break in the transverse direction for LLDPE films

Factor	Effect	SS	df	MS	f probe	p-value	95% CI
A	-106.86	45673.61	1.00	45673.61	18.38	0.0027	57.47
B	-167.85	112688.43	1.00	112688.43	45.35	0.0001	57.47
C	104.06	43313.27	1.00	43313.27	17.43	0.0031	57.47
AB	28.32	3208.45	1.00	3208.45	1.29	0.2887	57.47
AC	-7.04	198.00	1.00	198.00	0.08	0.7849	57.47
BC	-30.05	3611.47	1.00	3611.47	1.45	0.2624	57.47
ABC	4.33	75.12	1.00	75.12	0.03	0.8663	57.47
Total		228645.32	15.00				
Error		19876.96	8.00	2484.62			

Table 34: Full ANOVA table for the effect of radiation variables on the zero-shear viscosity of LLDPE films

Factor	Contrast (Pa.s)	Effect (Pa.s)	Sum of Squares	df	Mean Square	F0	p-value	90% CI
A	141055	17,632	1.24E+09	1	1.24E+09	0.04	0.85	170,551.84
B	1553268	194,159	1.51E+11	1	1.51E+11	4.48	0.07	170,551.84
C	-2132205	-266,526	2.84E+11	1	2.84E+11	8.45	0.02	170,551.84
AB	-520781	-65,098	1.70E+10	1	1.70E+10	0.50	0.50	170,551.84
AC	155440	19,430	1.51E+09	1	1.51E+09	0.04	0.84	170,551.84
BC	-1256856	-157,107	9.87E+10	1	9.87E+10	2.94	0.12	170,551.84
ABC	803517	100,440	4.04E+10	1	4.04E+10	1.20	0.31	170,551.84
Error			2.69E+11	8	3.36E+10	1.00	0.50	
Total			8.63E+11	15	5.75E+10	1.71	0.22	

Table 35: Full ANOVA table for the effect of radiation variables on the shear-thinning index of LLDPE films

Factor	Contrast	Effect	Sum of Squares	df	Mean Square	F_0	p-value	95% CI
A	-0.98	-0.12	0.06	1	0.06	22.22	1.51E-03	0.06
B	-0.88	-0.11	0.05	1	0.05	17.79	2.92E-03	0.06
C	1.08	0.13	0.07	1	0.07	26.88	8.38E-04	0.06
AB	0.06	0.01	0.00	1	0.00	0.09	0.78	0.06
AC	0.74	0.09	0.03	1	0.03	12.73	7.32E-03	0.06
BC	0.16	0.02	0.00	1	0.00	0.61	0.46	0.06
ABC	-0.50	-0.06	0.02	1	0.02	5.74	4.35E-02	0.06
Total			0.25	15	0.02			
Error			0.02	8	0.00			

Table 36: Full ANOVA table for the effect of radiation and compounding variables on the tensile stress at break of HDPE films in the machine direction

Factor	Contrast	Effect	df	SS	MS	F$_0$	p-value	95% CI
A	-7976.04	-498.50	1.00	1988038.04	1988038.04	52.11	9.17E-08	1754.81
B	4248.08	265.51	1.00	563944.25	563944.25	14.78	6.66E-04	1754.81
C	-934.90	-58.43	1.00	27313.61	27313.61	0.72	0.40	1754.81
D	412.89	25.81	1.00	5327.41	5327.41	0.14	0.71	1754.81
E	-858.01	-53.63	1.00	23005.54	23005.54	0.60	0.44	1754.81
AB	2142.36	133.90	1.00	143428.57	143428.57	3.76	0.06	1754.81
AC	-1127.64	-70.48	1.00	39736.72	39736.72	1.04	0.32	1754.81
AD	240.82	15.05	1.00	1812.31	1812.31	0.05	0.83	1754.81
AE	1679.18	104.95	1.00	88114.07	88114.07	2.31	0.14	1754.81
BC	439.03	27.44	1.00	6023.22	6023.22	0.16	0.69	1754.81
BD	-3163.76	-197.74	1.00	312793.64	312793.64	8.20	0.01	1754.81
BE	-1968.96	-123.06	1.00	121150.13	121150.13	3.18	0.09	1754.81
CD	-569.24	-35.58	1.00	10126.00	10126.00	0.27	0.61	1754.81
CE	213.36	13.34	1.00	1422.61	1422.61	0.04	0.85	1754.81
DE	-285.65	-17.85	1.00	2549.95	2549.95	0.07	0.80	1754.81
ABC	-1406.73	-87.92	1.00	61839.99	61839.99	1.62	0.21	1754.81
ABD	496.64	31.04	1.00	7707.97	7707.97	0.20	0.66	1754.81
ABE	-323.84	-20.24	1.00	3277.34	3277.34	0.09	0.77	1754.81
ACD	-2749.07	-171.82	1.00	236167.72	236167.72	6.19	0.02	1754.81
ACE	-492.41	-30.78	1.00	7577.19	7577.19	0.20	0.66	1754.81
ADE	117.46	7.34	1.00	431.12	431.12	0.01	0.92	1754.81
BCD	663.74	41.48	1.00	13767.27	13767.27	0.36	0.55	1754.81
BCE	241.55	15.10	1.00	1823.37	1823.37	0.05	0.83	1754.81
BDE	-448.93	-28.06	1.00	6298.07	6298.07	0.17	0.69	1754.81

CDE	-2150.33	-134.40	1.00	144497.18	144497.18	3.79	0.06	1754.81
ABCD	-397.03	-24.81	1.00	4926.03	4926.03	0.13	0.72	1754.81
ABCE	775.36	48.46	1.00	18787.04	18787.04	0.49	0.49	1754.81
ABDE	-1544.69	-96.54	1.00	74564.43	74564.43	1.95	0.17	1754.81
ACDE	-1441.45	-90.09	1.00	64930.19	64930.19	1.70	0.20	1754.81
BCDE	1800.62	112.54	1.00	101319.92	101319.92	2.66	0.11	1754.81
ABCDE	1242.38	77.65	1.00	48234.70	48234.70	1.26	0.27	1754.81
Total			31	36,188,567.90	1,167,373.16			
Error			27	1,029,991.95	38,147.85			

Table 37: Full ANOVA table for the effect of radiation and compounding variables on the tensile strain at break of HDPE films in the machine direction

Factor	Contrast	Effect	df	SS	MS	F_0	p-value	95% CI
A	91.724	5.73	1	262.92	262.92	15.76	4.80E-04	30.28
B	-59.077	-3.69	1	109.06	109.06	6.54	0.02	30.28
C	-17.989	-1.12	1	10.11	10.11			30.28
D	-30.537	-1.91	1	29.14	29.14			30.28
E	-22.665	-1.42	1	16.05	16.05			30.28
AB	-69.971	-4.37	1	153.00	153.00	9.17	0.01	30.28
AC	-35.272	-2.20	1	38.88	38.88			30.28
AD	-25.279	-1.58	1	19.97	19.97			30.28
AE	-9.580	-0.60	1	2.87	2.87			30.28
BC	4.066	0.25	1	0.52	0.52			30.28
BD	20.901	1.31	1	13.65	13.65			30.28
BE	22.490	1.41	1	15.81	15.81			30.28
CD	36.048	2.25	1	40.61	40.61			30.28
CE	-9.570	-0.60	1	2.86	2.86			30.28
DE	12.822	0.80	1	5.14	5.14			30.28
ABC	6.484	0.41	1	1.31	1.31			30.28
ABD	46.473	2.90	1	67.49	67.49			30.28
ABE	32.906	2.06	1	33.84	33.84			30.28
ACD	8.036	0.50	1	2.02	2.02			30.28
ACE	-15.925	-1.00	1	7.93	7.93			30.28
ADE	-15.801	-0.99	1	7.80	7.80			30.28
BCD	-56.449	-3.53	1	99.58	99.58	5.97	0.02	30.28
BCE	11.228	0.70	1	3.94	3.94			30.28
BDE	-10.702	-0.67	1	3.58	3.58			30.28

CDE	-16.121	-1.01	1	8.12	8.12			30.28
ABCD	-53.197	-3.32	1	88.44	88.44	5.30	0.03	30.28
ABCE	49.972	3.12	1	78.04	78.04			30.28
ABDE	-0.804	-0.05	1	0.02	0.02			30.28
ACDE	-24.876	-1.55	1	19.34	19.34			30.28
BCDE	12.071	0.75	1	4.55	4.55			30.28
ABCDE	2.733	0.17	1	0.23	0.23			30.28
Total			31	1,146.81	36.99			
Error			26	433.82	16.69			

Table 38: Full ANOVA table for the effect of radiation and compounding variables on the tensile stress at break in the transverse direction of HDPE films

Factor	Contrast	Effect	df	SS	MS	F₀	p-value	95% CI
A	20.508	1.282	1	13.14	13.14	0.22	0.645	69.88
B	-118.385	-7.399	1	437.97	437.97	7.24	0.012	69.88
C	-107.897	-6.744	1	363.80	363.80	6.01	0.021	69.88
D	-18.286	-1.143	1	10.45	10.45	0.17	0.681	69.88
E	-69.359	-4.335	1	150.33	150.33	2.48	0.126	69.88
AB	19.997	1.250	1	12.50	12.50	0.21	0.653	69.88
AC	-51.190	-3.199	1	81.89	81.89	1.35	0.254	69.88
AD	-10.447	-0.653	1	3.41	3.41	0.06	0.814	69.88
AE	12.169	0.761	1	4.63	4.63	0.08	0.784	69.88
BC	-37.942	-2.371	1	44.99	44.99	0.74	0.396	69.88
BD	39.178	2.449	1	47.97	47.97	0.79	0.381	69.88
BE	35.167	2.198	1	38.65	38.65	0.64	0.431	69.88
CD	-24.488	-1.531	1	18.74	18.74	0.31	0.582	69.88
CE	60.778	3.799	1	115.44	115.44	1.91	0.178	69.88
DE	14.480	0.905	1	6.55	6.55	0.11	0.745	69.88
ABC	-138.550	-8.659	1	599.88	599.88	9.92	0.004	69.88
ABD	42.557	2.660	1	56.60	56.60	0.94	0.342	69.88
ABE	-28.384	-1.774	1	25.18	25.18	0.42	0.524	69.88
ACD	7.144	0.447	1	1.59	1.59	0.03	0.872	69.88
ACE	22.464	1.404	1	15.77	15.77	0.26	0.614	69.88
ADE	68.803	4.300	1	147.93	147.93	2.45	0.129	69.88
BCD	96.146	6.009	1	288.87	288.87	4.77	0.037	69.88
BCE	-19.012	-1.188	1	11.30	11.30	0.19	0.669	69.88
BDE	39.795	2.487	1	49.49	49.49	0.82	0.373	69.88

CDE	82.866	5.179	1	214.59	214.59	3.55	0.070	69.88
ABCD	80.058	5.004	1	200.29	200.29	3.31	0.080	69.88
ABCE	-53.617	-3.351	1	89.84	89.84	1.48	0.233	69.88
ABDE	14.268	0.892	1	6.36	6.36	0.11	0.748	69.88
ACDE	11.236	0.702	1	3.95	3.95	0.07	0.800	69.88
BCDE	-0.099	-0.006	1	0.00	0.00	0.00	0.998	69.88
ABCDE	38.656	2.416	1	46.70	46.70	0.77	0.387	69.88
Total			31	36,675.90	1,183.09	19.56	0.000	69.88
Error			28	1,693.99	60.50	1.00	0.500	69.88

Table 39: Full ANOVA table for the effect of radiation variables on the tensile stress at break in the machine direction of photosensitized HDPE films

Source of Variation	Contrast	Effect	Sum of Squares	Degrees of Freedom	Mean Square	F_0	$C_{ritical}$	95% CI	p-value
A	-33.26	-8.32	138.31	1	138.31	85.58	7.71	2.86	0.0008
B	-10.78	-2.69	14.52	1	14.52	8.99	7.71	2.86	0.0400
C	38.21	9.55	182.47	1	182.47	112.90	7.71	2.86	0.0004
AB	2.07	0.52	0.53	1	0.53	0.33	7.71	2.86	0.5962
AC	-0.33	-0.08	0.01	1	0.01	0.01	7.71	2.86	0.9312
BC	-3.18	-0.80	1.27	1	1.27	0.78	7.71	2.86	0.4260
ABC	-0.75	-0.19	0.07	1	0.07	0.04	7.71	2.86	0.8446
Total			561.78	13	43.21				
Pure Error			6.46	4	1.62				
Lack of Fit			218.12	1	218.12	134.96	7.71		Effect is significant

Table 40: Full ANOVA table for effect of radiation variables on the tensile strain at break in the transverse direction of photosensitized HDPE films

Source of Variation	Contrast	Effect	Sum of Squares	Degrees of Freedom	Mean Square	F_0	$C_{ritical}$	95% CI	p-value
A	1.23954	0.30988	0.19206	1	0.19206	0.65023	7.71	1.22	0.465
B	7.38650	1.84663	6.82005	1	6.82005	23.09014	7.71	1.22	0.009
C	-3.18151	-0.79538	1.26525	1	1.26525	4.28365	7.71	1.22	0.107
AB	1.73666	0.43416	0.37700	1	0.37700	1.27637	7.71	1.22	0.322
AC	-1.44918	-0.36230	0.26252	1	0.26252	0.88878	7.71	1.22	0.399
BC	-3.46930	-0.86732	1.50450	1	1.50450	5.09368	7.71	1.22	0.087

ABC	-1.16139	-0.29035	0.16860	1	0.16860	0.57083	7.71	1.22	0.492
Total			16.56176	13	1.27398				
Pure Error			1.18147	4	0.29537				
Lack of Fit			4.79031	1	4.79031	16.21820	7.71		Effect is significant

Table 41: Full ANOVA table for the effect of radiation variables on the tensile strain at break in the machine direction of photosensitized HDPE films

Source of Variation	Contrast	Effect	Sum of Squares	Degrees of Freedom	Mean Square	F_0	$C_{critical}$	95% CI	p-value
A	-50.22921	-12.55730	315.37174	1	315.3717424	156.9109453	7.71	3.19	0.0002
B	21.54177	5.38544	58.00596	1	58.0059603	28.86044892	7.71	3.19	0.0058
C	37.08328	9.27082	171.89619	1	171.8961884	85.52571389	7.71	3.19	0.0008
AB	12.79174	3.19794	20.45358	1	20.45358292	10.17653328	7.71	3.19	0.0332
AC	-27.49985	-6.87496	94.53022	1	94.53021875	47.03283137	7.71	3.19	0.0024
BC	-30.47913	-7.61978	116.12214	1	116.1221402	57.77573681	7.71	3.19	0.0016
ABC	-3.64561	-0.91140	1.66131	1	1.661305388	0.826570564	7.71	3.19	0.41
Total			866.75604	13	66.67354157				
Pure Error			8.03951	4	2.009877271				
Lack of Fit			80.67539	1	80.67539297	40.13946232	7.71		Effect is significant

Table 42: Full ANOVA table for the effect of radiation variables on the tensile strain at break of HDPE films in the transverse direction

Source of Variation	Contrast	Effect	Sum of Squares	Degrees of Freedom	Mean Square	F_0	$C_{ritical}$	95% CI	p-value
A	-1.86659	-0.46665	0.43552	1	0.43552	92.22262	7.71	0.15	0.0007
B	0.16750	0.04187	0.00351	1	0.00351	0.74260	7.71	0.15	0.4374
C	0.38888	0.09722	0.01890	1	0.01890	4.00281	7.71	0.15	0.1160
AB	1.96035	0.49009	0.48037	1	0.48037	101.71968	7.71	0.15	0.0005
AC	0.11710	0.02927	0.00171	1	0.00171	0.36294	7.71	0.15	0.5794
BC	0.38888	0.09722	0.01890	1	0.01890	4.00281	7.71	0.15	0.1160
ABC	0.11710	0.02927	0.00171	1	0.00171	0.36294	7.71	0.15	0.5794
Total			1.22723	13	0.09440				
Pure Error			0.01889	4	0.00472				
Lack of Fit			0.24770	1	0.24770	52.45110242	7.71		Effect is significant